The removal of selected pharmaceuticals from a municipal membrane bioreactor secondary effluent with an electrochemical oxidation process

by

Kareema Smith

A thesis submitted in fulfilment of the requirements for the degree

Master of Engineering: Chemical Engineering

in the

Faculty of Engineering and the Built Environment

at the

Cape Peninsula University of Technology

Supervisor: **Prof Mujahid Aziz**

February 2023

Declaration

I, Kareema Smith, hereby declare that the contents of this dissertation/ thesis represent my unaided work and that the dissertation/ thesis has not previously been submitted for academic examination towards any qualification. Furthermore, it represents my own opinions and not necessarily those of the Cape Peninsula University of Technology

Signed:  Date: February 2023

Abstract

Municipal secondary membrane bioreactor (MBR) wastewater effluent in South Africa (SA) contains various types of pharmaceuticals that form part of a class of chemical contaminants of emerging concern (CECs). These contaminants cause harmful influences on the natural environment. While typical tertiary remedy methods efficiently remove micropollutants, residues of these products exist in water masses at low concentrations, emphasising the need for additional treatment. Advanced, pioneering and sensitive analytical technologies are needed to identify their low concentration in complex matrices such as MBR secondary wastewater. Under these circumstances, electrochemical oxidation (EO) is a possible solution for removing pharmaceuticals.

This study investigates the removal of inorganics and pharmaceuticals in secondary municipal MBR effluent. A lab-scale EO unit with Ti/Pt and Ti/ $IrO_2Ta_2O_5$ electrodes was used. The EO process produced effluent discharge for recycling application.

Three pharmaceuticals were selected, i.e., ibuprofen (IBU), carbamazepine (CBZ) and diclofenac (DCF). IBU and DCF are from the same pharmaceutical group, a non-steroidal anti-inflammatory drug (NSAID), while CBZ is from the anti-epileptic group. Ammonia and COD were also treated in this process.

The electrochemical oxidation process with Ti/Pt and Ti/$IrO_2Ta_2O_5$ electrodes was applied to treat the secondary municipal MBR effluent in a batch reactor at constant pH of 4 and a working volume of 3L. The electrolyte (NaCl) concentration and current density were varied at room temperature. At a current density of 10 mA/cm^2 and 0.08M electrolyte anode, Ti/$IrO_2Ta_2O_5$ showed better results than Ti/Pt for CBZ, DCF and IBU of more than 99% pharmaceutical removal. The inorganic ammonia compound was successfully removed at a maximum removal of 99% (Ti/$IrO_2Ta_2O_5$ anode) and 75% (Ti/Pt anode). However, Ti/Pt has a maximum reduction of 86% for COD.

A Response Surface Methodology (RSM) and central composite design (CCD) characterised the electrochemical oxidation experiments. Polynomial quadratic models were successfully developed to remove COD, ammonia, and colour. Their removal was found to be significant.

Research outputs

Smith K & Aziz M; 2022, The removal of selected pharmaceuticals from a municipal membrane bioreactor secondary effluent with an electrochemical oxidation process, Inter-institutional Postgraduate Symposium, STIAS, Stellenbosch University, Stellenbosch, South Africa, 30 September 2022

Smith K & Aziz, M; 2023, The elimination of selected pharmaceuticals from a municipal membrane bioreactor secondary effluent with an electrochemical oxidation process. Science of the Total Environment. Submitted XX February 2023 [Paper ID.: XX-XX-XX]

Acknowledgements

I thank Allah for giving me the strength to succeed with this project, for protecting me, and blessing me with my family and friends.

This research project was undertaken within the Chemical Engineering Department at the Cape Peninsula University of Technology between January 2019 and February 2023.

I want to express my sincere gratitude to the following people for their contributions towards the completion of this thesis:

My Supervisor, Prof Mujahid Aziz, for his incomparable supervision, persistent guidance, motivation, encouragement, and technical expertise in this research field. I am thankful for his sustained academic, moral and caring assistance throughout my academic journey

The technical and administrative staff in the Chemical Engineering Department. Mr Alwyn Bester and Mrs Hannelene Small always willing to assist

The Environmental Engineering Research Group (*EnvERG*) in the Department of Chemical Engineering.

Rheinmetall Denel Munition (Pty) Ltd South Africa, for their support and student scholarship.

Ms Pei-Yin Lieberich, for her continuous assistance, guidance, and technical expertise in the field of GCMS analysis.

To my friends: Noora Salie, Ilhaam Railoun Gafoor, Maryam Manuel, Nurah Jacobs, Zilungile Mqoqi, Clive Adams, Wafieqah Mandoll, Jade Claasen and Randall Smith for their moral support, prayers and encouragement.

Prof Shaheed Hartley, for the countless hours he invested in me and his contribution to my academic and personal growth

Thank you for your constant encouragement to my family, siblings, cousins, uncles, aunties and grandparents.

To my parents, Dawood Smith and Shamiela Darries, who instilled the importance of education and the value of hard work and perseverance. Thank you for your continued support throughout the years.

Finally, thank you to my husband, Kayyum, for everything.

Dedication

To my parents, Dawood Smith and Shamiela Darries

Table of Contents

List of tables

List of Figures

List of Acronyms

AOP	Advanced Oxidation Process
BDD	Boron Doped Diamond
CAS	Conventional Activated Sludge
CBZ	Carbamazepine
CCT	City of Cape Town
DC	Direct Current
DCF	Diclofenac
DSA	Dimensionally Stable Anode
DWS	Department of Water and Sanitation
EDC	Endocrine – Disrupting Contaminant
EO	Electrochemical Oxidation
GD	Green Drop
MBR	Membrane bioreactor
MEng	Master of Engineering
MMO	Mixed Metal Oxide
NSAID	Nonsteroidal anti-inflammatory drug
PPCP	Pharmaceuticals and Personal Care Products
SA	South Africa
SRT	Sludge Retention Time
SS	Stainless Steel
TP	Transformation Products
TSS	Total Suspended Solids
WWTW	Wastewater Treatment Works

List of symbols

Symbol	Definition	Unit
I	Applied Current	A
A	Area	cm^2
COD_t	Chemical oxygen demand at time T	mg/ml
J	Current density	mA/cm^2
V	Electrolyte volume	L
F	Faraday's constant	C/mol
COD_i	Initial COD	mg/l
m	Mass	g
Vm	Mean cell voltage	V
E	Mean energy consumption	kWh/m^3
M	molarity	Mol/l
Δt	Reaction time	seconds
T	Temperature	°C

Chapter 1

Introduction

Chapter 1: Introduction

1. Background

"South Africa (SA) is a developing country" (Archer et al., 2017). This statement is based on the population statistics of a 70.9% - 83.5% increase in 2011. This population increase means that not only the water demand increased but also the demand for sanitation services.

All wastewater treatment works (WWTW) in SA aim to improve the water quality of the sewage influent. Release secondary effluent to the environment must comply with the Department of Water and Sanitation (DWS) criteria. The DWS founded the Green Drop (GD) program in 2008 to evaluate the performance of WWTW (Archer et al., 2017). Should the WWTW comply, the plant will receive a GD status. However, the WWTW in SA is reported to be overloaded, resulting in few GD statuses and ineffective wastewater treatment (Madikizela et al., 2018).

Water pollution occurs from either direct- or indirect contamination. Abdi & Kazemi (2015) describes direct contamination as effluent discharge into water masses, while indirect contamination is organic or inorganic water pollutants. Municipal wastewater contains many contaminants, such as domestic waste, antibiotics, pharmaceuticals, bacteria, and personal care products (PPCP). Researchers have taken a closer look at pharmaceuticals entering the WWTW.

Pharmaceuticals have recently become one of the critical elements in the investigation. These pharmaceuticals enter the sewage system mostly from hospitals and through domestic use (Loos et al., 2018). Removal of pharmaceuticals from secondary effluent is vital because it is classified as a threat to the environment and aquatic life. There are various methods to remove pharmaceuticals from secondary effluent. However, studies have shown that electrochemical oxidation is promising (Benito et al., 2017; Coria et al., 2014; García-Montoya et al., 2015).

1.1. Problem statement

Municipal secondary membrane bioreactor (MBR) wastewater effluent in SA contains various types of pharmaceuticals that form part of a class of chemical contaminants of emerging concern (CECs) (Madikizela et al., 2018; Olujimi et al., 2012). These contaminants cause harmful influences on the natural environment. While typical tertiary remedy methods efficiently remove micropollutants, residues of these products exist in water masses at low concentrations, emphasising the need for additional treatment. Advanced, pioneering and sensitive analytical technologies are needed to identify their low concentration in complex matrices such as MBR secondary wastewater. Under these circumstances, electrochemical oxidation (EO) is a possible solution for removing pharmaceuticals.

1.2. Research question

- How effective would removing inorganics and COD using EO be at varying current density and NaCl electrolyte concentration?

- What effect will the current density and NaCl electrolyte concentration have on the removal of the pharmaceuticals, ibuprofen (IBU), diclofenac (DCF) and carbamazepine (CBZ)?

1.3. Aim and objectives

This study investigates the removal of inorganics and pharmaceuticals in secondary municipal MBR effluent with Ti/Pt and Ti/ $IrO_2Ta_2O_5$ electrodes using an EO unit for yielding effluent discharge for recycling application.

The research objectives were:

- Evaluate two types of electrodes (Ti/Pt and Ti/ $IrO_2Ta_2O_5$) based on the effect of current density and NaCl electrolyte concentration to measure the best quality of effluent with the removal of targeted inorganics and COD.

- Investigate the removal efficiencies of selected pharmaceuticals: carbamazepine (CBZ), ibuprofen (IBU) and diclofenac (DCF) using solid-phase extraction (SPE) and gas chromatography-mass spectrometry (GCMS) for quantification in the water.

1.4. Significance of the study

Effective municipal MBR secondary effluent treatment may result in compliance with wastewater discharge standards and potential recycling applications.

1.5. Delineation

This study focused on removing selected Inorganics, COD and pharmaceuticals, carbamazepine, diclofenac and ibuprofen from secondary municipal membrane bioreactor wastewater effluent using EO tertiary treatment process. A lab-scale EO unit was used as a tertiary treatment process, and GCMS was used to analyse and quantify the pharmaceuticals removed. This research focused on the effect of current density, NaCl electrolyte concentration, and feed pH on evaluating the removal efficiencies and performance of the electrodes (Ti/Pt and Ti/ $IrO_2Ta_2O_5$). All other factors were delineated.

1.6. Structure of the thesis

Chapter 1: Introduction

The chapter introduces the reader to the background of the project and the problem statement that the project addresses. The aims and objectives are included for addressing the issues stated and the delineation.

Chapter 2: Literature Review

The literature review looks at all the studies other researchers conducted within the same or similar field. It may also identify gaps within research and highlight the literature on this study's focus points.

Chapter 3: Methodology

The chapter contains the materials and methods used for executing the project from the aims and objectives of the project. Also included are the instruments and equipment used.

Chapter 4: Results and Discussion

This section contains the results and the discussion. The area is separated into three sections. The results are on COD removal, inorganic pollutants, and chemical analysis.

Chapter 5: Optimisation using Response Surface Methodology (RSM)

This section dealt with the optimisation of the EO removal process using RSM. This includes developing the multilevel factorial design, central composite design and central composite predictive models. The best-fitted models were optimized to identify the optimum condition for COD, sulphate removal and colour removal in municipal MBR secondary effluent by evaluation and verification using Design Expert Software.

Chapter 6: Conclusion and Recommendation

This section concludes the overall project collected from the experiments in chapters 4 and 5. This chapter also includes recommendations observed during this study for further research.

Appendix:

This section includes tables, graphs and calculations that formed part of the methods and discussions in Chapters 3, 4 and 5.

Chapter 2

Literature Review

Chapter 2: Literature Review

2. Introduction

All living species are dependent on clean and drinkable water. The recent water shortage resulting in stringent measures to save water in the Western Cape Province emphasises the need to ensure the availability of clean and potable water in an ever-expanding human population. Parsons & Jeffersons (2006) confirmed that improvement in water quality improves human health.

2.1. Types of Water

Municipal wastewater comprises different types of wastewater. The two significant types of wastewater are industrial- and domestic wastewater. Wastewater is a form of pollution not only to the environment but also the aquatic life. Naturally, these different types of wastewater in Figure 2.1 contain various pollutants. Domestic wastewater comprises greywater (home wastewater) and blackwater (*Von Sperling*, 2007).

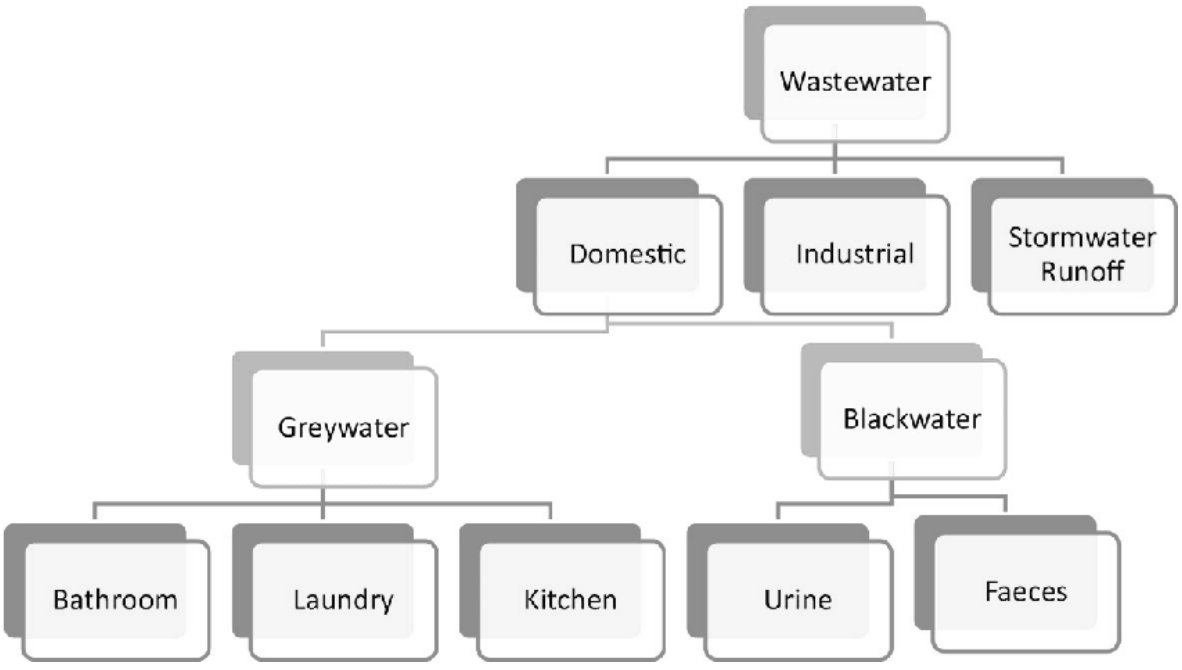

Figure 2.1: Types of wastewater(Edokpayi et al., 2017)

2.2. Composition of Wastewater

Domestic wastewater comprises 99.9% water, while the remaining 0.1% consists of biodegradable compounds, suspended solids (SS), metals, and pathogenic microorganisms (Templeton & Butler, 2011). However, domestic and industrial wastewater comprises many chemicals such as antibiotics, pharmaceuticals, bacteria, and personal care products. This composition species increases the number of pollutants within municipal wastewater significantly. Madikizela, Ncube and Chimuka (2018) reported various pharmaceuticals discovered in water masses (e.g. surface water) across South Africa. Therefore, the removal of these pharmaceuticals is needed.

2.3. Wastewater Treatment

As mentioned, South Africa is a growing economy (Archer et al., 2017). The water demand is excellent, and the sewage or municipal wastewater has also significantly increased. Treating wastewater is vital for the environment, aquatic life, and recycling purposes. There are several types of water treatment and recycling technologies, as shown in Figure 2.2.

Wastewater treatment is done in steps depending on the wastewater received at the WWTW. Generally, primary- and secondary treatment followed by disinfectant is usually implemented at most WWTW in South Africa. However, Pre- treatment and tertiary treatment are also implemented. Since the membrane unit removes TSS significantly, tertiary water treatment for MBR processes is usually implemented for solid waste rather than secondary effluent. However, there are still pollutants within the effluent because the size of the membranes allows particles, e.g. pharmaceuticals, to enter the secondary effluent.

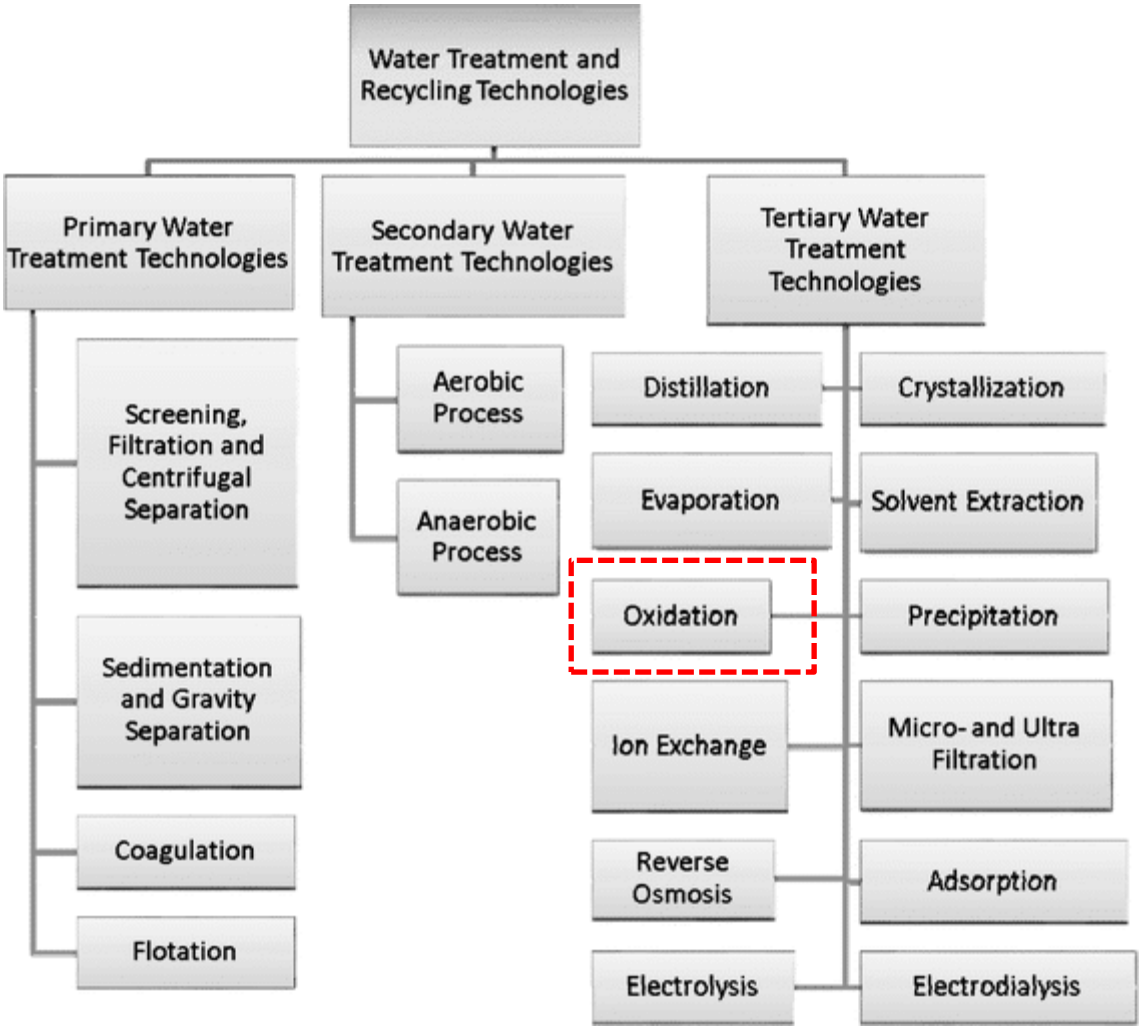

Figure 2.2: Water treatment technologies (Gupta et al., 2012)

2.4. Secondary Treatment

In South African municipal wastewater treatment works (MWWTWs), the most popular secondary treatments are either the conventional activated sludge (CAS) process or the membrane bioreactor (MBR).

2.4.1. Conventional Activated Sludge (CAS)

The CAS unit contains a reactor and secondary settling tanks/ clarifiers (Figure 2.3). Generally, the reactor removes organic matter biologically by nitrification and denitrification (Templeton & Butler, n.d.)and phosphate removal processes. Secondary effluent is obtained through sedimentation in the secondary settling tanks/ clarifiers.

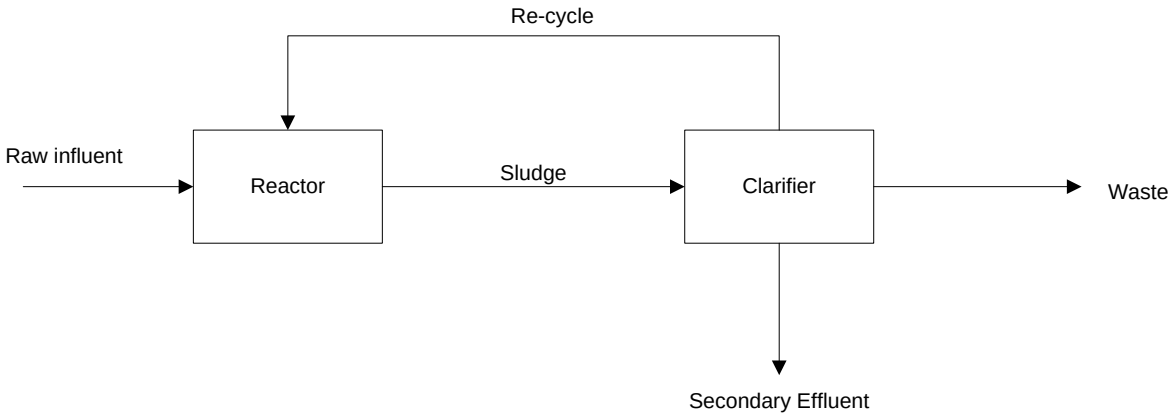

Figure 2.3: BFD of general CAS plant

A comparative study shows that although the CAS plants have low costs and energy consumption, it does not have an excellent environmental footprint. Instead, the membrane bioreactor (MBR) has much better results for the secondary effluent.

2.4.2. Membrane Bioreactor (MBR)

The MBR has two units, i.e. the biological reactor and the membrane unit (Figure 2.4). There are three zones within a biological reactor: anaerobic, aerobic and anoxic. These zones allow biological reactions and processes, including phosphate removal, nitrification and denitrification (Martín et al., 2015).

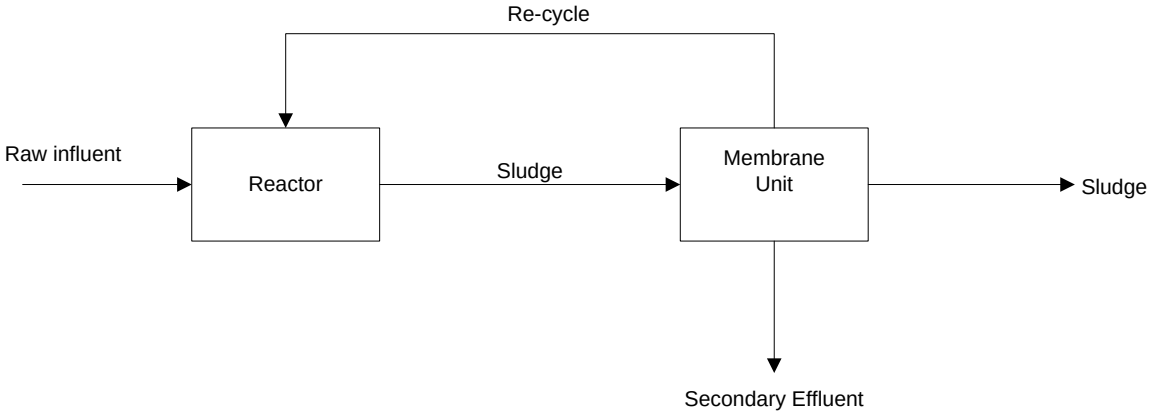

Figure 2.4: BFD of general MBR.

Unlike the CAS plant, the MBR produces better-quality secondary effluent. The membrane unit contains micro-porous membranes instead of secondary settling tanks/clarifiers. The membrane unit separates the liquid (permeate) from the solid. However, not all contaminants are removed through secondary treatment. The MBR secondary treatment, such as pharmaceuticals, is inefficient for removing non-biodegradable contaminants (Wanda et al., 2018). Hence, tertiary treatment is required.

2.5. Tertiary Treatment

WWTW is not equipped to remove pharmaceuticals efficiently. Therefore tertiary treatment is proposed. There are many possible treatment suggestions, such as adsorption (Akpotu et al., 2020), electrocoagulation (Zaidi et al., 2019), ozonation (Lee et al., 2014)and photo-catalysis (Orimolade et al., 2020). However, based on research (Hurwitz et al., 2014), electrochemical oxidation seems a promising approach for tertiary treatment because it is "the most mature approach" (Radjenovic & Sedlak, 2015) for tertiary water treatment

2.5.1. Advanced Oxidation Processes (AOP)

AOP is classified as an effective method to degrade pharmaceuticals and an environmentally friendly process (Rajab, Greco, et al., 2013). These processes are typically done on secondary treated effluent to decrease the treated compounds and lower operational costs.

Advanced oxidation processes can either be homogeneous or heterogeneous. Brugnera, de Araújo Souza and Zanoni (2016) state that a reaction that occurs without a solid catalyst or a process with substances in the same phase can be classified as homogeneous, while a heterogeneous system occurs with the presence of a solid catalyst to form hydroxyl radicals or is a process involving substances in different phases. These authors' second deduction is that heterogeneous and homogeneous reactions may appear with or without irradiation. Various advanced oxidation technologies are characterised by heterogeneous (with/without irradiation) and homogeneous (with/ without irradiation), as shown in Figure 2.5.

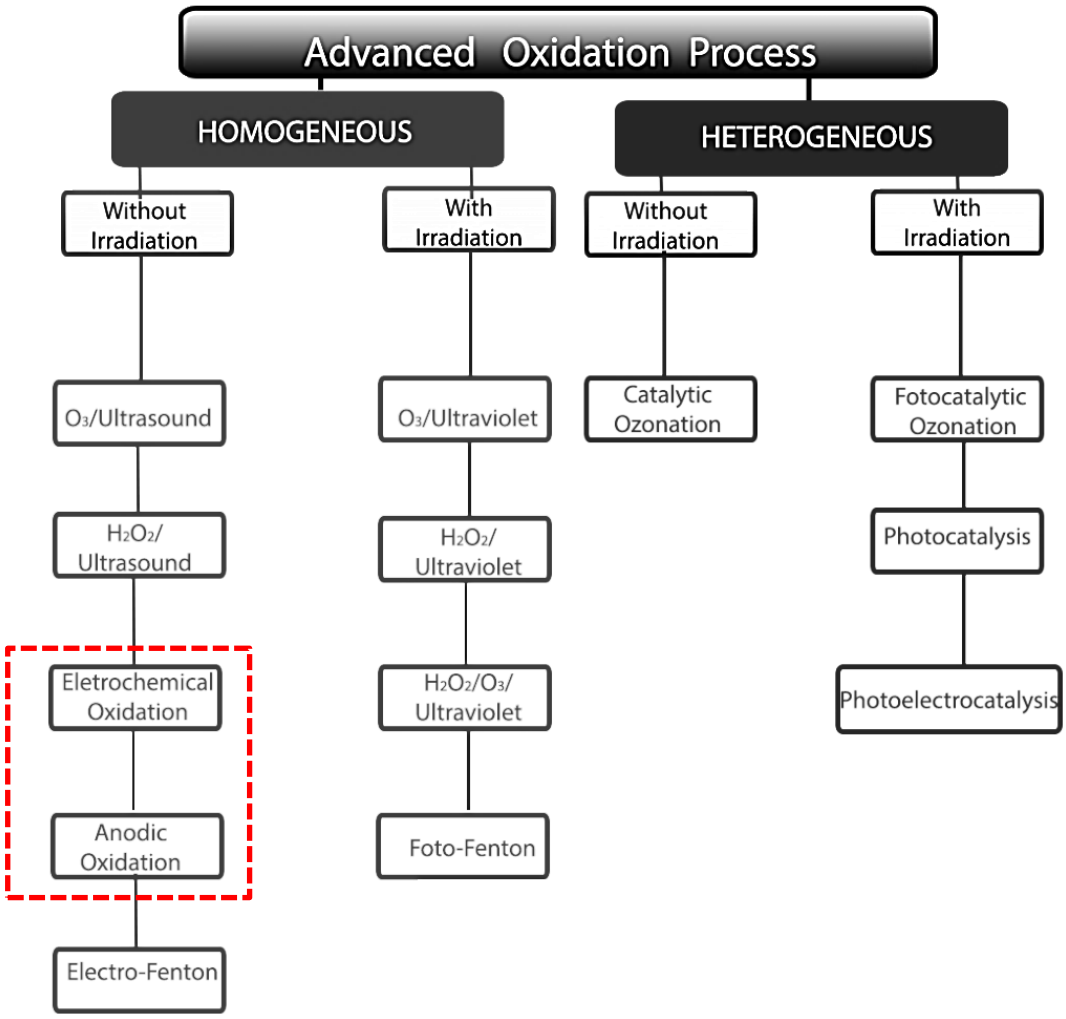

Figure 2.5: Advanced oxidation processes(Brugnera, de Araújo Souza and Zanoni., 2016).

2.5.2. Electrochemical Oxidation (EO)

Anodic or electrochemical oxidation (EO) is an advanced oxidation process (AOP) generally used to treat industrial effluent. Recent studies show that EO is used in industrial wastewater (García-Montoya et al., 2015)and municipal wastewater treatment (Babu et al., 2009; Rajab, Heim, et al., 2013). Secondary effluent ((Madikizela et al., 2020)contain pharmaceuticals that have become a global concern to the surface- and groundwater bodies.

EO systems generally consist of two electrodes (anode and cathode) and a power supply or electrolytic cell. The formation of oxidising species and degradation of contaminants occur with the addition of current/ energy supply and electrolyte. When complete minimisation is reached, water and carbon dioxide are released.

Advantages and Disadvantages of EO

There are numerous amounts of advantages that EO have over other technologies. Table 2.1 provides eight advantages some authors indicated.

Table 2.1: Advantages of EO.

Advantages	**Reference**
1. Environmental comparability	Peralta-Hernández et al. (2012); Radjenovic & Sedlak (2015); Rajab, Heim, et al. (2013)
2. Low Cost	Babu et al. (2009)
3. High effectiveness	Bagastyo et al. (2014)
4. No chemical additives	Radjenovic & Sedlak (2015)
5. No waste production	Radjenovic & Sedlak (2015)
6. Operation at ambient temperature and pressure	Heim et al. (2015)
7. Adaptable to other applications/ technologies	Babu et al. (2009)

It is noted that Radjenovic & Sedlak (2015) stated no waste is produced; however, it is also said that toxic by-products may form. The possibility of poisonous by-products refers to transformation products

that include pharmaceutical electrolysis. Research shows that the longer the EO process occurs, the by-products will also oxidise.

Table 2.2 shows two significant disadvantages that Radjenovic & Sedlak (2015) addressed, i.e. toxic by-products and high-energy consumption. The high consumption of energy can be lowered by combining low-cost biological processes (Martín et al., 2015) and RO (Zhou et al., 2011) with the EO process.

Table 2.2: Disadvantages of EO.

Disadvantages	**Reference**
1. High energy consumption	Radjenovic & Sedlak. (2015)
2. Toxic by-products	Radjenovic & Sedlak. (2015)

2.5.3. Direct- and indirect oxidation

Degeneration of contaminants such as pharmaceuticals using the EO technique is done with either:

Direct oxidation

The degradation of the pharmaceutical compound occurs directly over the anode (Peralta-Hernández et al., 2012)This happens through active oxygen on the surface of the anode or adsorbed hydroxide radicals ($°OH$). The following general equation describes direct oxidation.

$$M + H_2O \rightarrow M(°OH) + H^+ + e^- \qquad \text{(Peralta-Hernández et al., 2012)}$$

Equation 2.1

Where M is the adsorbed pollutant on the anode surface, after which degradation occurs through an anodic transfer reaction, this type of oxidation is called anodic- or direct oxidation as well as electrochemical incineration (Peralta-Hernández et al., 2012). The oxidation rate is determined based on the current density, pollutant diffusion rate and electrode activity (Babu et al., 2009).

Indirect oxidation

Degradation of compounds occurs in bulk solution through species generated in the electrode. The generation of common oxidants at the anode are Cl_2 , OH^* (Fenton reaction), hypochlorite, ozone and peroxodisulfate (Peralta-Hernández et al., 2012). The oxidation rate is determined based on the pH, diffusion rate for oxidants generated and temperature. Adding chloride salts (potassium, sodium, etc.) is required to increase the conductivity and generation of hypochlorite ions/ chlorine (Babu et al., 2009). However, indirect oxidation may also occur if chlorine radicals are adsorbed at the anode or active chlorine species (Hurwitz et al., 2014).

2.6. Electrodes

The efficiency of EO and the formation of by-products is dependent on the type of electrode used. There are different types of electrodes; however, the most researched electrodes for the anode are mixed metal oxide (MMO) electrodes, platinum electrodes and boron-doped diamond (BDD) electrodes

2.6.1. Mixed Metal Oxide (MMO) Electrodes

Mixed metal oxide (MMO) electrodes have been under investigation for the last decade. This type of electrode consists of a base material that is resistant to corrosion (e.g., titanium) and doped with metal oxides (e.g., $\boldsymbol{IrO_3}$). MMO electrodes are characterised to have active (e.g. $\boldsymbol{RuO_2}$) or nonactive (e.g. $\boldsymbol{SnO_2}$) anodes (Gherardini et al., 2001), where active anodes have a low over-potential for oxygen formation and non-active anodes have a high over-potential for oxygen formation. These electrodes are often used with a chloride electrolyte because of their limited ability to oxidise (Radjenovic et al., 2015). Below is a list of electrodes ranked for MMO or Dimensionally Stable Anode (DSA) material based on costs, stability and organic oxidation activity.

Table 2.3 MMO electrodes:

Electrode	Reference
IrO_3	Radjenovic et al. (2015)
RuO_2	
SnO_2	
PbO_2	
Ti/PbO_2	
$Ti/PdO - CO_3O_4$	
$Ti/RhO_x - TiO_2$	
$Ti/IrO_2Ta_2O_5$	
Ti/Pt	
$Ti/Pt - Ir$	
Ti coated with oxides of $Ru/Ir/Ta$	

2.6.2. Boron-Doped Diamond (BDD) Electrode

BDD anodes have high oxygen over-potential and are, therefore, suitable for direct oxidation.

Table 2. 4: Advantages of BDD electrode.

Advantages	Reference
1. High reactivity	Mordačíková et al. (2020)
1. High oxygen over-potential	
2. High chemical and corrosion stability	
3. Inert surface	
4. Low background current	
5. Wide potential window	

It has been proven that the high cost and energy consumption on a large-scale basis can be reduced by combining secondary treatment with EO.

Generation on BDD anode

Radjenovic et al. (2015) claim previous studies indicate that BDD ($^{\circ}OH$) have no spectroscopic evidence of the existence of free $^{\circ}OH$ radicals. Instead, at the BDD anode surface, $^{\circ}OH$ is formed because of the high oxygen over-potential. The following equation shows the formation of $^{\circ}OH$ at the anode.

$$BDD + H_2O \rightarrow BDD(^{\circ}OH) + H^+ + e^-$$

Equation 2.2

Generally, the BDD electrode's primary function is to oxidise organic contaminants. However, the anode produces ozone, H_2O_2, ferrate, peroxy dicarbonate with carbonate present, peroxy diphosphate with phosphate present and peroxy disulfate with sulphate ions present.

Substrates for BDD

The substrates for depositing the film of the BDD electrode include Si, Ti, Ta, W and Nb ((Mordačíková et al., 2020; Radjenovic & Sedlak, 2015).

2.7. Pharmaceuticals

Pharmaceutical residues in wastewater are classified as a threat to the environment and aquatic life. Baresel et al. (2015) explain that pharmaceuticals enter the environment through sewage treatment effluent. Treatment plants are generally not equipped to remove non-biodegradable dissolved compounds (Bagnis et al., 2018; Baresel et al., 2015). The following diagram shows alternative methods for pharmaceuticals to enter the environment.

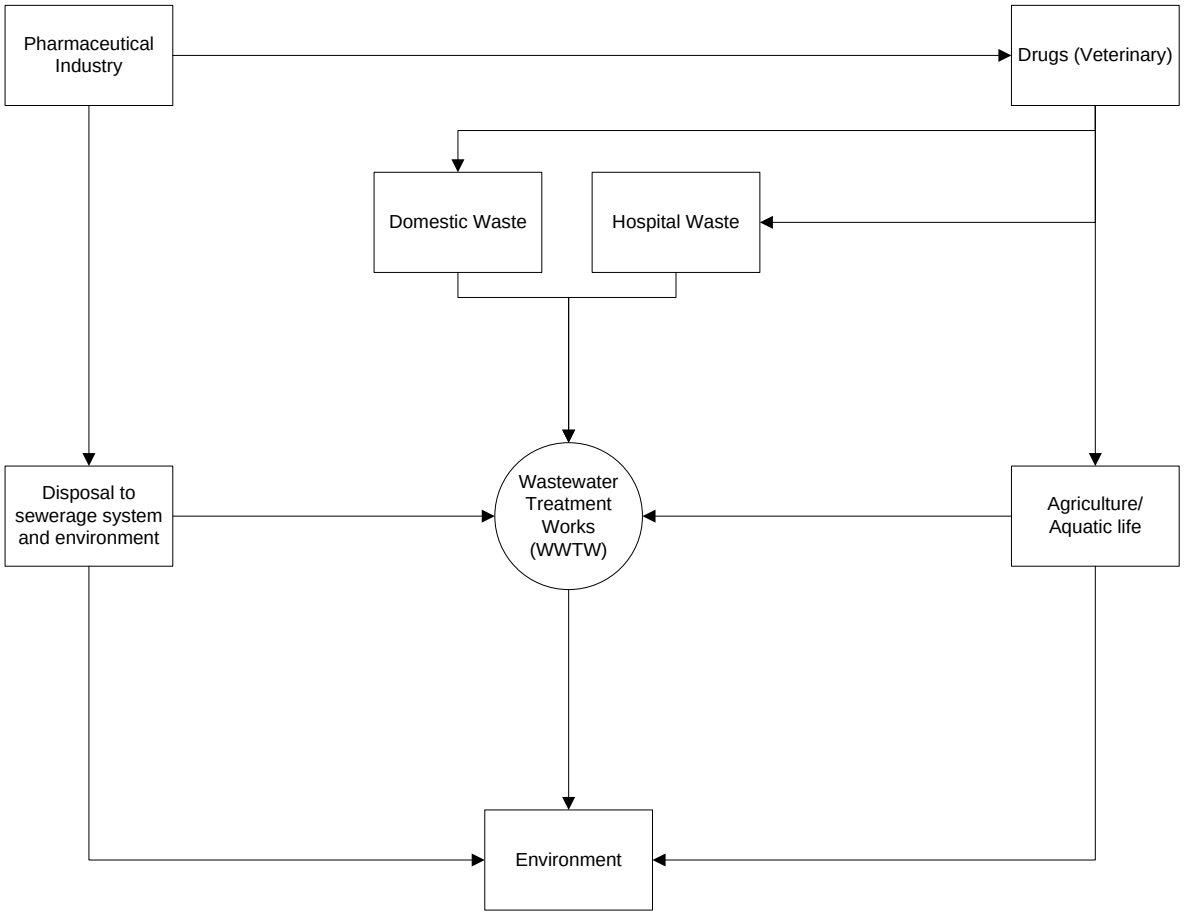

Figure 2.6: Schematic for pharmaceuticals entering the environment.

In South Africa, several studies on pharmaceuticals and the removal of pharmaceutical and personal care products (PPCPs), as well as endocrine-disrupting contaminants(EDCs) from wastewater, have been studied ((Archer et al., 2017; Aziz & Ojumu, 2020; Madikizela et al., 2020). Madikizela et al. (2018) reported various pharmaceuticals discovered in water masses (e.g. surface water) across South Africa. Therefore removal of these pharmaceuticals is needed

2.7.1. Impacts of pharmaceutical residue

Pharmaceutical residues in secondary effluent have an amplitude of negative impacts on the environment, animals and humans. Reportedly only long-term toxicity effects on aquatic life have been established, and no detection of the immediate toxicity effects of pharmaceuticals has been conveyed. However, more than one type of pharmaceutical in a water body may increase toxicity levels.(Rajab, Greco, et al., 2013).

2.7.2. Analytes

This research investigates the removal of three pharmaceuticals within a synthetic water matrix and real MBR secondary effluent. Diclofenac sodium (DCF), carbamazepine (CBZ), and ibuprofen (IBU) are the proposed pharmaceuticals because studies ((Hansen et al., 2016; Urtiaga et al., 2013; Verlicchi et al., 2012; Yao et al., 2018) have shown that residues of these pharmaceuticals are present in the WWTW secondary effluent.

Diclofenac (DCF)

When sludge undergoes treatment within the anoxic zone of the MBR, it partially degrades DCF, while acidic conditions with pH 4.4 increase the percentage removal. According to the literature, DCF depends not on the sludge retention time (SRT) but other operational factors. DCF is known as a nonsteroidal anti-inflammatory drug (NSAID) that reduces pain within the body.

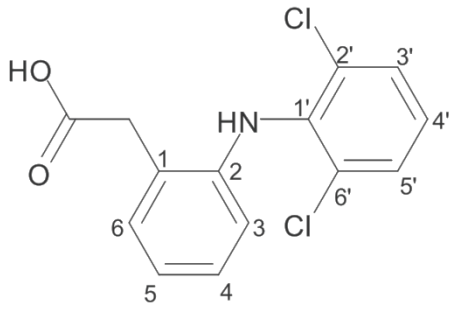

Figure 2.7: DCF structure.

Carbamazepine (CBZ)

CBZ is from the anti-epileptic group and is used to prevent seizures. CBZ is not dependent on the SRT and does not undergo degradation in any of the zones within the reactor of the MBR. In addition, acidic conditions (pH 4.4) do not significantly affect the % removal.

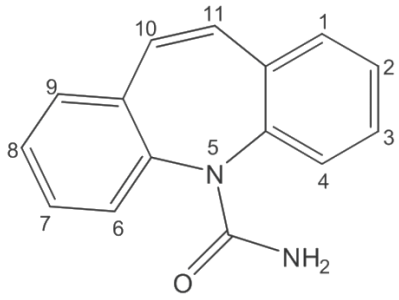

Figure 2.8: CBZ structure.

Ibuprofen (IBU)

IBU is also a form of the anti – epileptic group which prevents seizures.

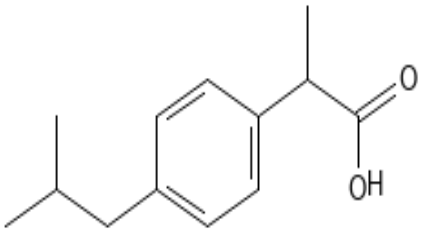

Figure 2.9: IBU structure.

2.7.3. Pharmaceutical Transformations (PTs)

Pharmaceutical transformations form during the degradation of pharmaceutical parent compounds. It is considered a primary concern since the TP's may be more harmful than the parent compounds (Rajab, Greco, et al., 2013).

Several studies (Bagastyo et al., 2014; Rajab, Greco, et al., 2013; Rajab, Heim, et al., 2013) indicate that PTs have a wide range of structural differences. Mohamad Rajab, Greco, et al. (2013) suggest that the type of degradation method and the composition of the water matrix significantly impact the number and structure of the TP's generated. When using AOP techniques, TP's are more "polar" and "smaller" than the parent compounds and may not have reference standards. Therefore, analysis is done using chromatographic techniques to obtain a comprehensive view of TP's produced (Rajab, Greco, et al., 2013).

The decrease in treatment time reduces energy consumption, while the increase in treatment time increases the removal efficiency of TP's. However, treatment time is indirectly proportional to the current density. Should the current density increase, the treatment time will decrease. Therefore, operational costs could also be reduced should a pharmaceutical's TP be deemed negligible. However, the hazardousness of TPs is unknown (Rajab, Heim, et al., 2013).

2.7.4. Pharmaceutical removal using EO treatment

Literature shows that BDD electrodes have shown excellent removal of pharmaceuticals (Rajab et al., 2013; da Silva et al., 2019; Mora- Gomez et al., 2020). The following equation calculates the % removal of pharmaceuticals in wastewater.

$$\frac{concentration\ of\ pharmaceutical\ in\ feed - concentration\ of\ pharmaceutical\ in\ effluent}{concentration\ of pharmaceutical\ in\ \ feed} \times 100$$

Equation 2.3

Table 2.5: Pharmaceutical removal

Pharmaceutical	Process	Initial concentration (mg / l)	Final concentration (mg/l)	% removal	Reference
Diclofenac (DCF)	EO	150	0	100	Coria et al. (2014)
		50	10.3	79.4	García-Montoya et al. (2015)
		50	8	84	Garcia- Montoya et al. (2015)
		50μM	0	100	Rajab et al. (2013)
		0.5	0.1	80	Loos et al. (2018)
Aniline		250	21.6	91.36	Benito et al. (2017)
		10	0	100	da Silva et al. (2018)
		100	49	51	Garcia- Montoya et al. (2015)
Sulfamethoxazole (SMX)		55.5μM	0	100	Rajab et al. (2013)
		0.5	0.1	80	Loos et al. (2018)
Carbamazepine (CBZ)		229.7	44.8	80.5	Álvarez-Torrellas et al. (2017)

2.8. Analysis Techniques

The most common and effective techniques for the analysis of pharmaceuticals are chromatographic techniques(Rajab, Greco, et al., 2013). These techniques are separation methods that can be used to separate compounds or solutes of a mixture.

Generally, solutes or compounds are placed between a mobile phase (liquid or gas) and a stationary phase (liquid or solid) with a continuous exchange of kinetic molecular motion between the phases. An origin or narrow zone occurs when a mixture of solutes is initiated into the process. The blend contains different species and is transported at different flow rates. The separation of the compounds or solutes occurs with both the moving fluid's driving force and the stationary phase's resistive force. One advantage of this separation method is that it can separate multicomponent chemical mixtures without extensive reference knowledge of the molecular compounds involved. A second advantage is that chromatography can detect molecular species ranging from tiny atoms (e.g. hydrogen) to large materials.

The most applied chromatography techniques that are used are:

a) Liquid chromatography (LC) - (Rajab, Greco, et al., 2013)
b) Gas chromatography (GC) - (Rajab, Greco, et al., 2013)
c) Ion exclusion chromatography (IC) - (Rajab, Greco, et al., 2013)

These analytical set-up techniques have produced innovative information about pharmaceutical compounds and their transformation products. Contrary to this, these techniques are highly time-consuming and require extensive resources. Alternatively, during the instance of compounds that have polarity on a larger scale, Mohamad Rajab, Greco, et al. (2013) suggest the following:

a) Hydrophilic interaction liquid chromatography (HILIC) - (Rajab, Greco, et al., 2013)
b) Reverse phase liquid chromatography (RPLC) - (Rajab, Greco, et al., 2013)
c) High-pressure liquid chromatography (HPLC) - (Rajab, Heim, et al., 2013)

Not only is the two methods more effective than LC, GC and IC, but combining both methods into one analytical set-up may provide fewer false negative results when the reference standards are unknown (Rajab, Greco, et al., 2013).

Mass spectrometers (MS) can produce high-accuracy results (Rajab, Greco, et al., 2013). Therefore MS will produce comprehensive results. The following types of MS were used in various studies:

a) Time of flight mass spectrometer (TOF-MS) -Mohamad Rajab, Greco, et al. (2013)
b) electrospray ionisation mass spectrometer(ESI – MS) - (Rajab, Heim, et al., 2013)
c) Gas chromatography-mass spectrometer (GC-MS) -(Togola & Budzinski, 2007)

As mentioned previously, chromatographic techniques, a combination of these techniques, produce a comprehensive analysis of pharmaceutical compounds. An example is Mohamad Rajab, Greco, et al. (2013) evaluation of "the feasibility and convenience on the serial coupling of RPLC and zwitterionic (ZIC-HILIC) with the time of flight mass spectrometer (TOF-MS) detection of TP's". The analysis was done using liquid chromatography (LC) combined with a mass spectrometer (MS) after the extraction of compounds using extracted ion chromatography (EIC). Another example is the GC coupling with an MS (GC – MS) for detecting and quantifying pharmaceutical compounds (Togola & Budzinski, 2007).

Chapter 3

Research Methodology

Chapter 3: Research Methodology

3. Introduction

This chapter comprises the experimental- and analytical procedures. A description of the instrumentation, equipment and materials utilised during each experimental run is included. All experiments were conducted at the Cape Peninsula University of Technology in Chemical Engineering Research Laboratory 1.18 in the Chemistry and Chemical Engineering Building.

3.1. Research Design

This thesis consisted of a quantitative design study while using an experimental approach. This project aimed to remove selected pharmaceuticals from municipal MBR secondary effluent through an Electrochemical Oxidation (EO) process. Select pharmaceuticals were monitored through Solid Phase Extraction (SPE) and Gas Chromatography-Mass Spectrometry (GC - MS). The EO system was optimised through Design Expert (DE) version 10.

3.2. Research Apparatus

The following glassware, equipment and materials were used during the experimental runs to collect data.

3.2.1. Glassware

All glassware was thoroughly washed and rinsed with deionised water, followed by a rinse with acetone. It was then placed in the autoclave between 120 – 140 °C for 45 minutes. The following glassware was used:

- The 4L glass beaker was used for feed sample preparation.
- The 3L glass beaker was used for the EO - treatment process.
- 500 ml glass bottles were used to store the effluent from the EO – treatment process.

3.2.2. Materials

The following chemicals were utilised:

Table 3.1: Chemicals utilised in research.

Compound	Chemical Formulae	Molecular Weight (Mw) (g/mol)
Ammonium phosphate	$(NH_4)_3PO_4$	149
Calcium sulphate	$CaSO_4$	136
Humic acid	$C_9H_9NO_6$	227
Magnesium sulphate heptahydrate	$MgSO_4 7H_2O$	120
Potassium chloride	KCl	75
Sodium bicarbonate	$NaHCO_3$	84
Sodium sulphite	Na_2SO_3	126
Carbemazepine (CBZ)	$C_{15}H_{12}N_2O$	236
Diclofenac sodium (DCF)	$C_{14}H_{10}Cl_2NNaO_2$	295
Ibuprofen (IBU)	$C_{13}H_{18}O_2$	206
Aspirin (ASP)	$C_9H_8O_4$	180
Dihexyl phthalate – 3,4,5,6-d_4	$C_{20}H_{30}O_4$	339

3.2.3. Equipment

The following equipment was utilised during the experimental runs and chemical analysis.

Photo 3.1: DO - meter.

DO – meter measures the dissolved oxygen every hour for 5 hours.

Photo 3.2: pH - meter.

The pH meter measures the pH every hour for 5 hours during experimental runs.

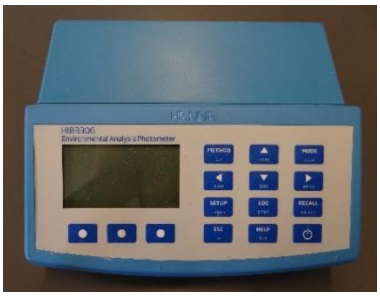

Photo 3.3: Multi - meter.

Multi – photometer measures ammonia and the water colour of the feed and effluent samples.

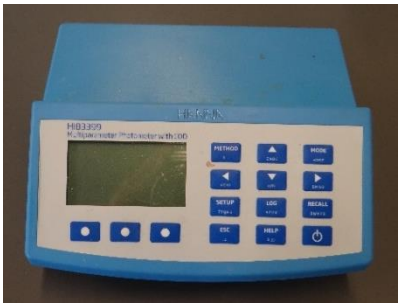

Photo 3.4: COD meter.

The COD meter measures the COD and sulphates in the feed and effluent samples.

Photo 3.5: TDS, EC and thermometer.

They were used for measuring the EC, TDS and temperature every 1 hour for 5 hours of the experimental runs.

3.3. Feed Preparation

The feed sample contains a synthetic water matrix modified to include similar characteristics to municipal membrane bioreactor (MBR) secondary effluent. The composition of the synthetic feed sample contains humic acid (4.2 mg/l), ammonium phosphate (60 mg/l), potassium chloride (4 mg/l), sodium bicarbonate (96 mg/l), magnesium sulphate heptahydrate (60 mg/l) and calcium sulphate (60 mg/l). The feed is prepared in a 4L glass reactor. Pharmaceuticals, i.e., carbamazepine (CBZ), diclofenac sodium (DCF) and ibuprofen (IBU) with a constant concentration of 900 µg/l each, are diluted with 0.1µL of methanol and added to the feed. With the increase in the conductivity of the synthetic feed, sodium chloride is added at different concentrations ranging from 0.02M – 0.08M, as specified in table 8. A magnetic bar is inserted in the reactor containing the 4L feed solution and placed onto the magnetic stirrer hotplate at 360rpm with an initial temperature of 25°C. The initial pH is 4 with 0,5M sulfuric acid and 0.125M sodium hydroxide. The feed solution is continuously stirred to obtain a uniform mixing. 1L of sample is removed from the reactor for feed analysis, while 3L is utilized for treatment.

3.4. Electrode Preparation

Sample contamination prevention starts with the decontamination of the electrodes before each experimental run. Initially, electrodes are rinsed and soaked in a 1L beaker of 0.5M sulfuric acid solution for 5 minutes to remove impurities from the electrode surface area. It is then rinsed with deionised water for 1 minute and air-dried. After each experimental run, electrodes are washed and rinsed before being air-dried.

3.5. Electrochemical Oxidation (EO)

EO treatment aims to reduce organic pollutants in municipal MBR secondary effluent effectively. The laboratory-scale EO – process contains a constant volume of 3L feed solution with pH 4. The solution is placed in a glass reactor at a continuous stirring rate of 360 rpm. Two types of electrodes, i.e., Ti/Pt or $Ti/IrO_2Ta_2O_5$, are used. Both types have a size of 100 x 100 x 1mm thickness and a surface area of 200 cm^2. Two electrodes (Ti/Pt or $Ti/IrO_2Ta_2O_5$) are used as an anode and cathode during an experimental run with an electrode spacing of 1cm apart inside the reactor. A direct current (DC) power supply with a maximum of 25V and a set current ranging between 1 – 2A is connected to the electrodes. A schematic diagram and photo of the experimental set-up are shown in Figure 3.1 and Photo 3.6.

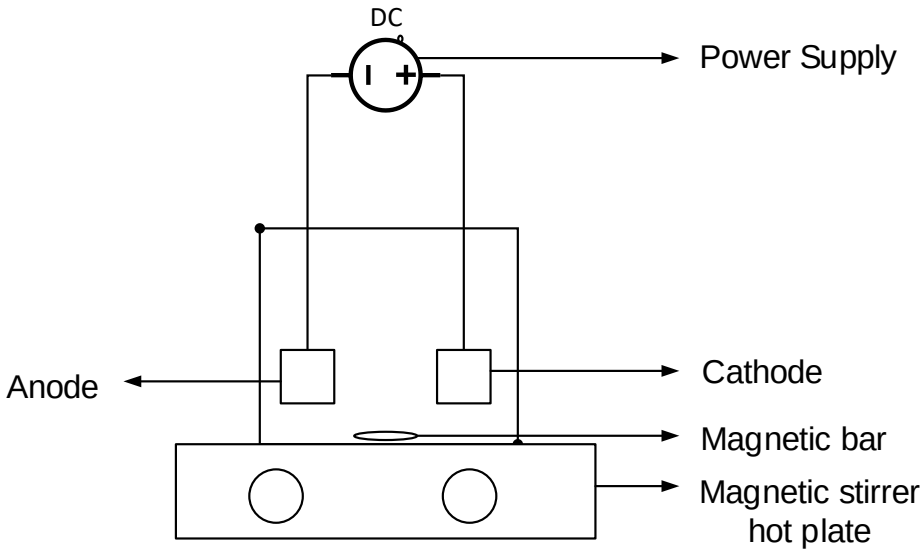

Figure 3.1: Experimental Set - up

Photo 3.6: Electrochemical oxidation batch reaction.

Based on the literature, experimental runs ranging from 1 – 5hrs showed significant results for Ti/Pt electrodes. Therefore, electrolysis time for all EO experimental runs was 5 hours to receive maximum removal. When investigating the effect of current density, the current was maintained at the desired range of 5 to 10 mA/cm^2. The parameters used were current density (5, 7.5 and 10mA/cm^2), NaCl electrolyte concentration (0.02, 0.05 and 0.08) and the comparison between the two electrodes (Ti/Pt or Ti/$IrO_2Ta_2O_5$). All Experimental runs were performed in duplication with statistical analysis for validation.

3.6. Inorganic Analysis

Feed and effluent samples are analyzed for inorganic pollutants, i.e., ammonia-, nitrites-, Sulphates-, Chlorine-free (Cl_F)-, chlorine total (Cl_T)-, colour-, and Chemical Oxygen Demand (COD). Respective chemical reagents are used to determine the quantity of the inorganic pollutants following the procedures provided by the Hanna Instruments (Pty) Ltd manuals.

3.7. Chemical Analysis

The chemical analysis done during this research is solid phase extraction (SPE) by using 200ml of feed and effluent, followed by a gas chromatography-mass spectrometer (GC-MS) to determine the concentration of the pharmaceuticals removed.

3.7.1. Solid Phase Extraction (SPE)

Photo 3.7 illustrates the SPE set –up. SPE is done to extract a concentrated sample containing IBU, DCF and CBZ. The extraction is done as follows:

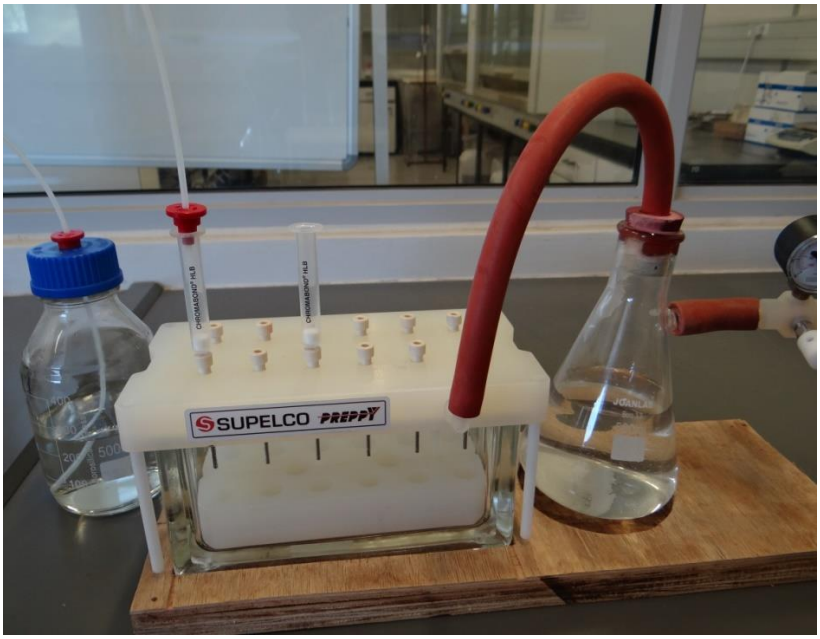

Photo 3.7: SPE set - up.

A. Pre- SPE

1. 200ml of the sample is collected and filtered under vacuum using a glass fibre filter.
2. Add internal standard with a standard concentration of 1µl of Dihexyl phthalate – 3,4,5,6-d_4 (2mg/ml) into the filtered sample.
3. Adjust the pH of the sample to 2.

B. Condition

4. Use 3ml to condition cartridge Chromabond $HLB_{60mg/3ml}$ at a 50:50 ratio of acetone and ethyl acetate.
5. Add 3ml Methanol.
6. Add 3ml of water in an acidic medium (pH 2) to the Chromabond $HLB_{60mg/3ml}$ cartridge
7. Use a vacuum (12 – 15ml/min) when adding 200ml water samples to allocated cartridges.
8. Allow samples to filter through the cartridge until samples are depleted.

C. Washing

9. Use 3ml of water and methanol at a ratio of 60:40
10. Leave cartridge under vacuum for drying at 1hr.

D. Elution

11. Filter 9ml of ethyl acetate and acetone at a 50:50 ratio through the cartridge into a tube.
12. Insert the closed tube into a vortex for 10 minutes at 5000 rpm.
13. Remove the sample from the vortex.
14. While drying under nitrogen gas, place samples in a heating block at 42°C
15. Keep samples in an upright position at all times.
16. The dry sample under nitrogen gas

E. Derivatization

17. Re-dissolve sample in 80 µl ethyl acetate.
18. Add 30µl of MSTFA for acidic compounds
19. Incubate samples for 35min at 65°C

The sample is transferred to a GC-MS for further analysis.

3.7.2. Gas Chromatography-Mass Spectrometry (GC – MS)

The gas chromatography was done using a scan and selected – ion – monitoring (SIM) method. The full scan mode is utilized to detect the mass spectrum of each compound in the sample. The SIM method is primarily used for the quantification of pharmaceuticals. The retention times are determined using the mass-to-charge (m/z) ratios and act as a limitation of detection for qualitative measurements. Table 3.2 provides the GC – MS method conditions, while Table 3.3 show the m/z ratios and retention time.

Table 3.2: GC - MS scan mode method conditions

Parameter	**Condition**
Mode	MS1 scan mode
Agilent	7890A GC system 7000C GC/MS triple quad
Column	J&W 122-5532G DB 5ms + DG
Temperature setting	Inlet: 240°C Transfer line: 280°C Ion source: 230°C
Electron–impact (EI) mode	70eV
Injection volume	1°µl° (autosampler)
Oven temperature gradient	120°C: hold for 1 min 120 – 250°C: 12°C/min, hold 4 min 250 – 300°C: 20°C/min
Total run time	18.333 min
Solvent delay	7 min
Post run time	9.06min
Split ratio	14.1° (15 times diluted)
Constant ultrapure helium flow rate (column)	1 ml/min
Injector pressure	15.6psi
Gain factor	5

Table 3.3: GC-MS SIM method.

Parameter	m/z for SIM	Resolution dwell (ms)
Diclofenac	214	100
Carbamazepine	193	130
ibuprofen	160	70
Dihexyl phthalate – 3,4,5,6-d_4	153	40

SIM method is done at two cycles/sec and 506,7°ms/cycle.

3.7.3.

3.7.3. Pharmaceutical Quantification

To quantify pharmaceuticals, i.e. IBU, DCF and CBZ, standard curves of each pharmaceutical are designed. The compound method inserts 6 injection points with corresponding peak areas of each pharmaceutical and the internal standard, Dihexyl phthalate – 3,4,5,6-d_4. The data in table B2 in appendix B is normalized using the following equation;

$$Normalization\ of\ pharmaceutical = \frac{pharmaceutical\ peak\ area}{internal\ standard\ peak\ area}$$

Equation 3.1

Figures C1, C2 and C3 show the standard curve used to determine the concentration of each pharmaceutical after 5 hours of electrolysis.

C1 illustrates the standard curve for IBU. The straight line equation was calculated to be:

$$y_{IBU} = 0{,}0352x - 0.008$$

Equation 3.2

The corresponding R^2 value is found to be 0.9947.

.

C2 illustrates the standard curve for CBZ. The straight line equation was calculated to be:

$$y_{CBZ} = 0{,}1252x - 0{,}0352$$

Equation 3.3

The corresponding R^2 value is found to be 0,9942.

C3 illustrates the standard curve for DCF. The straight line equation was calculated to be:

$$y_{DCF} = 0{,}0259x - 0{,}0089$$

Equation 3.4

The corresponding R^2 value is found to be 0.9969.

3.8. Design of Experiments

The experiments were designed using Design Expert software version 10.0. Response Surface Methodology (RSM) and Central Composite design (CCD) were employed to generate 36 experimental runs. The factorial design is illustrated in Table 3.4. The electrode type is depicted under categorical factors: either electrode Ti/$IrO_2Ta_2O_5$ and Ti/Pt.

Table 3.4: Factorial Design of experiments.

	Name	Units	Low	Middle	High
A	electrolyte	M	0.02	0.05	0.08
B	Current density	mA/cm^2	5	7.5	10
C	Electrode	-	-	-	-

Table 3.5 describes all 18 random experimental runs, including duplicates making it 36 runs.

Table 3.5: Experimental runs and duplicates.

Experimental run	Electrolyte concentration (M)	Current Density (mA/cm^2)	Electrode
1	0,08	7,5	$IrO_2Ta_2O_5$
2	0,08	7,5	$IrO_2Ta_2O_5$
3	0,08	5	$IrO_2Ta_2O_5$
4	**0,08**	**5**	**$IrO_2Ta_2O_6$**
5	0,08	10	$IrO_2Ta_2O_5$
6	0,08	10	$IrO_2Ta_2O_5$
7	0,02	5	$IrO_2Ta_2O_5$
8	0,02	5	$IrO_2Ta_2O_5$
9	0,02	5	Pt
10	0,02	5	Pt
11	0,02	7,5	$IrO_2Ta_2O_5$
12	0,02	7,5	Pt
13	0,02	7,5	Pt
14	0,02	10	Pt

15	0,02	7,5	$IrO_2Ta_2O_5$
16	0,02	10	Pt
17	0,05	5	Pt
18	0,02	10	$IrO_2Ta_2O_5$
19	0,02	10	$IrO_2Ta_2O_5$
20	0,05	5	Pt
21	0,05	7,5	Pt
22	0,05	5	$IrO_2Ta_2O_5$
23	0,05	7,5	Pt
24	0,05	10	Pt
25	0,05	5	$IrO_2Ta_2O_5$
26	0,05	10	Pt
27	0,05	7,5	$IrO_2Ta_2O_5$
28	0,08	5	Pt
29	0,05	7,5	$IrO_2Ta_2O_5$
30	0,08	5	Pt
31	0,05	10	$IrO_2Ta_2O_5$
32	0,08	7,5	Pt
33	0,05	10	$IrO_2Ta_2O_5$
34	0,08	7,5	Pt
35	0,08	10	Pt
36	0,08	10	Pt

Table 3.6 is used to conduct ANOVA, regression and individual model coefficients using the RSM design.

Chapter 4

Results and Discussion

Chapter 4: Results and Discussion

4.1. Introduction

This chapter illustrates the results of removing pollutants from municipal MBR secondary effluent using a laboratory-scale EO treatment. The significant pollutants were COD, Inorganic (ammonia) - and organic (CBZ, DCF & IBU).

The results are represented under three major categories:

I. Chemical oxygen demand
II. Inorganic
III. Chemical

4.2. COD Removal

The COD is measured before and after 5 hours of electrolysis in a batch electrochemical oxidation reactor at pH 4. The COD spectrometer supplied by Hanna Instruments was used to analyse the COD concentration. Figure 4.1 illustrates the % COD removed versus the initial COD concentration. Experiment 17 (7.5 mA/cm^2; 0.08M NaCl) demonstrates 86% as the highest COD removal, while experiment 14 (7.5 mA/cm^2; 0.05M NaCl) shows 9.09% as the lowest COD % removal.
Figure 4.2 indicates the COD % removal at various experimental conditions, where a description of the COD % removal with the corresponding current densities and electrolyte (NaCl) concentrations for each of the 18 experimental runs.

Figure 4.1 and 4.2 illustrates the effect of NaCl concentration and current density on the COD % removal. It is noted that experiments 2, 16, 17 and 18 have a COD removal of above 66% with 0.08M NaCl electrolyte concentration. It can be observed that an increased NaCl concentration increases the removal of COD. In terms of electrodes, experiments 17 (Ti /Pt anode) and 4 (Ti/IrO2Ta2O5 anode) at 0.08M and 0.02M NaCl, respectively, have the highest COD removal. In contrast to this, experiment 14 is found to have the lowest COD removal of 9.09% (Ti/Pt) with 0.05M NaCl and a current density of 7.5 mA/cm2. Experiment 1, with COD removal of 14.17% (Ti/IrO2Ta2O5 anode), has the second lowest COD removal at 0.08M NaCl and 7.5mA/cm2. Based on the results, higher COD removal percentages are found at lower current densities.

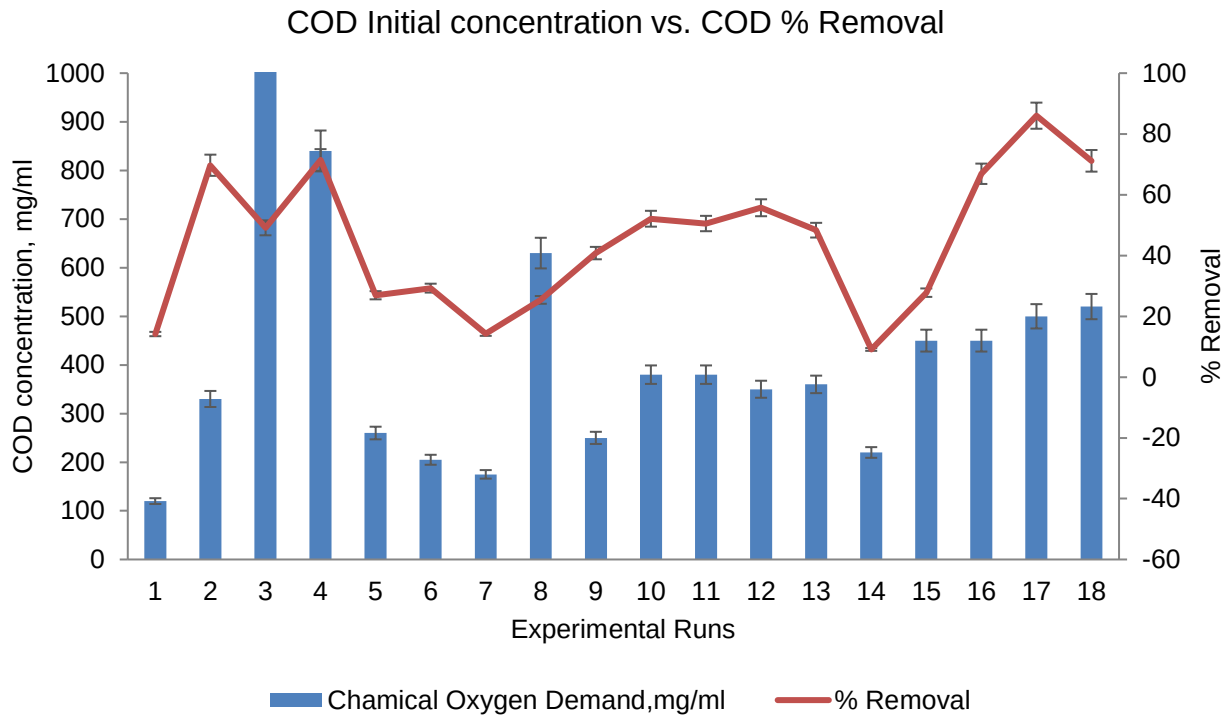

Figure 4.1: COD initial vs COD % removal.

Furthermore, the literature shows COD removal is due to direct and indirect oxidation. Direct oxidation occurs on the surface of the electrode, where products of the organic pollutants are oxidised and released into the bulk solution (Peralta-Hernández et al., 2012). Indirect oxidation occurs in the presence of an electrolyte. The electrolyte will react with the organic pollutants in the bulk solution and oxidises. This study comprises NaCl as an electrolyte ranging from 0.02M - 0.08M concentration

Hydrogen production occurs at the cathode and forms H_2O_2. In theory, the higher the applied current, the more hydrogen bubbles will be produced, resulting in a higher mixing rate (Benito et al., 2017). This also explains why Pt/Ti obtained a higher COD removal than Ti/ $IrO_2Ta_2O_5$. Dao et al. (2020) study also found that the Pt electrode performs better than the Ti/ IrO_2 electrodes. Dao et al. (2020) further state that the pH significantly affects the type of chloro – species forming. Since all experiments start at an initial pH of 4, the pH is not a parameter considered for the effect of COD. However, research indicates that an acidic medium produces a better COD % removal for EO systems in wastewater treatment. This is mainly due to the formation of chlorine, the most potent oxidant in chlorine-treated wastewater. Since both anodes have a NaCl concentration of 0.08M, illustrated in Table 4.1 as the highest COD % removal, it can be concluded that the NaCl concentration was sufficient to remove COD.

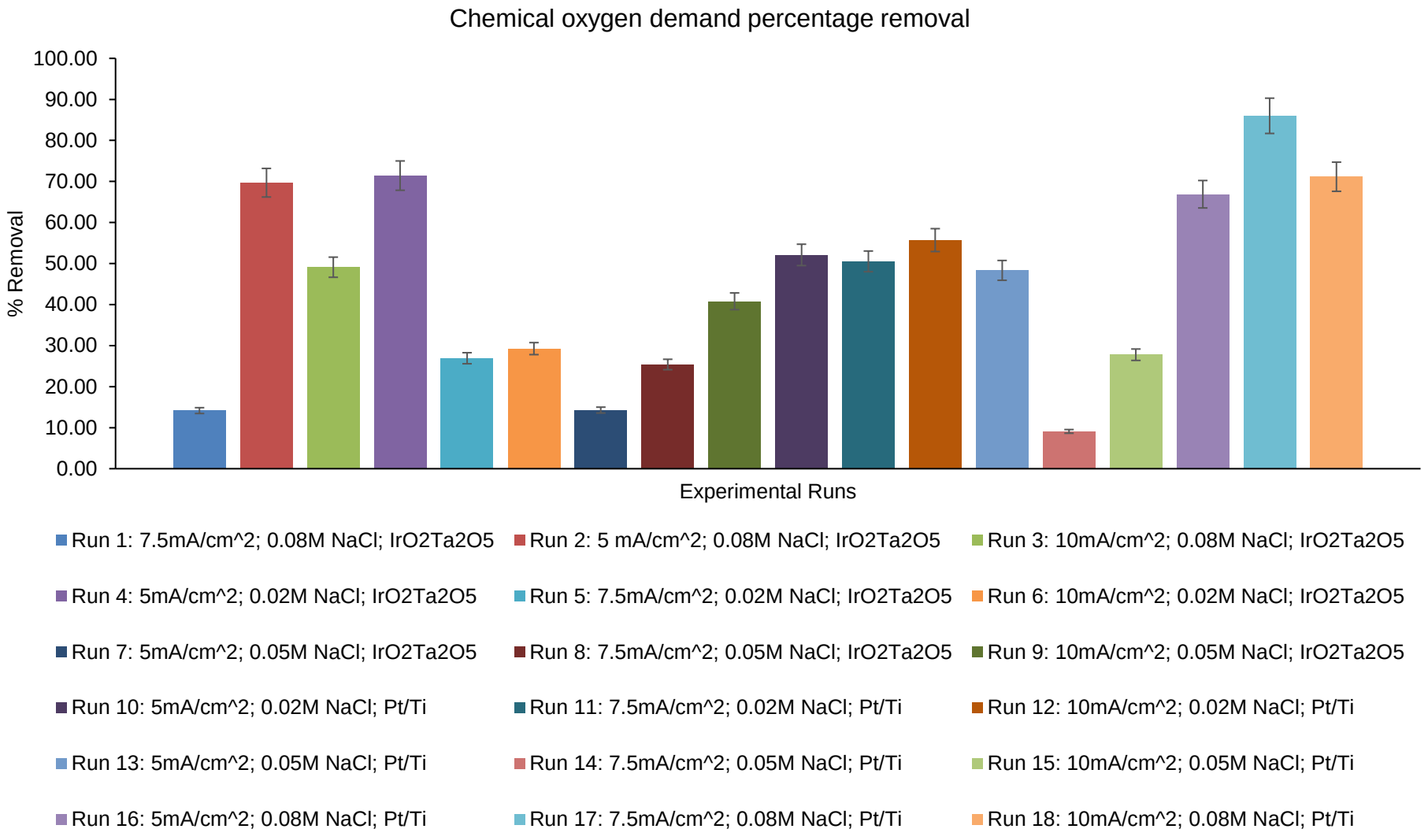

Figure 4.2: COD % removed.

Table 4.1 is a summary of the COD results in comparison with the current density (J) and electrolyte concentration. At a current density of 10 mA/cm^{2,} experimental runs 3, 6, 9, 12, 15 and 18 have a COD removal above 27%, with the highest at 71.15 (Ti/Pt; 0.08M NaCl). This confirms that increasing current density may increase the COD % removal.

Table 4.1 clearly shows the anode significantly affects the %COD removed. Ti/Pt have a higher oxidation potential than Ti/$IrO_2Ta_2O_5$ (Patel et al., 2013). This statement supports the data in Table 4.1, where the highest COD removal of Ti/Pt and Ti/ $IrO_2Ta_2O_5$ is 86% (7.5mA/cm^2; 0.08M NaCl) and 71.43% (5mA/cm^2; 0.02M NaCl) respectively. The current may affect the COD removal percentage since an increase in current density promotes the % COD removal. This may lead to higher energy consumption because current density increases energy consumption, as seen in Figure 4.8.

Table 4.1: COD results tabulated.

Current density (J) (mA/cm^2)	**Experimental Runs**	**Electrolyte (NaCl) (M)**	**Electrode**	**COD Removal (%)**
5	**2**	**0,08**	**Ti/ $IrO_2Ta_2O_5$**	**69,70**
	4	**0,02**	**Ti/ $IrO_2Ta_2O_5$**	**71,43**
	7	0,05	Ti/ $IrO_2Ta_2O_5$	14,29
	10	0,02	Ti/Pt	52,11
	13	0,05	Ti/Pt	48,33
	16	0,08	Ti/Pt	66,89
7,5	1	0,08	Ti/ $IrO_2Ta_2O_5$	14,17
	5	0,02	Ti/ $IrO_2Ta_2O_5$	26,92
	17	**0,08**	**Ti/Pt**	**86,00**
	14	0,05	Ti/Pt	9,09
	8	0,05	Ti/ $IrO_2Ta_2O_5$	25,40
	11	0,02	Ti/Pt	50,53
10	12	0,02	Ti/Pt	55,71
	3	0,08	Ti/ $IrO_2Ta_2O_5$	49,11
	9	0,05	Ti/ $IrO_2Ta_2O_5$	40,80
	15	0,05	Ti/Pt	27,78
	6	0,02	Ti/ $IrO_2Ta_2O_5$	29,27
	18	**0,08**	**Ti/Pt**	**71,15**

3.3. Inorganic Analysis

The inorganic analysis includes the removal of ammonia and colour pollutants utilizing the EO treatment process.

4.3.1. Ammonia Removal

High levels of ammonia in effluent wastewater are harmful to the environment. Madikizela et al. (2020) indicate that electrochemical oxidation assists with removing organic pollutants. Table 4.2 summarises the results obtained during the EO treatment process.

Experimental runs 2 and 3 (Table 4.2) at current densities 5 and 10mA/cm^2 performed well with 100 and 99% ammonia removal, respectively. Both had the same electrolyte concentration of 0.08M NaCl and Ti/$IrO_2Ta_2O_5$ electrode. The highest ammonia % removal for Ti/Pt was 80 at 0.05M and 10mA/$cm^{2,}$ while the lowest removal was 16 at a current density and electrolyte concentration of 10mA/cm^2 and 0.02M NaCl, respectively. Ammonia removal may be due to the chlorine salt, which increases the conductivity of the EO process. This is supported by Ghazouani et al. (2016), who found that the ammonia oxidises at the anode due to active chloro - species. From the results observed, it can be stated that the current density significantly impacts ammonia removal. The highest reduction was found at the lowest current density. Ensano et al. (2017) also found that the highest ammonia removal is at the lowest current density (0.3mA/cm^2; 26%). Table 4.2 indicates that NH_3, NH^{4+} and NH_3 - N significantly decreased with the EO – treatment process.

Table 4.2: Ammonia removal.

Current density	Electrode	Electrolyte (NaCl)	Experimental Run	% removal		
mA/cm²		**M**		**NH_3-N**	**NH_3**	**NH^{4+}**
5	Ti/ $IrO_2Ta_2O_5$	0,08	2	100,00 (45.05)	100,00 (44.04)	100,00 (44.99)
	Ti/ $IrO_2Ta_2O_5$	**0,02**	**4**	**35,91 (0.18)**	**35,89 (0.22)**	**35,97 (0.21)**
	Ti/ $IrO_2Ta_2O_5$	0,05	7	98,64 (0.19)	98,63 (0.23)	98,59 (0.22)
	Ti/Pt	0,02	10	35,34 (2.32)	35,27 (2.33)	35,28 (2.36)
	Ti/Pt	0,05	13	75,43 (1.83)	75,45 (1.83)	75,50 (1.77)
	Ti/Pt	**0,08**	**16**	**60,22 (11.10)**	**60,18 (11.07)**	**60,00 (11.12)**
7,5	I Ti/ $IrO_2Ta_2O_5$	0,08	1	35,59 (10.04)	35,62 (9.98)	35,63 (9.96)
	Ti/ $IrO_2Ta_2O_5$	**0,02**	**5**	**59,730 (0.32)**	**59,73 (0.27)**	**59,72 (0.33)**
	Ti/ $IrO_2Ta_2O_5$	0,05	8	99,15 (0.26)	99,19 (0.31)	99,12 (0.289)
	Ti/Pt	0,02	11	39,64 (45.44)	39,66 (45.54)	39,59 (45.47)
	Ti/Pt	0,05	14	59,15 (3.14)	59,16 (3.17)	59,20 (3.18)
	Ti/Pt	**0,08**	**17**	**66,22 (12.63)**	**65,56 (12.26)**	**65,26 (12.23)**
10	Ti/ $IrO_2Ta_2O_5$	**0,08**	**3**	**99,46 (14.84)**	**99,45 (14.86)**	**99,48 (14.91)**
	Ti/ $IrO_2Ta_2O_5$	0,02	6	90,63 (15.36)	90,69 (15.30)	90,70 (15.38)
	Ti/ $IrO_2Ta_2O_5$	0,05	9	99,31 (17.03)	99,32 (17.04)	99,35 (16.94)
	Ti/Pt	0,02	12	15,85 (9.79)	16,00 (12.45)	16,04 (6.46)
	Ti/Pt	0,05	15	80,28 (2.79)	80,35 (2.16)	80,33 (1.95)
	Ti/Pt	**0,08**	**18**	**74,51 (3.92)**	**75,00 (4.34)**	**74,81 (4.28)**

4.3.2. Colour Removal

Table 4.3 illustrates the colour removal for experimental runs in this study. At the current density of 10 mA/cm^{2,} the colour removal for experimental runs 3 (0.08M NaCl; Ti/ $IrO_2Ta_2O_5$); 6 (0.02M NaCl; Ti/ $IrO_2Ta_2O_5$); 9 (0.05M NaCl; Ti/ $IrO_2Ta_2O_5$) and 15 (0.05M NaCl; Ti/Pt) are above 80%. Ti/ $IrO_2Ta_2O_5$ have the highest removal of 100% (0.08M NaCl; 5 mA/cm^2) while Ti/Pt achieved maximum colour removal at 5mA/cm^2 of 75.43% (0.05M NaCl). The lowest colour removal of 15.85% (Ti/Pt) is at a current density of 10 mA/cm^2 and an electrolyte concentration of 0.02M NaCl.

Based on the results, it is a clear indication that an increase in the electrolyte concentration increases the removal of colour. This is supported by Sahu (2019) found that colour removal increased with an increase in the electrolyte. This may be due to the rise of electrical conductivity. Therefore, the electrolyte was sufficient to remove colour because the NaCl concentration varied from 0.02 – 0.08M. The initial pH of the EO treatment was 4, an acidic medium. This may also be the reason for the excellent removal of colour. Literature indicates that pH 4 is a suitable medium for removing colour. Umar et al. (2015) found colour removal of 80 - 84% at pH 4 and pH 5. Further studies (Sahu, 2019) show that as the pH increases to 6, the rate of colour removal decreases. Table 4.3 indicates that the salt concentration, current density and the type of anode impact the removal of colour.

Table 4.3: % Colour removal.

Current Density mA/cm²	**Electrode**	**Electrolyte (NaCl) M**	**Experimental Run**	**% Colour removal**
5	**Ti/ $IrO_2Ta_2O_5$**	**0,08**	**2**	**100,00 (23.15)**
	Ti/ $IrO_2Ta_2O_5$	0,02	4	35,91 (0.55)
	Ti/ $IrO_2Ta_2O_5$	0,05	7	98,64 (13.12)
	Ti/Pt	0,02	10	35,34 (12.93)
	Ti/Pt	**0,05**	**13**	**75,43 (9.09)**
	Ti/Pt	0,08	16	60,22 (2.37)
7,5	I Ti/ $IrO_2Ta_2O_5$	0,08	1	35,59 (9.40)
	Ti/ $IrO_2Ta_2O_5$	0,02	5	59,730 (3.88)
	Ti/ $IrO_2Ta_2O_5$	0,05	8	99,15 (17.52)
	Ti/Pt	0,02	11	39,64 (10.51)
	Ti/Pt	0,05	14	59,15 (55.59)
	Ti/Pt	0,08	17	66,22 (14.28)
10	Ti/ $IrO_2Ta_2O_5$	0,08	3	99,46 (20.80)
	Ti/ $IrO_2Ta_2O_5$	0,02	6	90,63 (12.96)
	Ti/ $IrO_2Ta_2O_5$	0,05	9	99,31 (16.11)
	Ti/Pt	0,02	12	15,85 (7.42)
	Ti/Pt	0,05	15	80,28 (24.85)
	Ti/Pt	0,08	18	74,51 (2.31)

3.4. Chemical Analysis

Three pharmaceuticals (IBU, DCF and CBZ) were spiked with a concentration of 900µg/l into 3 litres of synthetic municipal MBR secondary effluent. A total of 5 hours were used for each experimental run, and electrolysis was done using an electrochemical oxidation (EO) batch reactor system. Two types of anodes were compared, i.e. Ti/Pt and $Ti/IrO_2Ta_2O_5$.

3.4.1. Pharmaceutical removal using $Ti/ IrO_2Ta_2O_5$ Anode

Figures 4.3 and 4.4 illustrates the % removal of pharmaceuticals using a $Ti/IrO_2Ta_2O_5$ anode during EO - treatment.

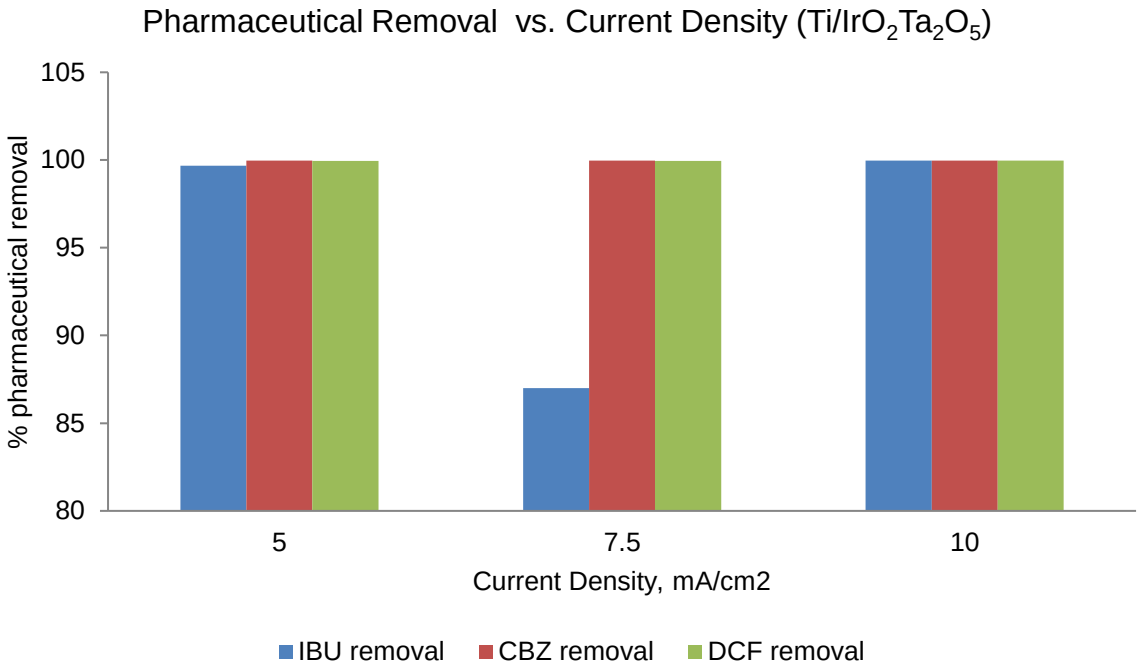

Figure 4.3: Pharmaceutical removal vs current density ($Ti/IrO_2Ta_2O_5$).

The experimental runs 3, 4 and 5 are illustrated in Figure 4.3. This is based on the COD results shown in Figure 4.1. These specific experiments produced the highest % COD removal at currents 5, 7.5 and 10 mA/cm^2 ($Ti/IrO_2Ta_2O_5$ electrode). At the current density of $5mA/cm^2$ (experimental run 4), CBZ, DCF and IBU have a removal rate of 99.96%, 99.95% and 99.67%, respectively. While at 10 $mA/cm^{2,}$ CBZ, DCF and IBU achieved optimum removal of 99.96%, 99.96% and 99.95% (experimental run 3).

CBZ and DCF are consistent with a reduction of ±99%; however, in Figure 4.3, IBU % removal presents a significant drop from 99% to 87% at the current density of 7.5mA/cm^2.

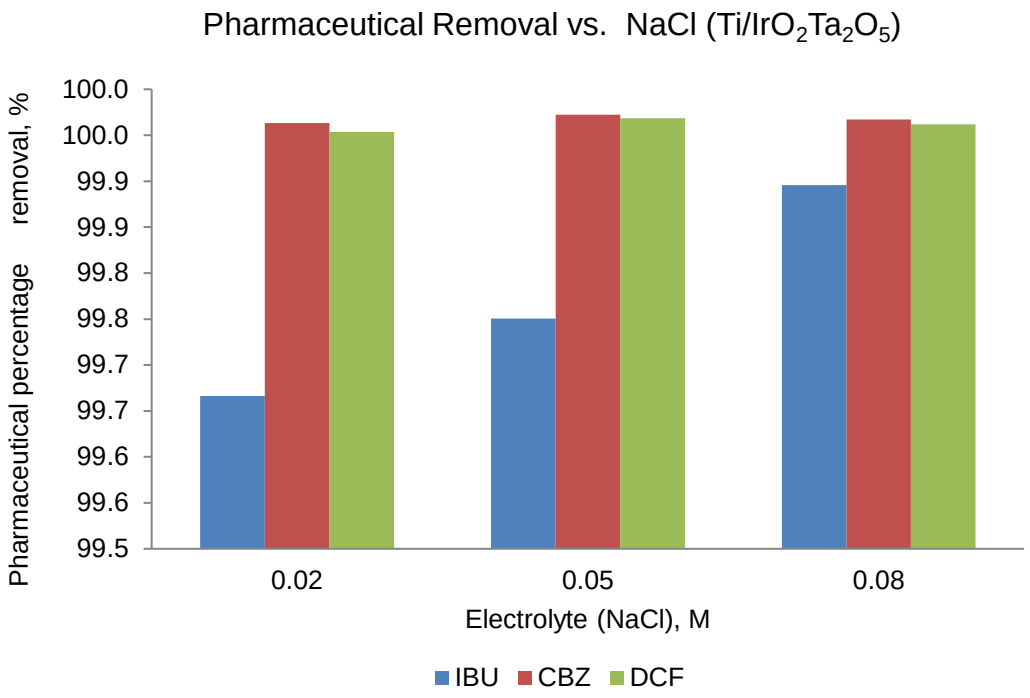

Figure 4.4: Pharmaceutical removal vs electrolyte (Ti/$IrO_2Ta_2O_5$).

The experimental runs 2,4, and 9 are illustrated in Figure 4.4 and are based on the COD results where the highest COD % removal at NaCl concentrations 0.02, 0.05 and 0.08M for the Ti/$IrO_2Ta_2O_5$ electrode are shown. In experimental run 4, at NaCl concentration 0.02M (Figure 4.4), CBZ experienced the highest removal rate of 99.96%, followed by DCF at 99.95% and IBU at 99.67%. During experimental run 9, at 0.05M NaCl (10mA/cm^2), CBZ, DCF, and IBU gained a % removal of 99.97, 99.97 and 99.75, respectively. At 0.08M NaCl (experimental run 2) with current density 5mA/cm^2 illustrates a reduction of 99.97, 99.96 and 99.90%, respectively. Based on the result in Figure 4.4, the % removal increases with an increase in an electrolyte and is apparent in the % removal of IBU.

This dimensionally stable anode (DSA) shows high performance in removing pharmaceuticals, as seen in Figures 4.3 and 4.4. The titanium-corrosion–resistant base material has a coated layer of metal oxide (Li et al., 2006). Since $Ti/IrO_2Ta_2O_5$ anode has low chlorine over-potential, with the presence of NaCl, it can effectively produce active chlorine species. Therefore, the formation of chlorine species affects the indirect oxidation in the bulk solution. Studies show that the removal is also due to direct and indirect oxidation (Dao et al., 2020; Patel et al., 2013). Based on observation, IBU increases with the increase of electrolytes. In Figure 4.3, similar results are noted. At current densities 5, 7.5 and 10 mA/cm^2, DCF and CBZ have removal of above 99%. They proved that the experimental conditions for these two pharmaceuticals were favourable. However, IBU has above 99% removal at 5 and $10mA/cm^{2;}$ at $7.5mA/cm^2$, it dropped to 87%. This may be due to the compound itself. The degradation of IBU may favour a basic medium instead of an acidic medium. IBU degradation may require more electrolytes or current, leading to higher energy consumption.

3.4.2. Pharmaceutical removal using Ti/Pt anode

Figure 4.5 illustrates the % removal of pharmaceuticals using a Ti/Pt anode during EO - treatment.

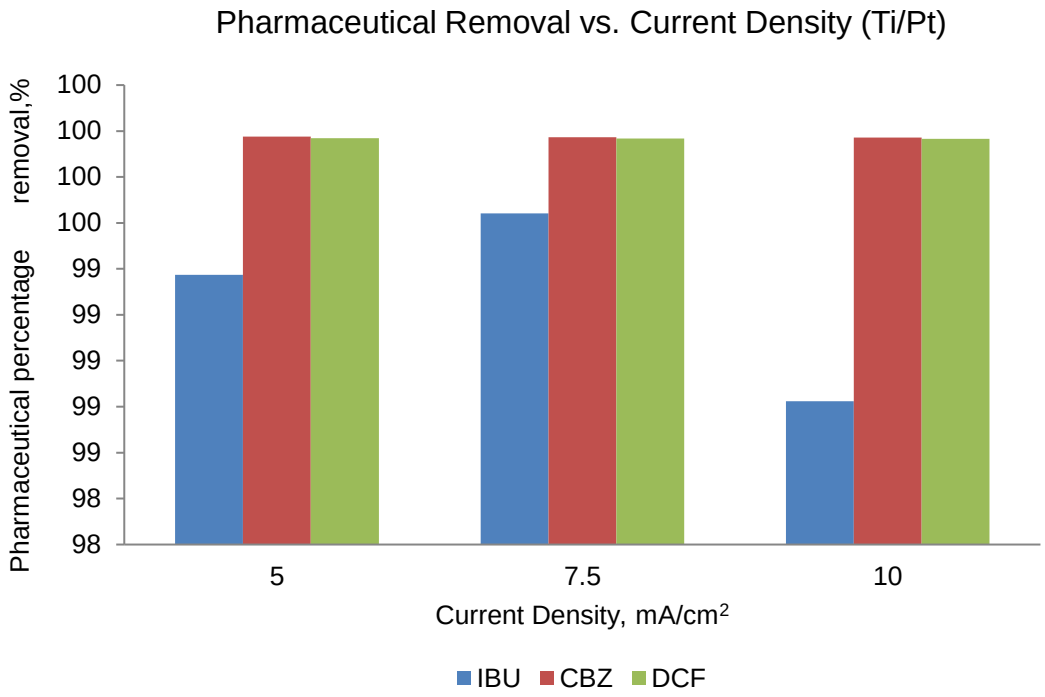

Figure 4.5: Pharmaceutical removal vs current density (Ti/Pt).

The experimental runs 16, 17 and 18 are illustrated in Figure 4.5 and linked to the COD results shown in Figure 4.1. The best COD removal is found at current densities 5, 7.5 and 10 mA/cm^2 for the Ti/Pt electrode. Experimental run 16 at current densities 5mA/cm^2 indicates that CBZ experienced the highest removal of 99.98%, followed by DCF at 99.97% and IBU at 99.37%. During experimental run 17, at 7.5mA/cm^2 (0.08M NaCl), CBZ, DCF and IBU gained a removal rate of 99.97%, 99.97% and 99.64%, respectively. At a current density of 10 mA/cm^2 (experimental run18) with NaCl at 0.08M illustrate CBZ, DCF and IBU with the removal of 99.97%, 99.97% and 99.82%. Based on the results in Figure 4.5, DCF and CBZ are almost at a consistent removal rate, while IBU fluctuates. IBU has the lowest removal rate at the highest current density, 10mA/cm^2. According to the literature, Ti/$IrO_2Ta_2O_5$ anode has a lower oxygen potential than Ti/Pt (Patel et al., 2013). It also means that direct oxidation may occur more on the surface area of the Ti/Pt anode. Results show ±99% CBZ and DCF were removed from both electrodes. However, IBU (7.5mA/cm^2) have more than 99% (7.5mA/cm^2) removal at the Ti/Pt anode and 87% at the Ti/$IrO_2Ta_2O_5$ anode, which is supported by the statement made by s Patel et al. (2013).

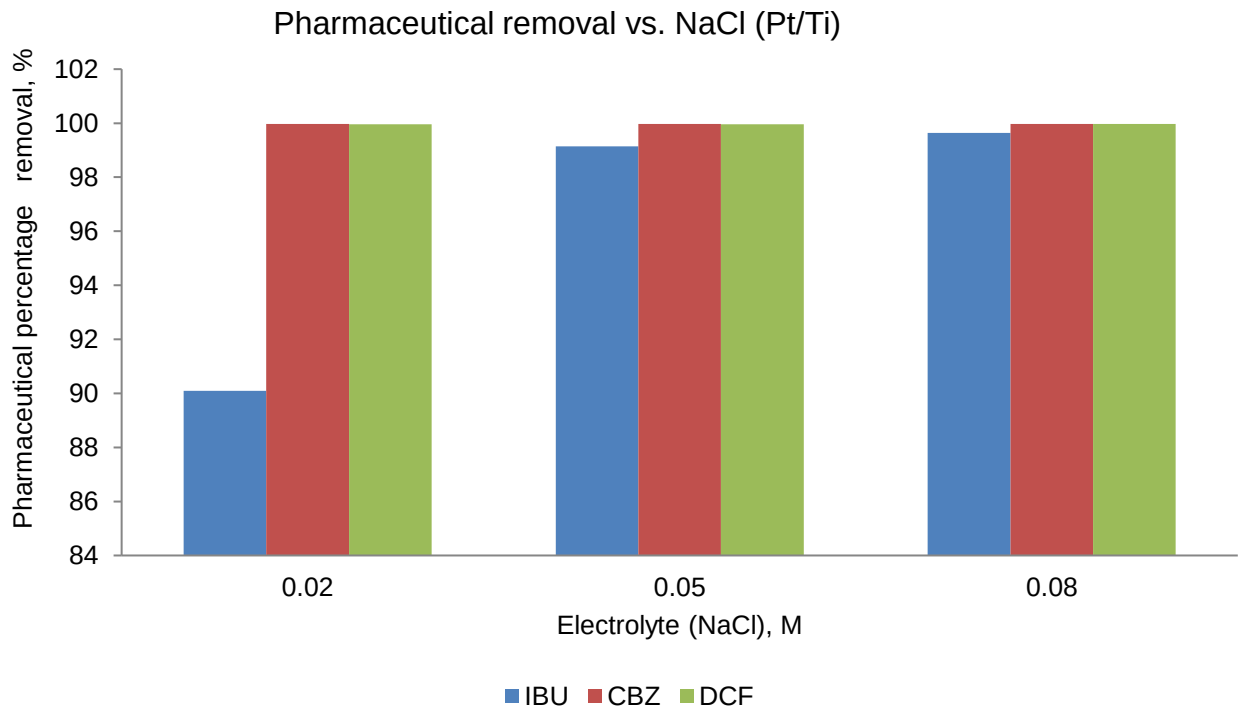

Figure 4.6: Pharmaceutical removal vs electrolyte (Ti/Pt).

The experimental runs 12, 13 and 17 are illustrated in Figure 4.6 and are based on the COD results shown in Figure 4.1. These experimental runs produced the best COD removal at NaCl concentrations 0.02, 0.05 and 0.08M for the Ti/Pt electrode. At 0.02M NaCl (10 mA/cm^2), CBZ, DCF, and IBU have a removal rate of 99.96%, 99.96% and 90.09%, respectively. IBU show a significant increase in the removal rate with 99.15% at 0.05M NaCl, while CBZ and DCF remain at 99.97% and 99.96%. At 0.08M NaCl, CBZ remains at 99.97% removal, but IBU and DCF show significant increases at 99.64% and 99.97% individually. Figure 4.6 shows a similar trend to Figure 4.4, where the rate of pharmaceutical removal increase with an increase in an electrolyte. It is observed that the electrolyte shows direct proportionality to % pharmaceutical removal.

When looking at electrolyte concentration, both anodes show an increase in IBU removal with an increase in NaCl concentration. This further supports Dao et al. (2020) statement that electrolyte affects the removal of organic compounds. It further indicates that indirect oxidation is also favoured for the disposal of IBU due to the increase in active chlorine species, which may be why Ti/Pt have a higher removal rate than Ti/$IrO_2Ta_2O_5$.

The pharmaceutical concentrations and standardised values of the effluent are presented in Table 4.4. Experimental runs 3, 4 and 5 with the highest COD removal for Ti/ $IrO_2Ta_2O_5$ electrode at current densities 10, 5 and 7.5 mA/cm^2 are highlighted in Table 4.4. The effluent concentration of IBU for electrode Ti/ $IrO_2Ta_2O_5$ at current densities of 10, 5, and 7.5 mA/cm^2 are 0.2667, 3.4200 and 123.45 μg/ml, respectively. These results support Figure 4.3, where the IBU has the lowest removal rate at a current density of 7.5 mA/cm^2. The effluent concentrations for CBZ (Ti/ $IrO_2Ta_2O_5$ electrode) are 0.3028, 0.3408 and 0.3645μg/ml at 10, 5, and 7.5 mA/cm^{2,} respectively, whilst DCF have an effluent concentration of 0.4537, 0.4411 and 0.3028μg/ml.

Experimental runs 16, 17 and 18 with electrode Ti/Pt and NaCl concentration at 0.08M are tabulated in Table 4.4 with current densities at 5, 7.5 and 10 mA/cm^2. The effluent concentration of IBU for electrode Ti/ Pt at current densities 5, 7.5 and 10 mA/cm^2 are 6.2788, 3.2276 and 13.225 μg/ml. These results support Figure 4.5, where the IBU have the lowest removal rate at a current density of 10 mA/cm^2. The effluent concentrations for CBZ (Ti/ Pt electrode) are 0.2925, 0.2918 and 0.2836μg/ml at 5, 7. 5, and 10 mA/cm^{2,} while DCF has an effluent concentration of 0.3624, 0.3484 and 0.3506μg/ml. Studies by Rajab et al., 2013; da Silva et al., 2019; Mora- Gomez et al., 2020 concur with these results regarding removing pharmaceuticals with EO.

Table 4.4: Pharmaceutical effluent concentration.

Current density (J)	Electrode	Experimental Run	Electrolyte (NaCl)	IBU	CBZ	DCF
mA/cm^2			M	µg/ml	µg/ml	µg/ml
5	Ti/ $IrO_2Ta_2O_5$	2	0,08	1,1194 ± 0.0181	0,2959 ± 0.0006	0,3634 ± 0.0007
	Ti/ $IrO_2Ta_2O_5$	**4**	**0,02**	**3,4200 ± 0.0262**	**0,3408 ± 0.0013**	**0,4537 ± 0.0014**
	Ti/ $IrO_2Ta_2O_5$	7	0,05	2,8249 ± 0.0020	0,4129 ± 0.0024	0,3748 ± 0.0022
	Ti/Pt	10	0,02	6,8413 0.0572	0,3084 ± 0.0012	0,4175 ± 0.0039
	Ti/Pt	13	0,05	9,1812 ± 8.9813	0,2909 ± 0.0101	0,3545 ± 0.0032
	Ti/Pt	**16**	**0,08**	**6,7288 ± 0.0506**	**0,2925 ± 0.0067**	**0,3624 ± 0.0028**
7,5	Ti/ $IrO_2Ta_2O_5$	1	0,08	0,5534 ± 0.0544	0,2941 ± 0.0027	0,3698 ± 0.0078
	Ti/ $IrO_2Ta_2O_5$	**5**	**0,02**	**123,4527 ± 4.2177**	**0,3645 ± 0.0041**	**0,4411 ± 0.0581**
	Ti/ $IrO_2Ta_2O_5$	8	0,05	0,5772 ± 2.4493	0,2959 ± 0.0026	0,3614 ± 0.0201
	Ti/Pt	11	0,02	1,7157 ± 0.1381	0,3112 ± 0.0008	0,3485 ± 0.0018
	Ti/Pt	14	0,05	4,6128 ± 0.0055	0,2947 ± 0.0018	0,3555 ± 0.0035
	Ti/Pt	**17**	**0,08**	**3,2276 ± 6.6995**	**0,2918 ± 0.0038**	**0,3484 ± 0.0030**
10	**Ti/ $IrO_2Ta_2O_5$**	**3**	**0,08**	**0,2667 ± 0.3024**	**0,3028 ± 0.0041**	**0,3472 ± 0.0051**
	Ti/ $IrO_2Ta_2O_5$	6	0,02	1,9212 ± 0.0814	0,4061 ± 0.0009	0,3706 ± 0.0038
	Ti/ $IrO_2Ta_2O_5$	9	0,05	2,8684 ± 0.0882	0,3177 ± 0.0007	0,3712 ± 0.0196
	Ti/Pt	12	0,02	111,5120 ± 0.1097	0,4137 ± 0.0045	0,3500 ± 0.0051
	Ti/Pt	15	0,05	2,2616 ± 0.1498	0,2910 ± 0.0033	0,6515 ± 0.0025
	Ti/Pt	**18**	**0,08**	**13,2252 ± 0.6471**	**0,2836 ± 0.0002**	**0,3506 ± 0.0036**

4.5. Energy and Efficiency

4.5.1. Instantaneous Current Efficiency (ICE)

The initial operational parameters of all experiments are tabulated in Table 3.6. To determine the effect of electrolyte (NaCl) concentration and current density on EO- the treatment process, the % ICE was calculated.

ICE is calculated using the equation:

$$\%ICE = \frac{FV\Delta COD}{8I\Delta t} \times 100$$

Equation 4.1

The % ICE is calculated over a total electrolysis time of 5 hours with a constant 1-hour interval. The calculated ICE experimental values of 18- experimental runs are tabulated in Appendix B. Experimental run 4 (Ti/ $IrO_2Ta_2O_5$ anode) with a current density; NaCl concentration of 5mA/cm^2 and 0.02M gained the highest %ICE of 120.63% after 5 hours. Experimental run 1 (Ti/ $IrO_2Ta_2O_5$ anode)) achieved 2.23% as the lowest %ICE value with initial parameters of 7.5 mA/cm^2 and 0.08M NaCl electrolyte.

Figure 4.7 compares the %ICE of the two anodes, i.e., Ti/Pt and Ti/$IrO_2Ta_2O_5$, in terms of current density. Based on the results, $IrO_2Ta_2O_5$ have an efficiency of 21.44% with 0.05 NaCl concentration, while Ti/Pt have an efficiency of 57.62% at 0.08M NaCl at a current density of 7.5mA/cm^2. It is primarily due to the overpotential of oxygen evolution of the anode (Dao et al., 2020). Since Ti/ $IrO_2Ta_2O_5$ have an oxygen over-potential growth of 0.25 V and Ti/Pt 0.3V, it stands to reason that the oxidation power of the anode will increase as the over-potential of the oxygen evolution increase (Dao et al., 2020). According to the literature, the % of ICE increase with a decrease in current density. At a current density of 5mA/cm^2, both anodes produced their highest efficiency of 120% and 55.28%, respectively. Due to the oxygen overpotential at the anode surface and mass transport limitations, higher ICE values are obtained at lower current densities (Zou et al., 2017).

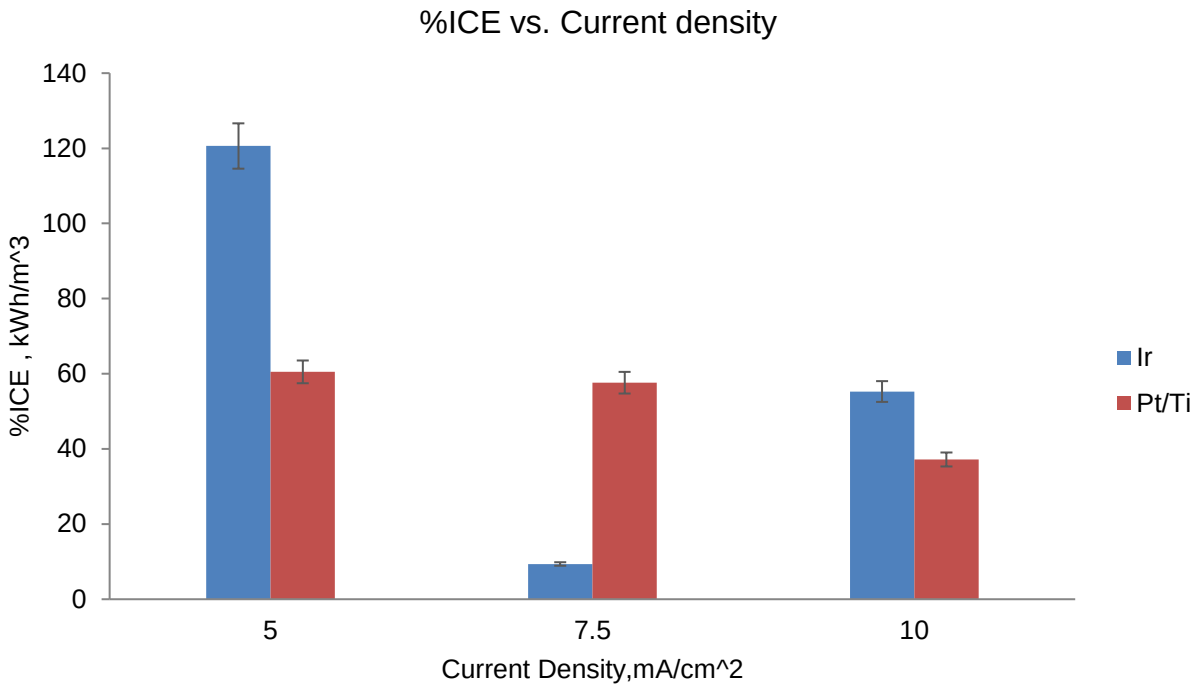

Figure 4.7: ICE vs current density.

4.5.2. Specific Energy Consumption (SEC)

The initial operational parameters of all experiments are tabulated in Table 3.6. The SEC was calculated to determine the energy consumption of electrolyte (NaCl) concentration and current density on EO- the treatment process. The following Energy Consumption equation is used (Ammar et al., 2016).

$$Ec = \frac{U_{cell} It}{3600V}$$

Equation 4.2

Where, $U_{cell}$is the average cell voltage (V); I is the current (A); t is the electrolysis time (s), and V is the volume (L).

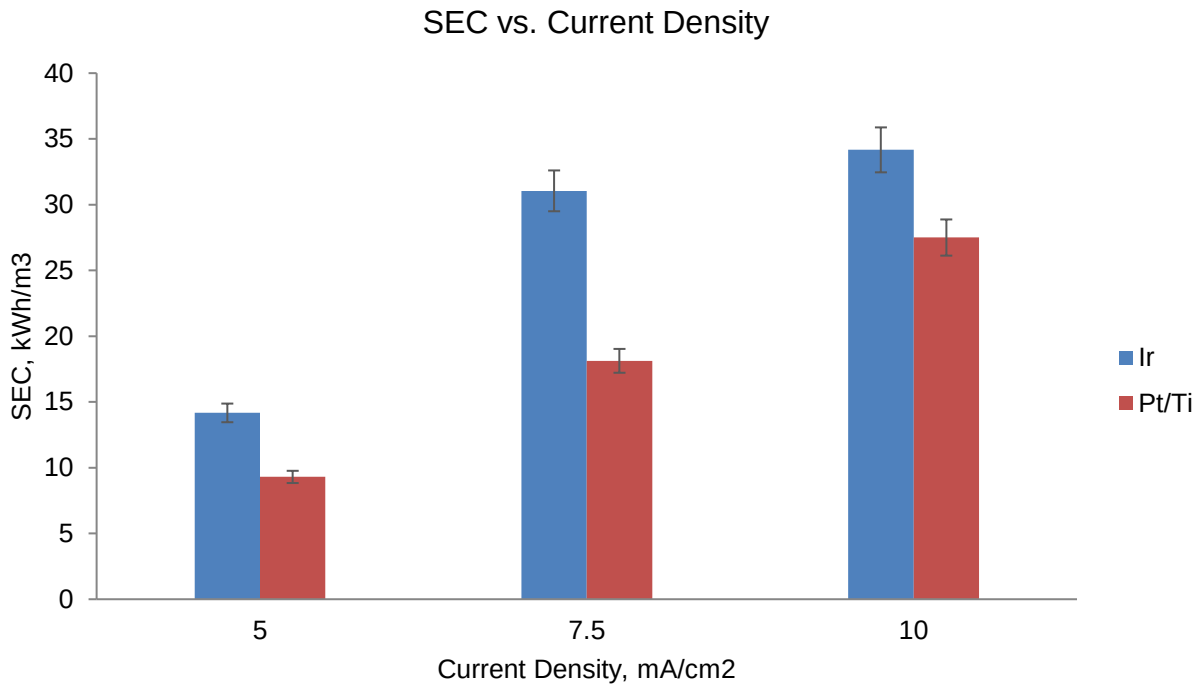

Figure 4.8: SEC vs current density

Figure 4.8 indicates the specific energy consumption (SEC) at current densities 5, 7.5 and 10mA/cm^2. The results show that SEC increases as current density increases for both anodes. According to Zou et al. (2017), energy consumption will increase as the applied current increases. Since current density is the applied current over the surface area of the reaction, Figure 4.8 is in accordance. Energy consumption shows significant growth with the increase in current density.

Figure 4.7 indicates that EO- treatment efficiency reaches a maximum at 5 mA/cm^{2,} while Figure 4.8 shows that the lowest energy consumption is also at 5 mA/cm^2. It, therefore, stands to reason that in terms of ICE and SEC, the most favourable current density is 5mA/cm^2 for both Ti/Pt and Ti/$IrO_2Ta_2O_5$ anodes.

Chapter 5

Optimisation using Response Surface Methodology (RSM)

Chapter 5: Optimisation using Response Surface Methodology (RSM)

5.1. Introduction

Modelling analysis was done using the Design Expert (DE) software version 10. The response surface methodology (RSM) and central composite design (CCD) generated 36 random experimental runs. This design provides information about the independent parameters used in this study and contributes to the desired response, i.e., minimum, maximum or optimum conditions (Teymouri et al., 2017).

This chapter uses the CCD model to optimize the EO treatment conditions for:

I. Chemical Oxygen Demand (COD).
II. Sulphate removal
III. Colour removal

COD, Inorganic compounds and colour removal were studied using three parameters, i.e. electrolyte (A), current density (B) and the type of electrode (C). The interaction effect of the three parameters is highlighted in this chapter.

5.2. COD

The COD in terms of removal efficiency ranges between 9.09 to 90.91%. The actual - and predicted removal efficiencies of COD are illustrated in Table 5.1.

Table 5.1: Central Composite Design output results for COD removal.

		Factors		COD removal (%)	
Run	**A: NaCl (M)**	**B: Current Density (mA/cm^2)**	**C: Electrode**	**Actual Value**	**Predicted Value**
1	0,08	7,5	$IrO_2Ta_2O_5$	14,17	12,35
2	0,08	7,5	$IrO_2Ta_2O_5$	10,53	12,35
3	0,08	5	$IrO_2Ta_2O_5$	69,7	80,31
4	**0,08**	**5**	**$IrO_2Ta_2O_6$**	**90,91**	**80,31**
5	0,08	10	$IrO_2Ta_2O_5$	49,11	50,36
6	0,08	10	$IrO_2Ta_2O_5$	51,61	50,36
7	0,02	5	$IrO_2Ta_2O_5$	71,43	72,08
8	0,02	5	$IrO_2Ta_2O_5$	72,73	72,08
9	0,02	5	Pt	52,11	41,41
10	0,02	5	Pt	30,71	41,41
11	0,02	7,5	$IrO_2Ta_2O_5$	26,92	24,57
12	0,02	7,5	Pt	50,53	51,76
13	0,02	7,5	Pt	53	51,76
14	0,02	10	Pt	55,71	48,8
15	0,02	7,5	$IrO_2Ta_2O_5$	22,22	24,57
16	0,02	10	Pt	41,89	48,8
17	0,05	5	Pt	48,33	37,87

18	0,02	10	$IrO_2Ta_2O_5$	29,27	29,64
19	0,02	10	$IrO_2Ta_2O_5$	30	29,64
20	0,05	5	Pt	27,42	37,87
21	0,05	7,5	Pt	9,09	19,36
22	0,05	5	$IrO_2Ta_2O_5$	14,29	14,72
23	0,05	7,5	Pt	29,63	19,36
24	0,05	10	Pt	27,78	35,68
25	0,05	5	$IrO_2Ta_2O_5$	15,15	14,72
26	0,05	10	Pt	43,59	35,68
27	0,05	7,5	$IrO_2Ta_2O_5$	25,4	51,73
28	0,08	5	Pt	66,89	48,55
29	0,05	7,5	$IrO_2Ta_2O_5$	78,06	51,73
30	0,08	5	Pt	30,21	48,55
31	0,05	10	$IrO_2Ta_2O_5$	40,8	37,8
32	0,08	7,5	Pt	86	79,57
33	0,05	10	$IrO_2Ta_2O_5$	34,79	37,8
34	0,08	7,5	Pt	73,15	79,57
35	0,08	10	Pt	71,15	64,14
36	0,08	10	Pt	57,14	64,14

The statistical analysis indicates that the fifth model can be used to explain the response of experiments (Table 5.1) based on accuracy and applicability. The following model equation (Equation 5.1) was generated to present the model:

$$\%\ COD_{\ removed} = 35.54 + 3.9A + 5.22B + 16.19C + 2.59AB - 10.01AC + 6.32BC + 6.52A^2 - 4.03B^2 + 0.54ABC - 11.4A^2B - 39.79A^2C + 16.37A^2B^2 - 18.24A^2BC + 10.82AB^2C + 48.74A^2B^2C$$

Equation 5.1

The model has a good response between the responses and variables, with an F-value of 4.49 and a low p-value of 0.0014 (Table 5.2). Teymouri et al. (2017) explain that a high F –value illustrates that more of the dataset can be fitted onto the statistical model. At the same time, the p–value indicates a probability value when there is no relationship between the model and the response. Based on this, the critical region of the model (Prob > F) indicates the significance level. The fifth model sufficiently fits the data since the Prob > F – value is less than 0.0500.

Table 5.2: Analysis of variance (ANOVA)

Source	Sum of Squares	Degree of Freedom	Mean Square	F - Value	p-value Prob > F
Model	14359,8	17	844,69	4,49	0,0014
A-Salt conc.	121,52	1	121,52	0,65	0,4321
B-Current	218,09	1	218,09	1,16	0,2959
C-Electrodes	1047,82	1	1047,82	5,57	0,0298
AB	107,17	1	107,17	0,57	0,4602
AC	801,2	1	801,2	4,26	0,0538
BC	319,16	1	319,16	1,7	0,2092
A^2	113,36	1	113,36	0,6	0,4477
B^2	43,23	1	43,23	0,23	0,6375
ABC	4,61	1	4,61	0,025	0,8773
A^2B	692,74	1	692,74	3,68	0,071
A^2C	4221,98	1	4221,98	22,44	0,0002
AB^2	34,19	1	34,19	0,18	0,675
B^2C	1226,51	1	1226,51	6,52	0,02
A^2B^2	476,51	1	476,51	2,53	0,129
A^2BC	1774,02	1	1774,02	9,43	0,0066
AB^2C	623,88	1	623,88	3,32	0,0853
A^2B^2C	4222,51	1	4222,51	22,44	0,0002
Pure Error	3387,28	18	188,18		
Cor Total	17747	35			

In terms of adequate precision, a value of more than 4 is desired. The model has a value ratio of 7.006. This indicates an adequate signal and can be used to navigate the design space. Table 5.3 shows the R^2 –value at 0.8091 while the adjusted value is 0.6369. The R^2 value is defined as the ratio of the dependent variable explained by the independent variable. Literature indicates that a good model fit should at least be 0.8. Therefore the quartic model is a good fit for the data.

Table5.3: ANOVA and Standard deviation results

Std. Dev.	13,72	**R^2**	**0,8091**
Mean	44,48	Adj R^2	0,6289
C.V. %	30,84	Pred R^2	0,2365
PRESS	13549,13	Adeq Precision	7,006

The relationship between the % probability of residuals and the externally studentized residuals indicates if a response transform would be necessary. The model validates that the normality of the data has no big problem, given that the residuals and probability share a linear relationship. Figure 5.1 show the linear relationship of the residuals. The validation of the actual values of the % COD removal is illustrated in Figure 5.2. The model indicates that most predicted values are to the actual experimental % COD removal data.

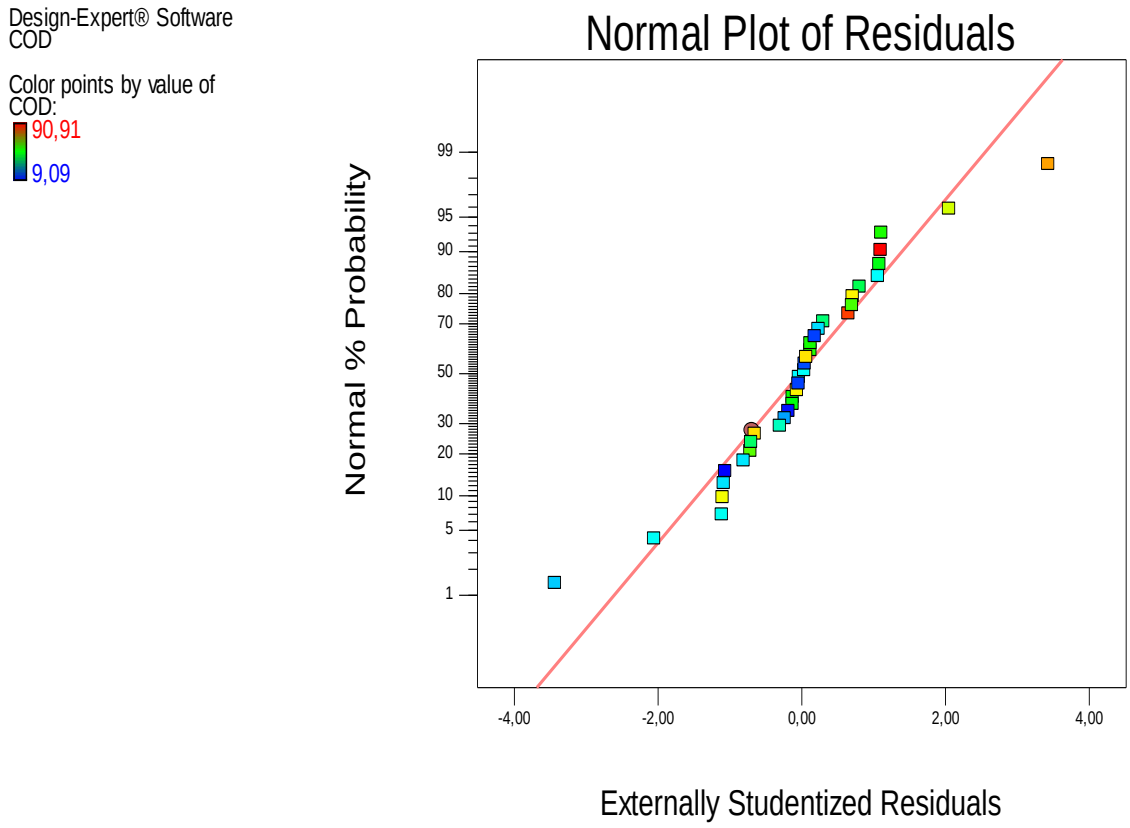

Figure 5.1: Normal plot of Residuals - COD

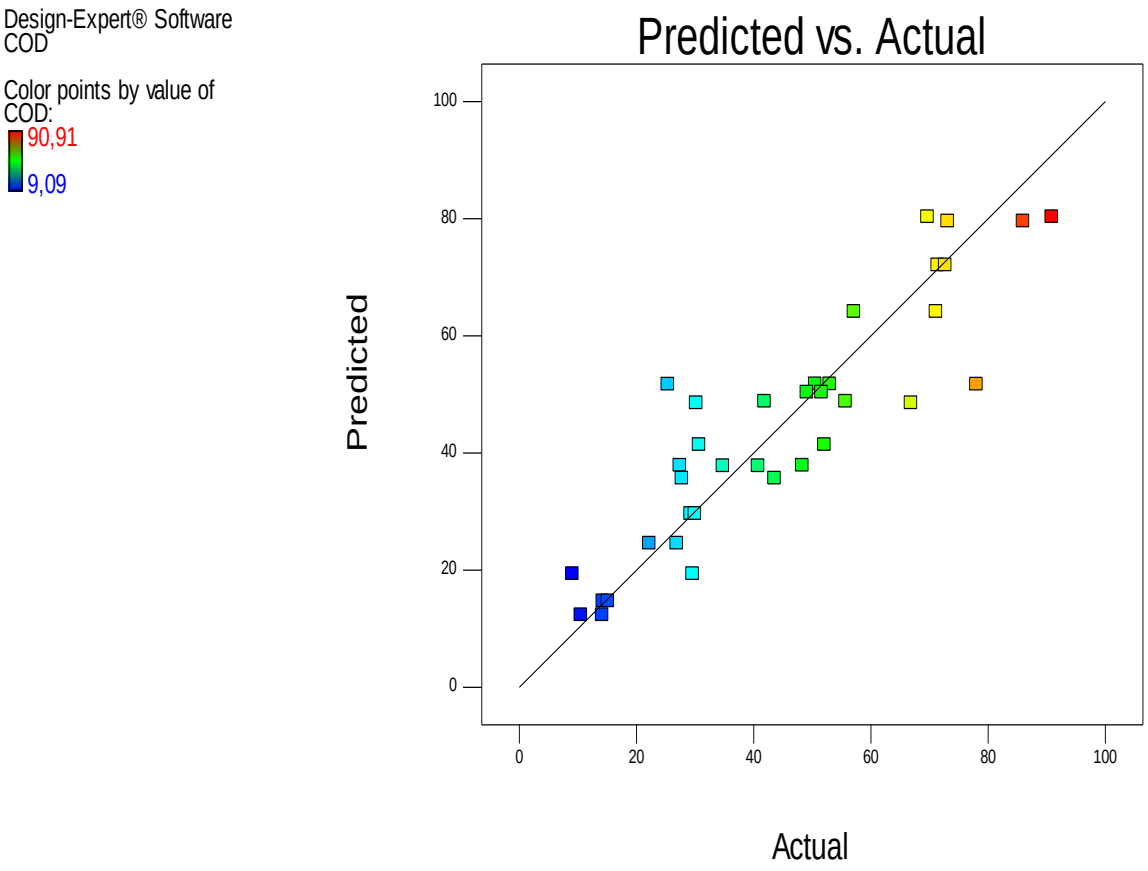

Figure 10: Predicted vs Actual values - COD.

Figures 5.3 and 5.4 show the 3D response surface and contour plot of the Ti/Pt electrode, while Figures 5.4 and 5.5 show that of the Ti /$IrO_2Ta_2O_5$ electrode. The 3D and contour plots illustrate the factors for A B, i.e. electrolyte and current density, while the electrode type remains constant. The 3D Figures show that although the model is significant with 0.0014 (Table 5. 2), there is a lack of interaction between A and B (electrolyte and current density). However, among the interactive terms C, AC, A^2C, A^2BC and AB^2C significantly affect the curvature. This indicates that the interaction between the electrolyte and electrode type may substantially impact the EO – treatment process.

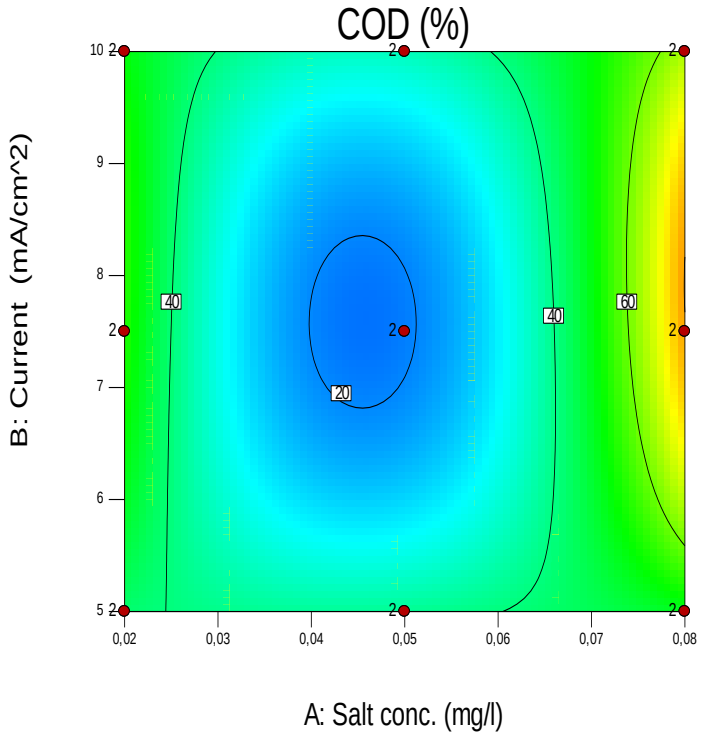

Figure 5.3: Contour plot (Ti/Pt - anode) -COD

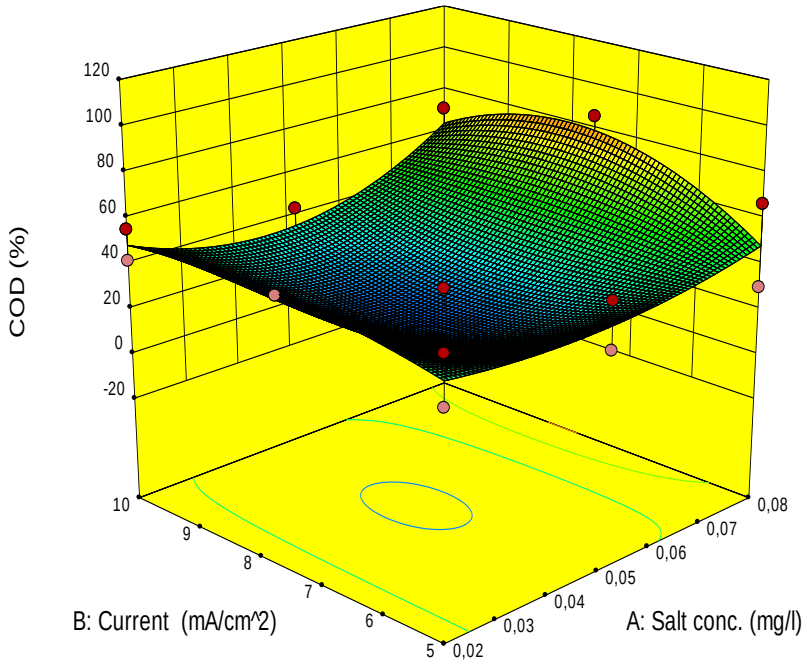

Figure 5.4: Response surface plot (Ti/Pt) - COD

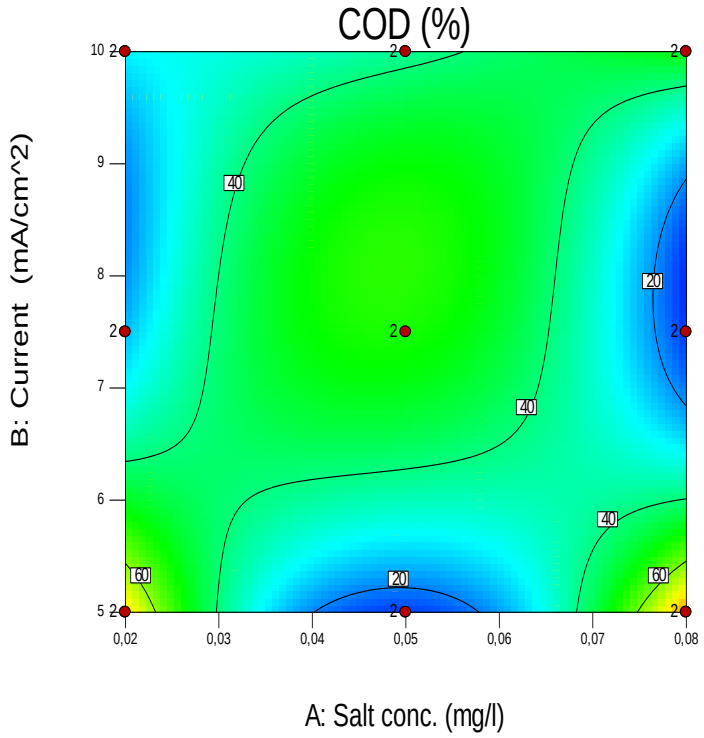

Figure 5.5: Contour plot – COD.

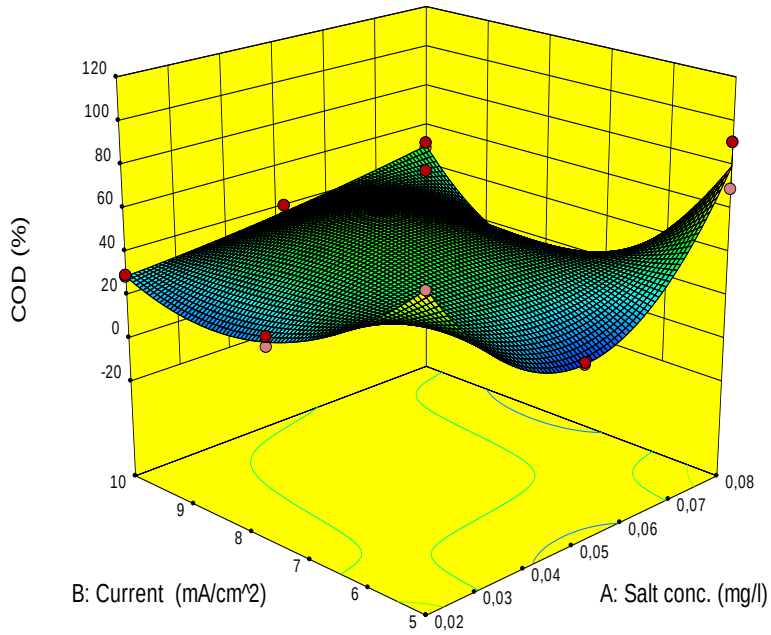

Figure 5.6: 3D plot - COD

The COD 3D graph and contour diagram is illustrated in Figures 5.5 and 5.6. The factors, electrolyte NaCl and current density, are kept constant to gain a relationship between factors A and

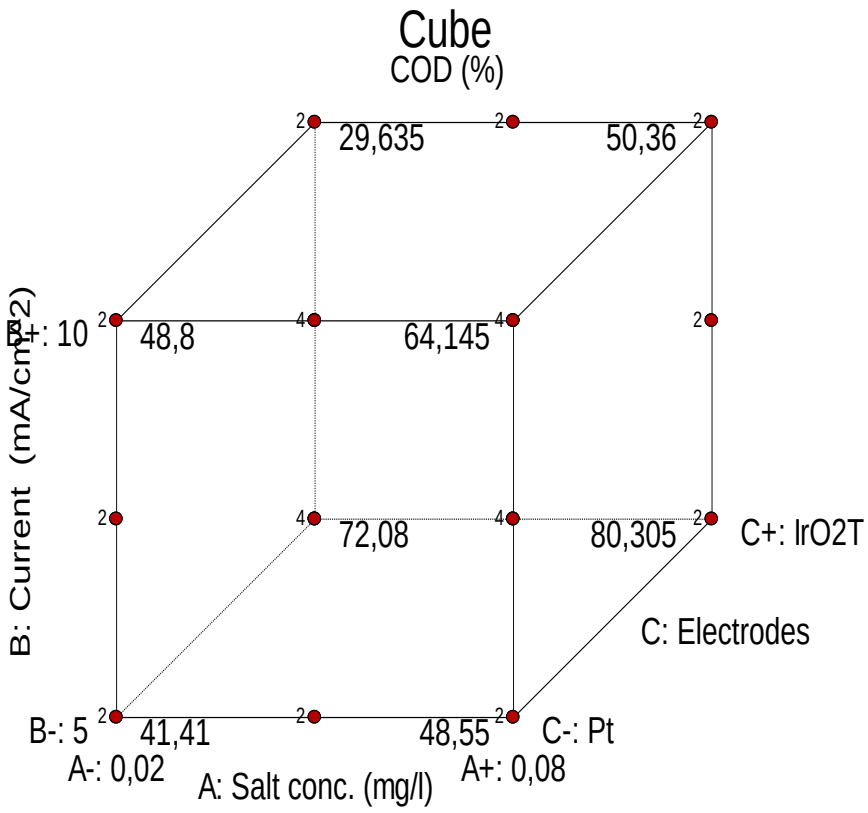

Figure 5.7: COD removal central composite design.

Figure 5.7 illustrates the cube generated for the removal of COD for factors electrolyte, current density and type of electrode. The critical factors described in this cube are electrode type and salt concentration 80.305% was removed with the Ti /$IrO_2Ta_2O_5$ with 0.08M NaCl electrolyte.

5.3. Amount of sulphate detected

The sulphate in terms of removal efficiency ranges between -50.1 to 22.58%. The actual - and predicted removal efficiencies of sulphate are illustrated in Table 5.4. The negative results indicate an increase in sulphate production. This may be due to the oxidation of sulphate molecules in the EO system.

Table 5.4: Central composite design results for sulphate removal.

	Factors			Sulphate removal (%)	
Run	**A: NaCl (M)**	**B: Current Density (mA/cm^2)**	**C: Electrode**	**Actual Value**	**Predicted Value**
1	0,08	7,5	$IrO_2Ta_2O_5$	2,52	-1,24
2	0,08	7,5	$IrO_2Ta_2O_5$	-9,09	-1,24
3	0,08	5	$IrO_2Ta_2O_5$	7,14	2,55
4	0,08	5	$IrO_2Ta_2O_6$	0	2,55
5	0,08	10	$IrO_2Ta_2O_5$	1,43	7,47
6	0,08	10	$IrO_2Ta_2O_5$	15,56	7,47
7	0,02	5	$IrO_2Ta_2O_5$	2,44	3,59
8	0,02	5	$IrO_2Ta_2O_5$	6,78	3,59
9	0,02	5	Pt	7,56	6,69
10	0,02	5	Pt	3,77	6,69
11	0,02	7,5	$IrO_2Ta_2O_5$	7,8	9,25
12	0,02	7,5	Pt	-43,94	-50,1
13	0,02	7,5	Pt	-52,17	-50,1
14	0,02	10	Pt	-15,94	-9,89
15	0,02	7,5	$IrO_2Ta_2O_5$	6,62	9,25
16	0,02	10	Pt	-5,88	-9,89
17	0,05	5	Pt	-12,9	-7,76

18	0,02	10	$IrO_2Ta_2O_5$	2,1	1,97
19	0,02	10	$IrO_2Ta_2O_5$	3,88	1,97
20	0,05	5	Pt	1,46	-7,76
21	0,05	7,5	Pt	-49	-25,53
22	0,05	5	$IrO_2Ta_2O_5$	2,52	8,26
23	0,05	7,5	Pt	-10,24	-25,53
24	0,05	10	Pt	-18,06	-22,55
25	0,05	5	$IrO_2Ta_2O_5$	9,92	8,26
26	0,05	10	Pt	-22,95	-22,55
27	0,05	7,5	$IrO_2Ta_2O_5$	15,38	14,89
28	0,08	5	Pt	-14,5	-8,86
29	0,05	7,5	$IrO_2Ta_2O_5$	22,58	14,89
30	0,08	5	Pt	-5,26	-8,86
31	0,05	10	$IrO_2Ta_2O_5$	10,53	11,21
32	0,08	7,5	Pt	5,51	5,26
33	0,05	10	$IrO_2Ta_2O_5$	7,8	11,21
34	0,08	7,5	Pt	9,09	5,26
35	0,08	10	Pt	-13,64	-15,95
36	0,08	10	Pt	-20,3	-15,95

The statistical analysis indicates that the quartic model can be used to explain the response of experiments (Table 5.4) based on accuracy and applicability. The following model equation (Equation 5.2) was generated to present the model:

$$\%\ Sulphate_{\ removed}$$

$$= -5.32 + 11.21A - 2.96B + 20.21C + 2AB - 16.46AC + 4.43BC - 3.89A2 + 2.61B2$$

$$-0.37ABC + 0.41A2\,B - 7A2C - 13.36AB2 - 7.77B2C + 5.04A2B2 - 1.06A2BC + 19.72AB2C$$

Equation 5.2

The model has a good response between the responses and variables with an F-value of 7.48 and a low p-value of <0.0001 (Table 5.4). The critical region of the model (Prob > F) indicates the significance level. The quartic model sufficiently fits the data since the Prob > F – value is less than 0.0500. According to the literature, a lack of fit F – value is good because it is desired to fit the model. The lack of fit F – value is 2.10, which implies that it is insignificant relative to the pure error.

Table 5.5: Analysis of variance (ANOVA) - Sulphate removal.

Source	Sum of Squares	Degree of Freedom	Mean Square	F Value	p-value Prob > F
Model	9074,81	16	567,18	7,48	< 0.0001
A-Salt conc.	1006,21	1	1006,21	13,27	0,0017
B-Current	70,09	1	70,09	0,92	0,3484
C-Electrodes	2941,44	1	2941,44	38,78	< 0.0001
AB	64,24	1	64,24	0,85	0,3689
AC	2168,11	1	2168,11	28,59	< 0.0001
BC	157,18	1	157,18	2,07	0,1663
A^2	40,3	1	40,3	0,53	0,4749
B^2	18,17	1	18,17	0,24	0,6302
ABC	2,16	1	2,16	0,028	0,8677
A^2B	0,92	1	0,92	0,012	0,9135
A^2C	391,81	1	391,81	5,17	0,0348
AB^2	951,59	1	951,59	12,55	0,0022
B^2C	482,47	1	482,47	6,36	0,0207
A^2B^2	45,23	1	45,23	0,6	0,4495
A^2BC	6,01	1	6,01	0,079	0,7814
AB^2C	2074,28	1	2074,28	27,35	< 0.0001
Residual	1440,98	19	75,84		
Lack of Fit	150,39	1	150,39	2,1	0,1647
Pure Error	1290,59	18	71,7		
Cor Total	10515,8	35			

In terms of adequate precision, a value of more than 4 is desired, and a value ratio of 10.860. This indicates an adequate signal and can be used to navigate the design space. Table 5.6 shows the R^2 –value at 0.863 while the adjusted value is 0.7476. The R^2 value is defined as the ratio of the dependent variable explained by the independent variable. Literature indicates that a good model fit should at least be 0.8. Therefore the quartic model is a good fit for the data. Also, the predicted R^2 of 0.5734 is in reasonable agreement with the adjusted R^2 value of 0.7476, which is less than 0.2. This indicates a desirable difference.

Table 5.6: ANOVA analysis.

Std. Dev.	8,71	**R-Squared**	**0,863**
Mean	-3,93	Adj R-Squared	0,7476
C.V. %	221,6	Pred R-Squared	0,5734
PRESS	4486,23	Adeq Precision	10,86

The relationship between the % probability of residuals and the externally studentized residuals indicates if a response transform would be necessary. The model validates that the normality of the data has no spacious problem, given that the residuals and probability share a linear relationship. Figure 5.8 show the linear relationship of the residuals. The validation of the actual values of the % Sulphate removal is illustrated in Figure 5.9. The model indicates that most of the predicted values are to the actual experimental % Sulphate removal data.

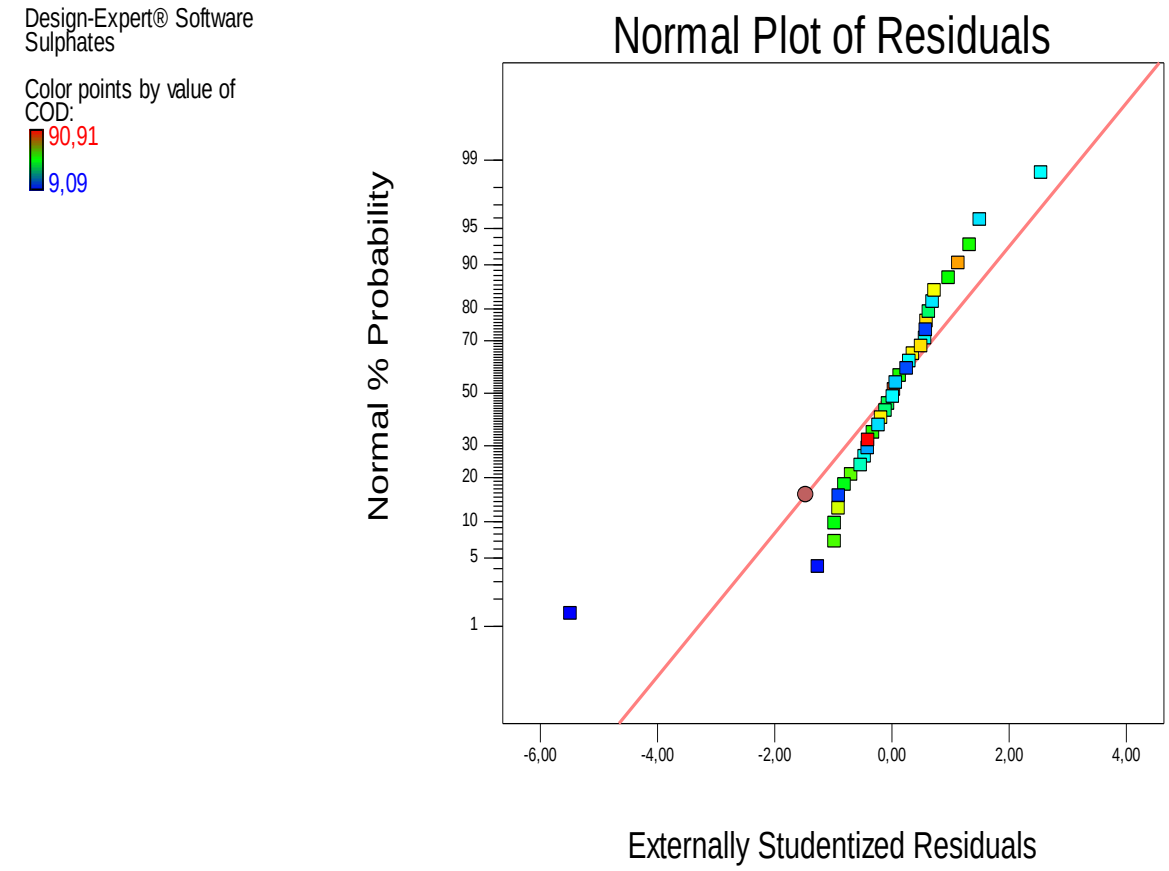

Figure 5.8: Normal plot vs. residuals - sulphate removal.

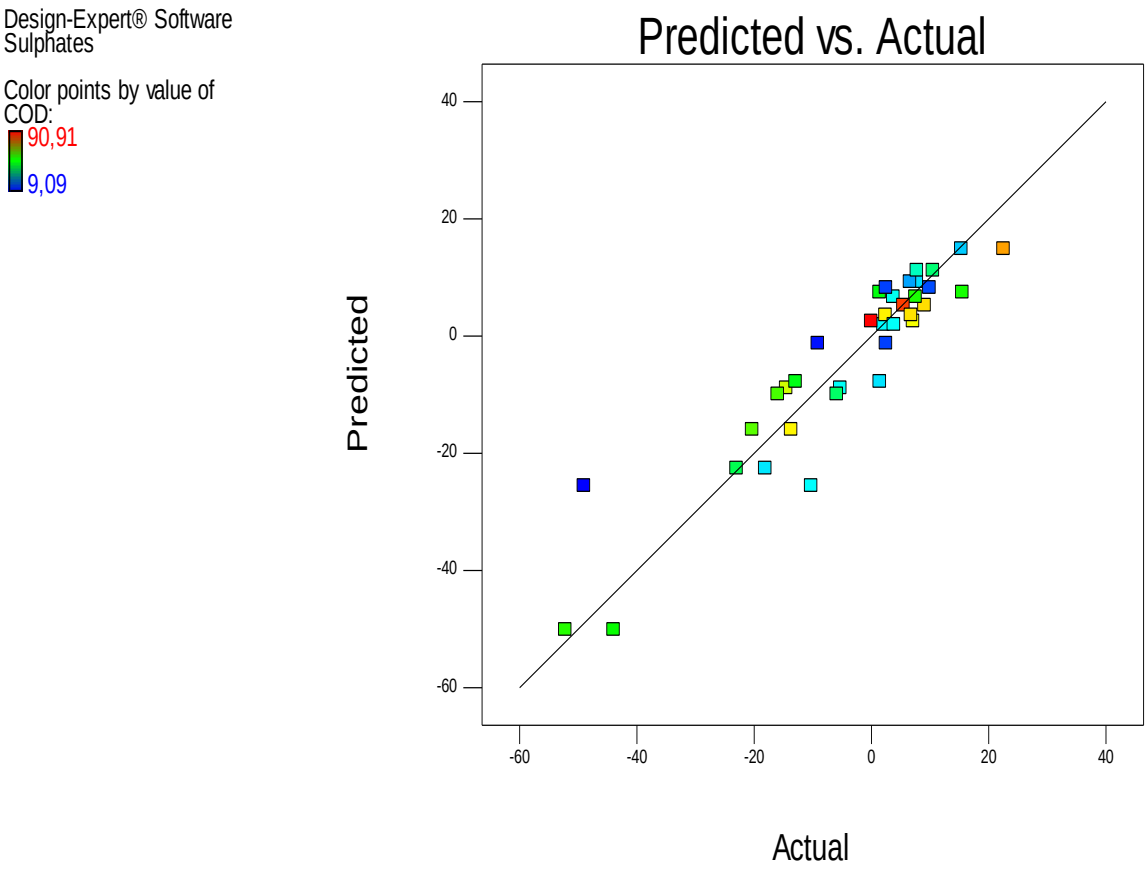

Figure 5.9: Predicted values vs actual values - sulphate removal.

Figures 5.10 and 5.11 show the 3D response surface and contour plot of the Ti/Pt electrode, while Figures 5.12 and 5.13 show that of the Ti /$IrO_2Ta_2O_5$ electrode. The 3D and contour plots illustrate the factors for A, B i.e. electrolyte and current density, while the electrode type remains constant. From the 3D Figures, it is noted that although the model is significant with <0.0001 (Table 5. 5), there is an interaction between A and C (electrolyte and type of electrode). More interactive terms are AC, A^2C, AB^2, B^2C and AB^2C, significantly affecting the curvature. This indicates that the interaction between the electrolyte, current density and the type of electrode may simultaneously impact the EO – treatment process.

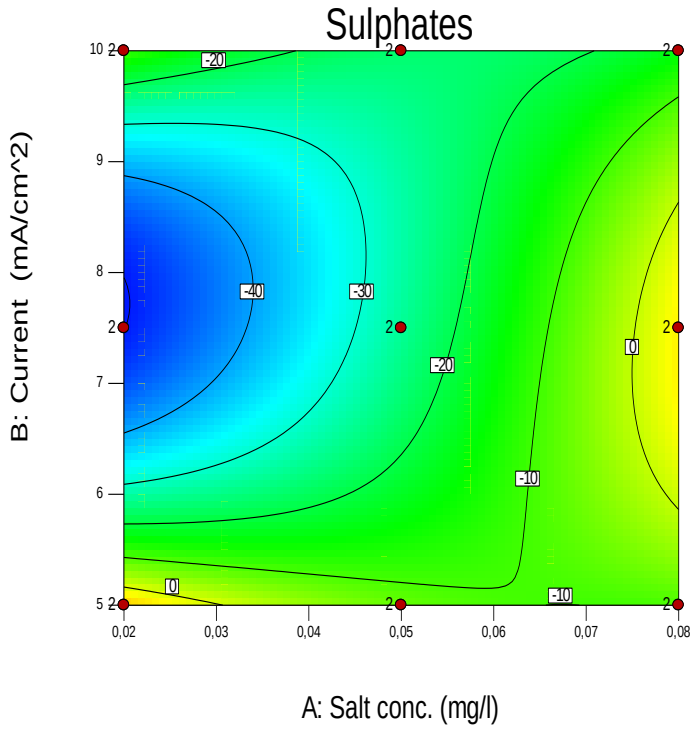

Figure 5.10: Contour plot- sulphate removal (Ti/Pt)

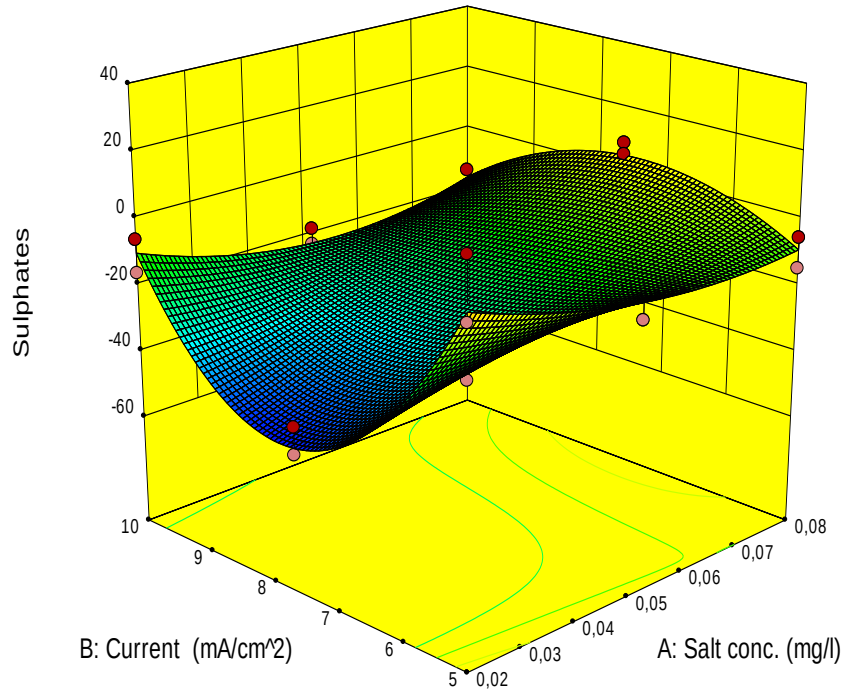

Figure 5.11: 3D plot - sulphate removal (Ti/Pt)

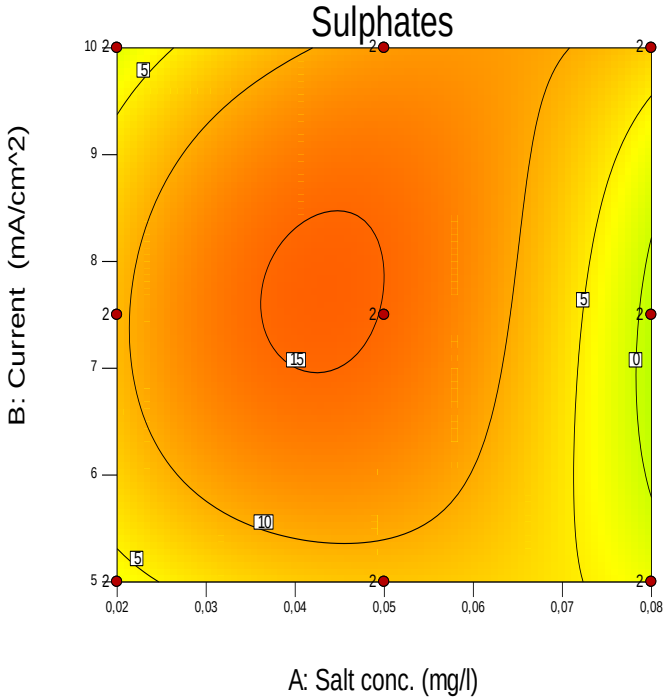

Figure 5.12: Contour plot - sulphate removal

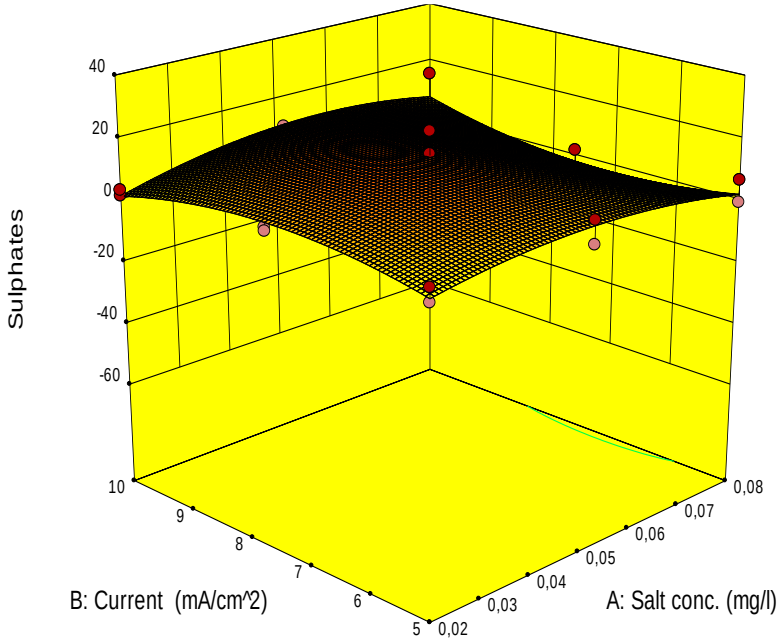

Figure 5.13: 3D plot sulphate remova.

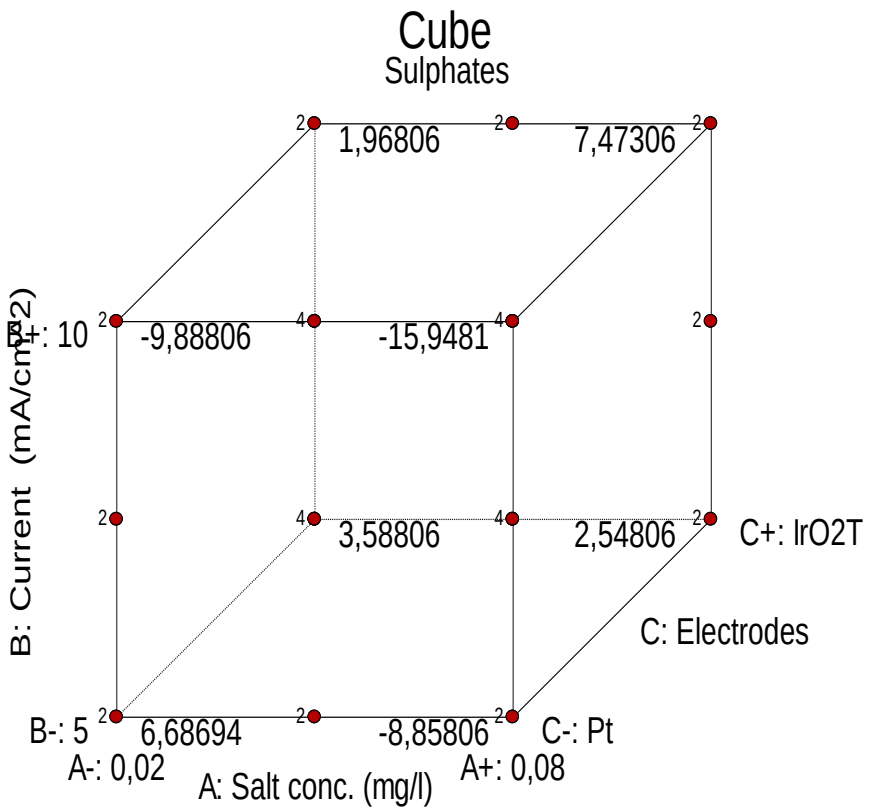

Figure 5.14: Sulphate removal CCD.

Figure 5.14 illustrates the cube generated for the removal of sulphates for factors electrolyte, current density and type of electrode. The critical factors described in this cube are electrode type and salt concentration. 22.58% was removed with the Ti /$IrO_2Ta_2O_5$ with 0.05M NaCl electrolyte.

5.4. Amount of colour detected

The colour in terms of removal efficiency ranges between 0 to 82.67%. The actual - and predicted removal efficiencies of colour are illustrated in Table 5.7. The negative results indicate an increase in colour. This may be due to the oxidation of sulphate molecules in the EO system.

Table 5.7: Central Composite design results – Colour removal

	Factors			Color removal (%)	
Run	**A: NaCl (M)**	**B: Current Density (mA/cm^2)**	**C: Electrode**	**Actual Value**	**Predicted Value**
1	0.08	7.5	$IrO_2Ta_2O_5$	68.97	51.37
2	0.08	7.5	$IrO_2Ta_2O_5$	36.23	51.37
3	0.08	5	$IrO_2Ta_2O_5$	43.04	36.13
4	0.08	5	$IrO_2Ta_2O_6$	42.25	36.13
5	0.08	10	$IrO_2Ta_2O_5$	62.21	62.73
6	0.08	10	$IrO_2Ta_2O_5$	43.66	62.73
7	0.02	5	$IrO_2Ta_2O_5$	18.29	11.02
8	0.02	5	$IrO_2Ta_2O_5$	0	11.02
9	0.02	5	Pt	8.47	12.8
10	0.02	5	Pt	23.33	12.8
11	0.02	7.5	$IrO_2Ta_2O_5$	29.73	20.1
12	0.02	7.5	Pt	-8.62	29.67
13	0.02	7.5	Pt	70	29.67
14	0.02	10	Pt	50.68	42.65
15	0.02	7.5	$IrO_2Ta_2O_5$	16.87	20.1

16	0.02	10	Pt	30.49	42.65
17	0.05	5	Pt	23.53	13.58
18	0.02	10	$IrO_2Ta_2O_5$	20.25	25.31
19	0.02	10	$IrO_2Ta_2O_5$	23.61	25.31
20	0.05	5	Pt	-5.88	13.58
21	0.05	7.5	Pt	52.54	33.52
22	0.05	5	$IrO_2Ta_2O_5$	25.37	34.98
23	0.05	7.5	Pt	34.21	33.52
24	0.05	10	Pt	51.76	49.58
25	0.05	5	$IrO_2Ta_2O_5$	38.67	34.98
26	0.05	10	Pt	28.99	49.58
27	0.05	7.5	$IrO_2Ta_2O_5$	42.11	47.15
28	0.08	5	Pt	-3.23	-8.45
29	0.05	7.5	$IrO_2Ta_2O_5$	36.62	47.15
30	0.08	5	Pt	-13.73	-8.45
31	0.05	10	$IrO_2Ta_2O_5$	82.67	55.43
32	0.08	7.5	Pt	24.62	14.56
33	0.05	10	$IrO_2Ta_2O_5$	57.89	55.43
34	0.08	7.5	Pt	-10.53	14.56
35	0.08	10	Pt	41.67	33.7
36	0.08	10	Pt	44.93	33.7

The statistical analysis indicates that the quadratic model can be used to explain the response of experiments (Table 5.7) based on accuracy and applicability. The following model equation (Equation 5.3) was generated to present the model:

$$\%\ Colour_{\ removed} = 40.33 + 4.04A + 14.11B + 6.81C + 3.08AB + 11.59AC - 3.89BC - 11.41A^2 - 1.94B^2$$

Equation 5.3

The model has a good response between the responses and variables with an F-value of 4.94 and a low p-value of 0.0008 (Table 5.8). This means there is only a 0.08% chance of error for the F –value. The critical region of the model (Prob > F) indicates the significance level. The quadratic model sufficiently fits the data since the Prob > F – value is less than 0.0500. According to the literature, a lack of fit F – value is good because it is desired to fit the model. The lack of fit F – value is 0.52, which implies that it is insignificant relative to the pure error.

Table 5.8: ANOVA results – Colour removal

Source	Sum of Squares	Degree of freedom	Mean Square	F Value	p-value Prob > F
Model	11653.15	8	1456.64	4.94	0.0008
A-Salt conc.	391.96	1	391.96	1.33	0.2591
B-Current	4779.9	1	4779.9	16.21	0.0004
C-Electrodes	1670.22	1	1670.22	5.66	0.0247
AB	151.29	1	151.29	0.51	0.48
AC	3225.5	1	3225.5	10.94	0.0027
BC	363.17	1	363.17	1.23	0.2769
A^2	1040.97	1	1040.97	3.53	0.0711
B^2	30.13	1	30.13	0.1	0.7517
Residual	7963.13	27	294.93		
Lack of Fit	1645.99	9	182.89	0.52	0.8405
Pure Error	6317.14	18	350.95		
Cor Total	19616.28	35			

In terms of adequate precision, a value of more than 4 is desired, and a value ratio of 8.290. This indicates an adequate signal and can be used to navigate the design space. Table 5.9 shows the R^2 –value at 0.5941 while the adjusted value is 0.4738. The R^2 value and the R^2 adjusted – value have a difference of less than 0.2. This indicates a desirable difference for this data set.

Table 5.9: Standard deviation – colour removal

Std. Dev.	17.17	**R-Squared**	**0.5941**
Mean	31.44	Adj R-Squared	0.4738
C.V. %	54.63	Pred R-Squared	0.3234
PRESS	13272.4	Adeq Precision	8.29

The relationship between the % probability of residuals and the externally studentized residuals indicates if a response transform would be necessary. The model validates that the normality of the data has no spacious problem, given that the residuals and probability share a linear relationship. Figure 5.15 show the linear relationship of the residuals. The validation of the actual values of the % colour removal is illustrated in Figure 5.16. The model indicates that most of the predicted values are to the real experimental % colour removal data.

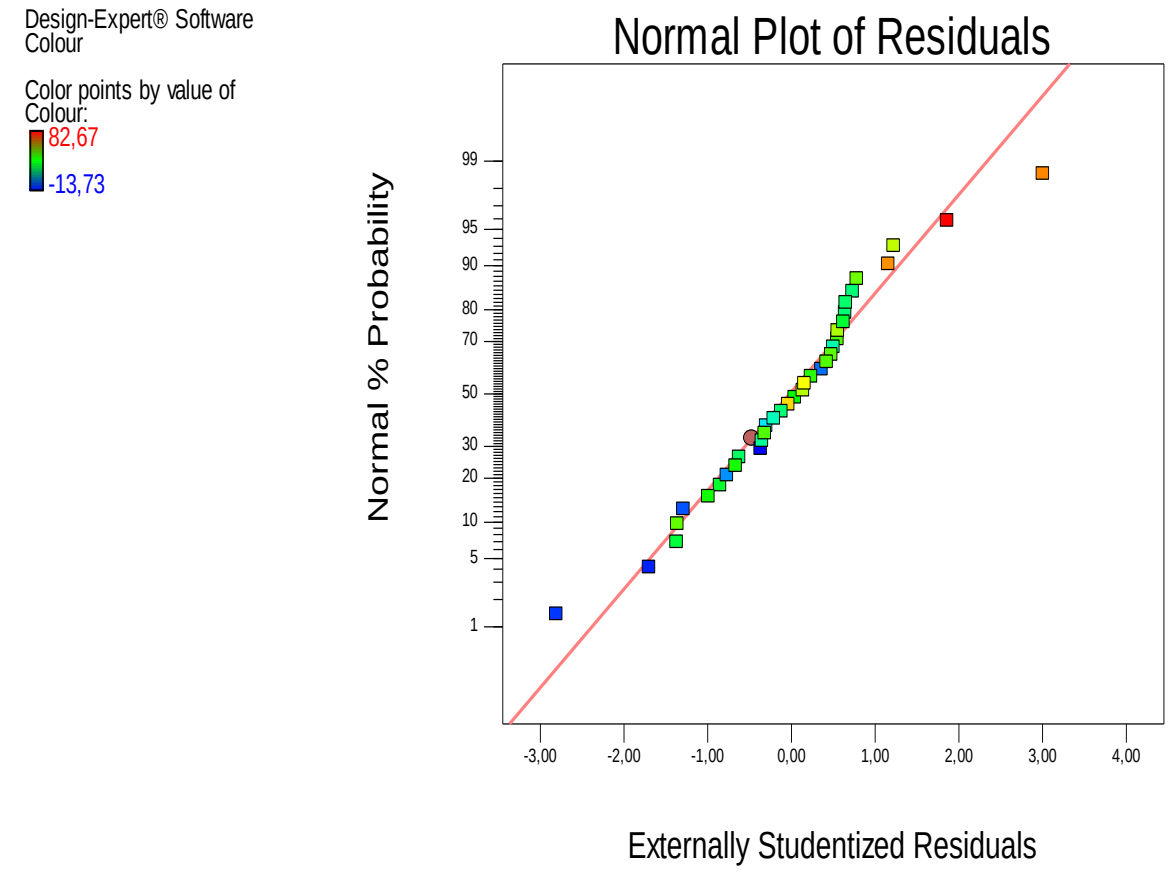

Figure 5.15: Normal plot vs. residuals - colour removal.

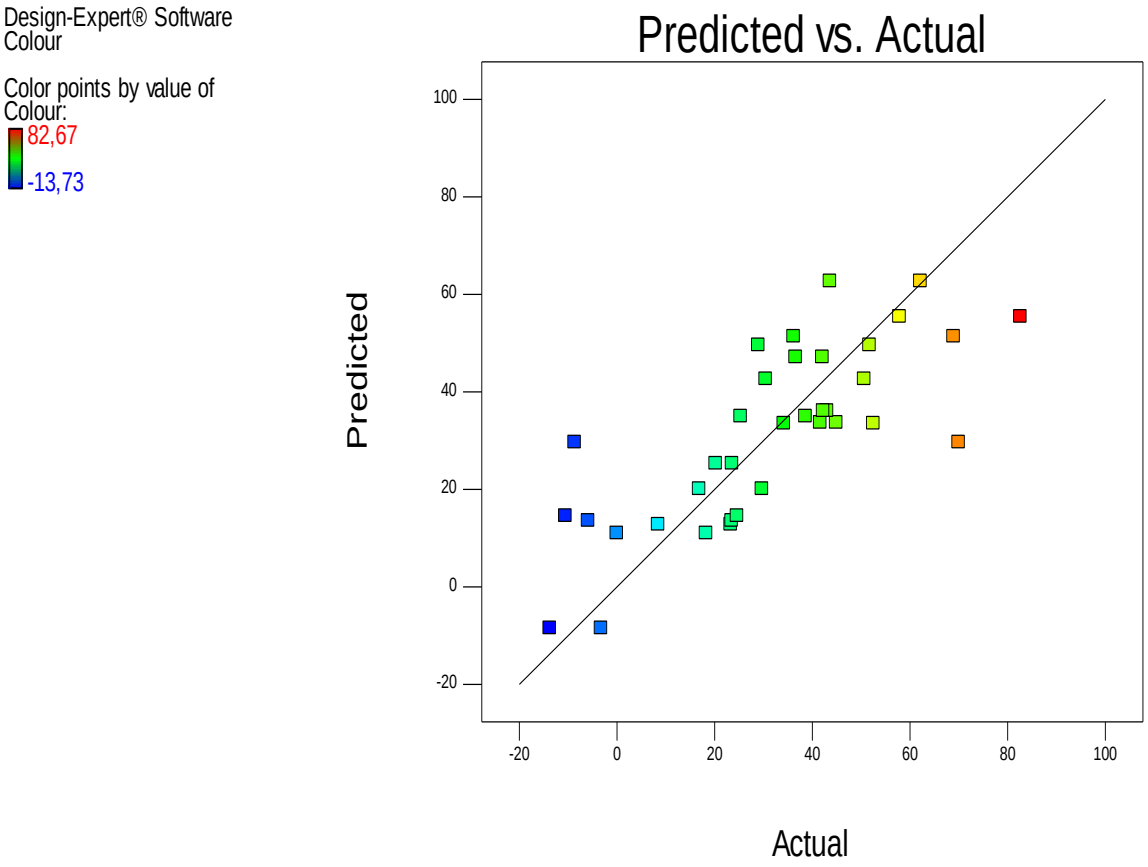

Figure 5.16: Predicted values vs Actual values - colour removal.

Figures 5.17 and 5.18 show the 3D response surface and contour plot of the Ti/Pt electrode, while Figures 5.19 and 5.20 show that of the Ti /$IrO_2Ta_2O_5$ electrode. The 3D and contour plots illustrate the factors for A, B i.e. electrolyte and current density, while the electrode type remains constant. The 3D Figures show that although the model is significant with 0.0008 (Table 5. 8), there is an interaction between B and C (Current density and type of electrode). More interactive terms are AC and A^2, which significantly affect the curvature. This indicates that the interaction between the electrolyte and current density may simultaneously impact the EO – treatment process.

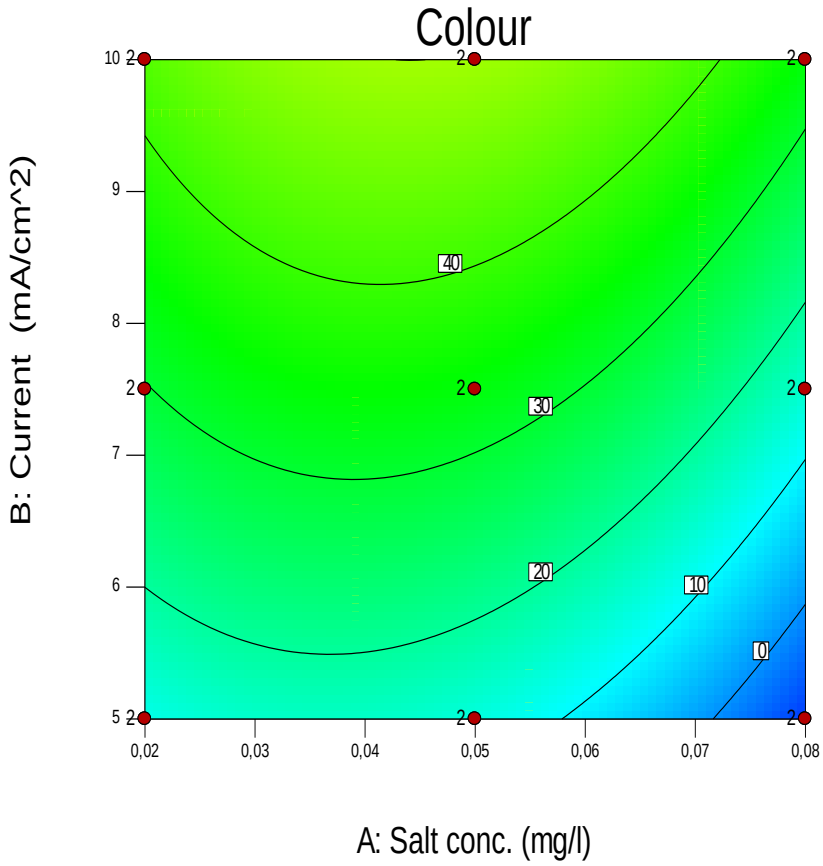

Figure 5.17: Contour plot - colour (Ti/Pt)

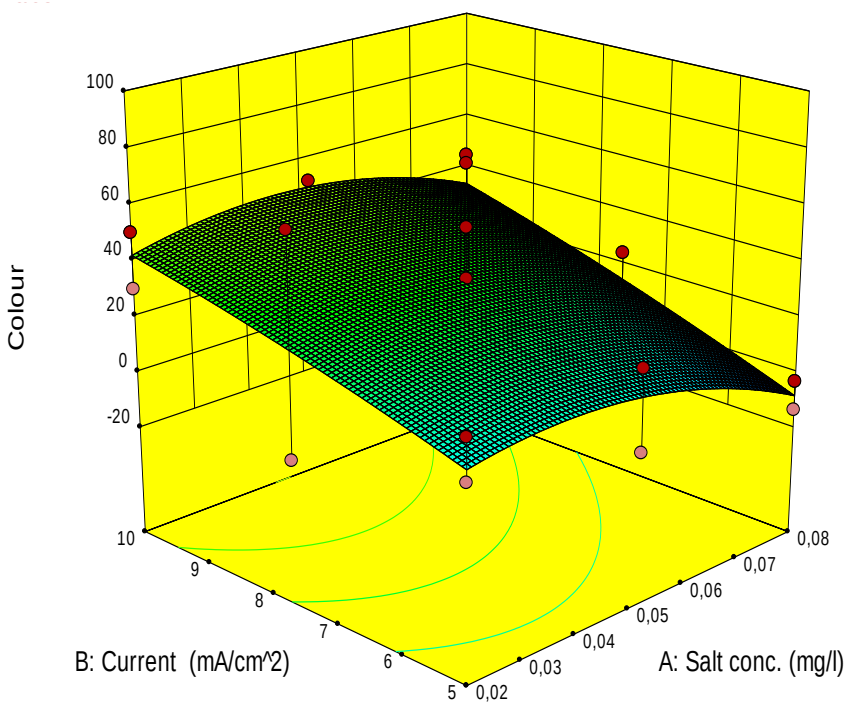

Figure 5.18:3D - Colour plot (Ti/Pt)

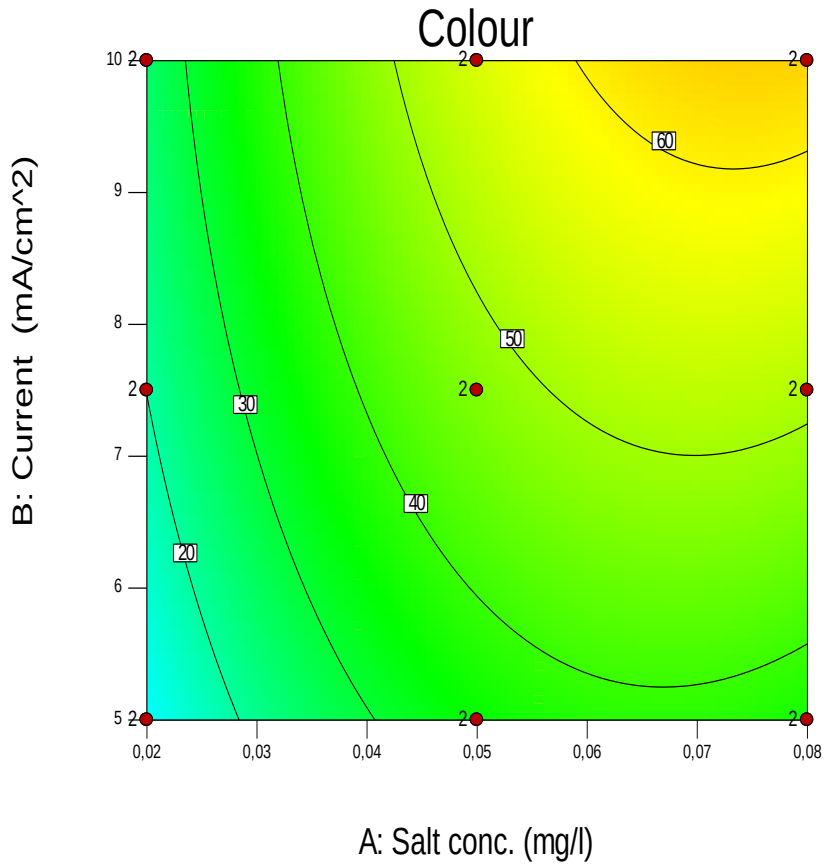

Figure 5.19: Contour plot - colour removal.

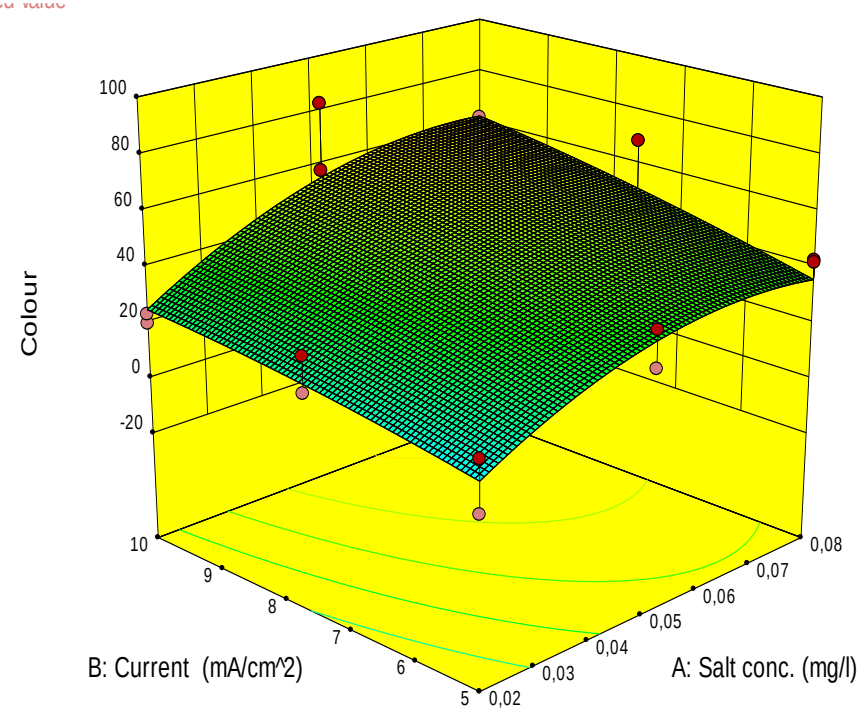

Figure 5.20: 3D colour removal plot.

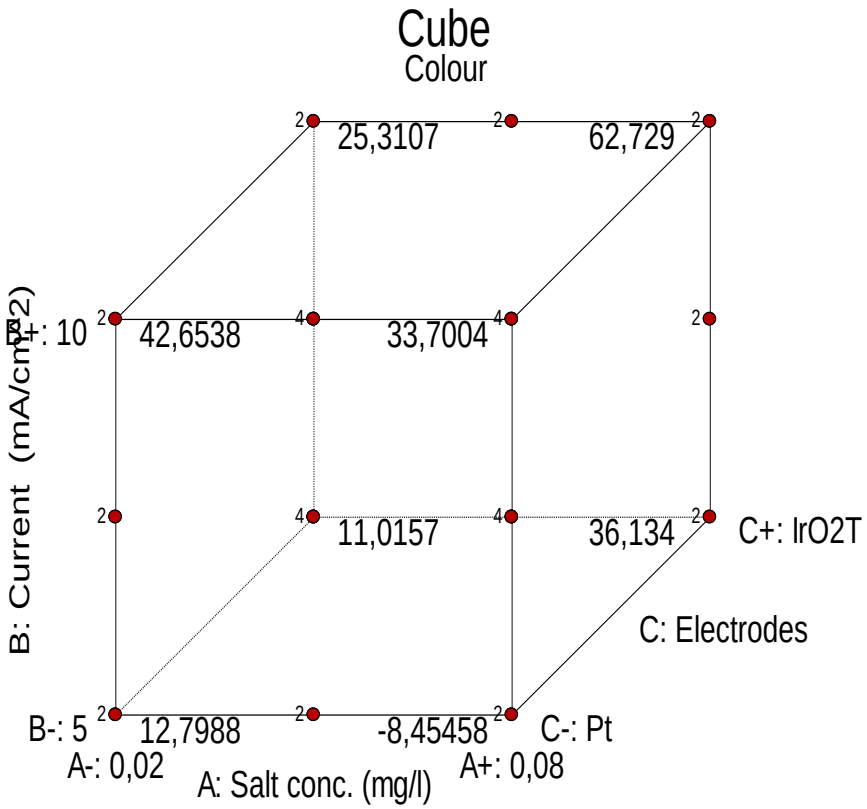

Figure 5.21: Colour removal CCD.

Figure 5.21 illustrates the cube generated for the removal of colour for factors electrolyte, current density and the type of electrode. The critical factors described in this cube are the type of electrode. 82.67% was removed with the Ti /$IrO_2Ta_2O_5$ with 0.05M NaCl electrolyte.

Chapter 6

Conclusion & Recommendation

Chapter 6: Conclusion and Recommendation

6.1. Conclusion

The reduction of COD, micropollutants and contaminants of emerging concerns in municipal secondary MBR wastewater by EO process with Ti/$IrO_2Ta_2O_5$ and Ti/Pt anodes for effluent discharge or possible recycle application was investigated. The research was done on changing the EO system's physical parameters (current densities and electrolyte concentration) and whether those changes efficiently enhance the elimination of COD, ammonia, and CECs.

The inorganic ammonia compound was successfully removed at a maximum removal of 99% (Ti/$IrO_2Ta_2O_5$ anode) and 75% (Ti/Pt anode). However, Ti/Pt has a maximum reduction of 86% for COD. The highest COD removal of Ti/Pt and Ti/ $IrO_2Ta_2O_5$ was 86% (7.5mA/cm^2; 0.08M NaCl) and 71.43% (5mA/cm^2; 0.02M NaCl), respectively. It can be seen that the current density affects COD removal, whereas the increase in current density promotes COD removal. Pt/Ti obtained a higher COD removal than Ti/ $IrO_2Ta_2O_5$. Hydrogen production occurs at the cathode and forms H_2O_2 due to the higher applied current that produces more hydrogen bubbles.

Select pharmaceuticals were monitored through Solid Phase Extraction (SPE) and Gas Chromatography-Mass Spectrometry (GC - MS). A standard curve for each pharmaceutical selected was used to quantify the GC-MS results. At a current density of 10 mA/cm^2 and 0.08M electrolyte anode, Ti/$IrO_2Ta_2O_5$ showed better results than Ti/Pt for CBZ, DCF and IBU of more than 99% pharmaceutical removal due to the increase of electrolyte, specifically IBU.

The optimization of the EO process was conducted using the Central Composite Design (CCD). The ANOVA results showed that the P-value was less than 0.0001 for the model developed, achieving an R^2 value of 0.80 when experimental and modelled results were compared. A quadratic equation obtained from the CCD was developed to predict the removal of COD and colour from secondary municipal MBR effluent. The optimum conditions were both Ti/$IrO_2Ta_2O_5$ and Ti/Pt anodes; NaCl concentration 0.08 and 0.05 M; current density of 5 and 10 mA/cm^2 to obtain a maximum removal efficiency of 80% and 82% for COD and colour, respectively.

Finally, COD, ammonia, and selected pharmaceuticals (IBU, CBZ and DCF) removal using an EO bench-scale unit with Ti/$IrO_2Ta_2O_5$ and Ti/Pt anodes at the predetermined process variables was successful.

6.2. Recommendations

Future studies should investigate the effect of pH on different pharmaceutical compounds, specifically Ibuprofen in acidic, neutral and basic mediums. Also, the toxicity of the pharmaceutical compounds should be investigated. The mother-compound and transformation products of pharmaceuticals should be analysed simultaneously—a comparative study of the effects of different types of electrolytes on the removal of pharmaceuticals.

References

7. **References**

Abdi, O. & Kazemi, M. 2015. A review study of biosorption of heavy metals and comparison between different biosorbents. J. Mater. Environ. Sci.Vol 6, 1386-1399

Access, O. (n.d.). *We are IntechOpen , the world ' s leading publisher of Open Access books Built by scientists , for scientists TOP 1 %*.

Akpotu, S. O., Lawal, I. A., Moodley, B., & Ofomaja, A. E. (2020). Covalently linked graphene oxide/reduced graphene oxide-methoxylether polyethylene glycol functionalised silica for scavenging of estrogen: Adsorption performance and mechanism. *Chemosphere*, *246*. https://doi.org/10.1016/j.chemosphere.2019.125729

Álvarez-Torrellas, S., Peres, J. A., Gil-Álvarez, V., Ovejero, G., & García, J. (2017). Effective adsorption of non-biodegradable pharmaceuticals from hospital wastewater with different carbon materials. *Chemical Engineering Journal*, *320*, 319–329. https://doi.org/10.1016/j.cej.2017.03.077

Ammar, H. B., Brahim, M. Ben, Abdelhédi, R., & Samet, Y. (2016). Green electrochemical process for metronidazole degradation at BDD anode in aqueous solutions via direct and indirect oxidation. *Separation and Purification Technology*, *157*, 9–16. https://doi.org/10.1016/j.seppur.2015.11.027

Archer, E., Wolfaardt, G. M., & van Wyk, J. H. (2017). Pharmaceutical and personal care products (PPCPs) as endocrine disrupting contaminants (EDCs) in South African surface waters. In *Water SA* (Vol. 43, Issue 4, pp. 684–706). South African Water Research Commission. https://doi.org/10.4314/wsa.v43i4.16

Aziz, M., & Ojumu, T. (2020). Exclusion of estrogenic and androgenic steroid hormones from municipal membrane bioreactor wastewater using UF/NF/RO membranes for water reuse application. *Membranes*, *10*(3). https://doi.org/10.3390/membranes10030037

Babu, B. R., Venkatesan, P., Kanimozhi, R., & Basha, C. A. (2009). Removal of pharmaceuticals from wastewater by electrochemical oxidation using cylindrical flow reactor and optimization of treatment conditions. *Journal of Environmental Science and Health - Part A Toxic/Hazardous Substances and Environmental Engineering*, *44*(10), 985–994. https://doi.org/10.1080/10934520902996880

Bagastyo, A. Y., Batstone, D. J., Kristiana, I., Escher, B. I., Joll, C., & Radjenovic, J. (2014). Electrochemical treatment of reverse osmosis concentrate on boron-doped electrodes in undivided and divided cell configurations. *Journal of Hazardous Materials*, *279*, 111–116. https://doi.org/10.1016/j.jhazmat.2014.06.060

Bagnis, S., Fitzsimons, M., Snape, J., Tappin, A., & Comber, S. (2018). Sorption of active pharmaceutical ingredients in untreated wastewater effluent and effect of dilution in freshwater:

Implications for an “impact zone” environmental risk assessment approach. *Science of the Total Environment*, *624*, 333–341. https://doi.org/10.1016/j.scitotenv.2017.12.092

Baresel, C., Cousins, A. P., Hörsing, M., Ek, M., Ejhed, H., Allard, A.-S., Magnér, J., Westling, K., Wahlberg, C., Fortkamp, U., & Söhr, S. (2015). *Pharmaceutical residues and other emerging substances in the effluent of sewage treatment plants Review on concentrations, quantification, behaviour, and removal options*. www.ivl.se

Benito, A., Penadés, A., Lliberia, J. L., & Gonzalez-Olmos, R. (2017). Degradation pathways of aniline in aqueous solutions during electro-oxidation with BDD electrodes and UV/H2O2 treatment. *Chemosphere*, *166*, 230–237. https://doi.org/10.1016/j.chemosphere.2016.09.105

Coria, G., Nava, J. L., & Carreño, G. (2014). Electrooxidation of Diclofenac in Synthetic Pharmaceutical Wastewater Using an Electrochemical Reactor Electrooxidation of Diclofenac in Synthetic Pharmaceutical Wastewater Using an Electrochemical Reactor Equipped with a Boron Doped Diamond Electrode Article. In *Chem. Soc* (Vol. 58, Issue 3).

da Silva, S. W., Navarro, E. M. O., Rodrigues, M. A. S., Bernardes, A. M., & Pérez-Herranz, V. (2018). The role of the anode material and water matrix in the electrochemical oxidation of norfloxacin. *Chemosphere*, *210*, 615–623. https://doi.org/10.1016/j.chemosphere.2018.07.057

Dao, K. C., Yang, C. C., Chen, K. F., & Tsai, Y. P. (2020). Recent trends in removal pharmaceuticals and personal care products by electrochemical oxidation and combined systems. In *Water (Switzerland)* (Vol. 12, Issue 4). MDPI AG. https://doi.org/10.3390/W12041043

Edokpayi, J. N., Odiyo, J. O., & Durowoju, O. S. (2017). Impact of Wastewater on Surface Water Quality in Developing Countries: A Case Study of South Africa. *Water Quality*. https://doi.org/10.5772/66561

Ensano B.M.B., Borea L., Naddeo V., Belgiorno V., De Luna M.D.G., & Ballesteros F.C. (2017). Removal of pharmaceutical compounds by electrochemical processes in real wastewater. *Proceedings of the 15th International Conference on Environmental Science and Technology*, *September*, 2015–2018.

García-Montoya, M. F., Gutiérrez-Granados, S., Alatorre-Ordaz, A., Galindo, R., Ornelas, R., & Peralta-Hernández, J. M. (2015). Application of electrochemical/BDD process for the treatment wastewater effluents containing pharmaceutical compounds. *Journal of Industrial and Engineering Chemistry*, *31*, 238–243. https://doi.org/10.1016/j.jiec.2015.06.030

Ghazouani, M., Akrout, H., Jomaa, S., Jellali, S., & Bousselmi, L. (2016). Enhancing removal of nitrates from highly concentrated synthetic wastewaters using bipolar Si/BDD cell: Optimization and mechanism study. *Journal of Electroanalytical Chemistry*, *783*, 28–40. https://doi.org/10.1016/j.jelechem.2016.10.048

Gherardini, L., Michaud, P. A., Panizza, M., Comninellis, C., & Vatistas, N. (2001). Electrochemical Oxidation of 4-Chlorophenol for Wastewater Treatment: Definition of Normalized Current Efficiency (φ). *Journal of The Electrochemical Society*, *148*(6), D78. https://doi.org/10.1149/1.1368105

Hansen, K. M. S., Spiliotopoulou, A., Chhetri, R. K., Escolà Casas, M., Bester, K., & Andersen, H. R. (2016). Ozonation for source treatment of pharmaceuticals in hospital wastewater - Ozone lifetime and required ozone dose. *Chemical Engineering Journal*, *290*, 507–514. https://doi.org/10.1016/j.cej.2016.01.027

Heim, C., Ureña de Vivanco, M., Rajab, M., Müller, E., Letzel, T., & Helmreich, B. (2015). Rapid inactivation of waterborne bacteria using boron-doped diamond electrodes. *International Journal of Environmental Science and Technology*, *12*(10), 3061–3070. https://doi.org/10.1007/s13762-014-0722-9

Hurwitz, G., Hoek, E. M. V., Liu, K., Fan, L., & Roddick, F. A. (2014). Photo-assisted electrochemical treatment of municipal wastewater reverse osmosis concentrate. *Chemical Engineering Journal*, *249*, 180–188. https://doi.org/10.1016/j.cej.2014.03.084

Lee, Y., Kovalova, L., McArdell, C. S., & von Gunten, U. (2014). Prediction of micropollutant elimination during ozonation of a hospital wastewater effluent. *Water Research*, *64*, 134–148. https://doi.org/10.1016/j.watres.2014.06.027

Li, B. S., Lin, A., & Gan, F. X. (2006). Preparation and electrocatalytic properties of Ti/IrO2-Ta2O5 anodes for oxygen evolution. *Transactions of Nonferrous Metals Society of China (English Edition)*, *16*(5), 1193–1199. https://doi.org/10.1016/S1003-6326(06)60400-7

Loos, G., Scheers, T., Van Eyck, K., Van Schepdael, A., Adams, E., Van der Bruggen, B., Cabooter, D., & Dewil, R. (2018). Electrochemical oxidation of key pharmaceuticals using a boron doped diamond electrode. *Separation and Purification Technology*, *195*(October 2017), 184–191. https://doi.org/10.1016/j.seppur.2017.12.009

Madikizela, L. M., Ncube, S., & Chimuka, L. (2018). Uptake of pharmaceuticals by plants grown under hydroponic conditions and natural occurring plant species: A review. In *Science of the Total Environment* (Vol. 636, pp. 477–486). Elsevier B.V. https://doi.org/10.1016/j.scitotenv.2018.04.297

Madikizela, L. M., Ncube, S., & Chimuka, L. (2020). Analysis, occurrence and removal of pharmaceuticals in African water resources: A current status. In *Journal of Environmental Management* (Vol. 253). Academic Press. https://doi.org/10.1016/j.jenvman.2019.109741

Martín, J., Santos, J. L., Aparicio, I., & Alonso, E. (2015). Pharmaceutically active compounds in sludge stabilization treatments: Anaerobic and aerobic digestion, wastewater stabilization ponds

and composting. *Science of the Total Environment*, *503–504*, 97–104. https://doi.org/10.1016/j.scitotenv.2014.05.089

Mordačíková, E., Vojs, M., Grabicová, K., Marton, M., Michniak, P., Řeháček, V., Bořík, A., Grabic, R., Bruncko, J., Mackuľak, T., & Vojs Staňová, A. (2020). Influence of boron doped diamond electrodes properties on the elimination of selected pharmaceuticals from wastewater. *Journal of Electroanalytical Chemistry*, *862*. https://doi.org/10.1016/j.jelechem.2020.114007

Orimolade, B. O., Zwane, B. N., Koiki, B. A., Tshwenya, L., Peleyeju, G. M., Mabuba, N., Zhou, M., & Arotiba, O. A. (2020). Solar photoelectrocatalytic degradation of ciprofloxacin at a FTO/BiVO4/MnO2 anode: Kinetics, intermediate products and degradation pathway studies. *Journal of Environmental Chemical Engineering*, *8*(1). https://doi.org/10.1016/j.jece.2019.103607

Patel, P. S., Bandre, N., Saraf, A., & Ruparelia, J. P. (2013). Electro-catalytic materials (electrode materials) in electrochemical wastewater treatment. *Procedia Engineering*, *51*, 430–435. https://doi.org/10.1016/j.proeng.2013.01.060

Peralta-Hernández, J. M., Méndez-Tovar, M., Guerra-Sánchez, R., Martínez-Huitle, C. A., & Nava, J. L. (2012). A Brief Review on Environmental Application of Boron Doped Diamond Electrodes as a New Way for Electrochemical Incineration of Synthetic Dyes. *International Journal of Electrochemistry*, *2012*, 1–18. https://doi.org/10.1155/2012/154316

Radjenovic, J., & Sedlak, D. L. (2015). Challenges and Opportunities for Electrochemical Processes as Next-Generation Technologies for the Treatment of Contaminated Water. In *Environmental Science and Technology* (Vol. 49, Issue 19, pp. 11292–11302). American Chemical Society. https://doi.org/10.1021/acs.est.5b02414

Rajab, M., Greco, G., Heim, C., Helmreich, B., & Letzel, T. (2013). Serial coupling of RP and zwitterionic hydrophilic interaction LC-MS: Suspects screening of diclofenac transformation products by oxidation with a boron-doped diamond electrode. *Journal of Separation Science*, *36*(18), 3011–3018. https://doi.org/10.1002/jssc.201300562

Rajab, M., Heim, C., Greco, G., Helmreich, B., & Letzel, T. (2013). Removal of Sulfamethoxazole from Wastewater Treatment Plant Effluents by a Boron-doped Diamond Electrode. *International Journal of Environmental Pollution and Solutions*. https://doi.org/10.7726/ijeps.2013.1008

Sahu, O. (2019). Electro-oxidation and chemical oxidation treatment of sugar industry wastewater with ferrous material: An investigation of physicochemical characteristic of sludge. *South African Journal of Chemical Engineering*, *28*, 26–38. https://doi.org/10.1016/j.sajce.2019.01.004

Templeton, M. R., & Butler, P. D. (n.d.). *Introduction to Wastewater Treatment*.

Teymouri, M., Karkhane, M., Marzban, M., & Marzban, A. (2017). Designing a Response Surface Model for Removing Phosphate and Organic Compound from Wastewater by Pseudomonas

Strain MT1. *Proceedings of the National Academy of Sciences India Section B - Biological Sciences*, *87*(4), 1167–1176. https://doi.org/10.1007/s40011-015-0686-7

Togola, A., & Budzinski, H. (2007). Analytical development for analysis of pharmaceuticals in water samples by SPE and GC-MS. *Analytical and Bioanalytical Chemistry*, *388*(3), 627–635. https://doi.org/10.1007/s00216-007-1251-x

Umar, M., Roddick, F. A., Fan, L., Autin, O., & Jefferson, B. (2015). Treatment of municipal wastewater reverse osmosis concentrate using UVC-LED/H2O2 with and without coagulation pre-treatment. *Chemical Engineering Journal*, *260*, 649–656. https://doi.org/10.1016/j.cej.2014.09.028

Urtiaga, A. M., Pérez, G., Ibáñez, R., & Ortiz, I. (2013). Removal of pharmaceuticals from a WWTP secondary effluent by ultrafiltration/reverse osmosis followed by electrochemical oxidation of the RO concentrate. *Desalination*, *331*, 26–34. https://doi.org/10.1016/j.desal.2013.10.010

Verlicchi, P., Al Aukidy, M., & Zambello, E. (2012). Occurrence of pharmaceutical compounds in urban wastewater: Removal, mass load and environmental risk after a secondary treatment-A review. *Science of the Total Environment*, *429*, 123–155. https://doi.org/10.1016/j.scitotenv.2012.04.028

Wanda, E. M. M., Nyoni, H., Mamba, B. B., & Msagati, T. A. M. (2018). Application of silica and germanium dioxide nanoparticles/ polyethersulfone blend membranes for removal of emerging micropollutants from water. *Physics and Chemistry of the Earth*, *108*, 28–47. https://doi.org/10.1016/j.pce.2018.08.004

Wastewater Characteristics, Treatment and Disposal. (2007). IWA Publishing.

Yao, W., Ur Rehman, S. W., Wang, H., Yang, H., Yu, G., & Wang, Y. (2018). Pilot-scale evaluation of micropollutant abatements by conventional ozonation, UV/O3, and an electro-peroxone process. *Water Research*, *138*, 106–117. https://doi.org/10.1016/j.watres.2018.03.044

Zaidi, S., Chaabane, T., Sivasankar, V., Darchen, A., Maachi, R., & Msagati, T. A. M. (2019). Electro-coagulation coupled electro-flotation process: Feasible choice in doxycycline removal from pharmaceutical effluents. *Arabian Journal of Chemistry*, *12*(8), 2798–2809. https://doi.org/10.1016/j.arabjc.2015.06.009

Zhou, M., Liu, L., Jiao, Y., Wang, Q., & Tan, Q. (2011). Treatment of high-salinity reverse osmosis concentrate by electrochemical oxidation on BDD and DSA electrodes. *Desalination*, *277*(1–3), 201–206. https://doi.org/10.1016/j.desal.2011.04.030

Zou, J., Peng, X., Li, M., Xiong, Y., Wang, B., Dong, F., & Wang, B. (2017). Electrochemical oxidation of COD from real textile wastewaters: Kinetic study and energy consumption. *Chemosphere*, *171*, 332–338. https://doi.org/10.1016/j.chemosphere.2016.12.065

Appendix A (Sample Calculations)

Moles of Sodium Chloride ($NaCl$) at 0,08M

$$Molarity(M) = \frac{Moles\ of\ solute\ (n_{solvent})}{Volume\ (V)}$$

$$0{,}08M = \frac{n}{1l}$$

$$n = 0{,}08\ mol\ NaCl$$

Mass of Sodium Chloride ($NaCl$) at 0,08M

$$Moles\ (n) = \frac{mass\ (m)}{Molar\ mass\ (M_w)}$$

$$0{,}08\ mol\ NaCl = \frac{m}{58{,}44\frac{g}{mol}}$$

$$m = 4{,}67g\ NaCl$$

Volume of sulfuric Acid (H_2SO_4) for 0,5M

$$Volume\ of\ 1M\ H_2SO_4\ with\ 98\%\ Assay:$$

$$Volume(ml) = \frac{Molecular\ mass\ (M_w)}{Specific\ Gravity(d)}$$

$$Volume = \frac{98{,}08\ g/mol}{1{,}84}$$

$$Volume = 53{,}03\ ml$$

$$\sim 98\%\ H_2SO_4 = \ 53{,}03\ ml$$

$$\sim 100\%\ H_2SO_4 = \quad ?$$

$$V_{1M} = \frac{53{,}03 \times 100}{98}$$

$$V_{1M} = 54{,}38ml$$

$$\therefore 1M \equiv 1000ml \equiv 54{,}38\ ml\ H_2SO_4$$

$$\therefore V_{0{,}5M} = \frac{54{,}38 \times 0{,}5}{1}$$

$$\therefore V_{0{,}5M} = 27{,}19ml\ H_2SO_4/1000ml\ H_2O$$

Experimental Run 1 Sample Calculations

Current density at 2A

$$Current\ Density\ (J) = \frac{Current\ (I)}{Anode\ surface\ area\ (A)}$$

$$J = \frac{2A}{10cm \times 10cm \times 2} \times 1000$$

$$J = 10mA/cm^2$$

%COD Removal

$$\%\ COD\ Removal = \frac{COD_{initial} - COD_{final}}{COD_{initial}} \times 100$$

$$= \frac{330 - 100}{330} \times 100$$

$$= 69.7\%$$

Instantaneous current efficiency

$$\%ICE = \frac{FV\Delta COD}{8I\Delta t}$$

$$= \frac{(96487)(0.003)(120 - 103)}{(8)(1.5)(18000)}$$

$$= 2.28\%$$

Appendix B (Inorganic and Organic compounds data)

Table B1 COD removal

Table B1:**Electrode**	**Experimental Run**	**Electrolyte (NaCl)**	**Current density**	**Average Voltage**	**Feed**	**COD Effluent**	**COD removal**
		M	mA/cm^2	V	mg/l	mg/l	%
$Ti/IrO_2Ta_2O_5$	1	0,08	7,5	5,45	120	103	14,17
	2	0,08	5	4,42	330	100	**69,70**
	3	0,08	10	10,25	1120	570	**49,11**
	4	0,02	5	8,5	840	240	**71,43**
	5	0,02	7,5	12,42	260	190	26,92
	6	0,02	10	12,83	205	145	29,27
	7	0,05	5	6,58	175	150	14,29
	8	0,05	7,5	9,25	630	470	25,40
	9	0,05	10	9,33	250	148	40,80
Ti/Pt	10	0,02	5	9	380	182	52,11
	11	0,02	7,5	10,08	380	188	50,53
	12	0,02	10	14	350	155	55,71
	13	0,05	5	5,98	360	186	48,33
	14	0,05	7,5	7,92	220	200	9,09
	15	0,05	10	8,92	450	325	27,78
	16	0,08	5	5,58	450	149	**66,89**
	17	0,08	7,5	7,25	500	70	**86,00**
	18	0,08	10	8,25	520	150	71,15

Table B2 Ammonia removal.

Electrode	**Experimental Run**	**Electrolyte (NaCl)**	**Current density**	**% Removal**		
		M	mA/cm^2	NH3-N	NH3	NH4+
$Ti/IrO_2Ta_2O_5$	1	0,08	7,5	35,59	35,62	35,63
	2	0,08	5	100,00	100,00	100,00
	3	0,08	10	99,46	99,45	99,48
	4	0,02	5	35,91	35,89	35,97
	5	0,02	7,5	59,73	59,73	59,72
	6	0,02	10	90,63	90,69	90,70
	7	0,05	5	98,64	98,63	98,59
	8	0,05	7,5	99,15	99,19	99,12
	9	0,05	10	99,31	99,32	99,35
Ti/Pt	10	0,02	5	35,34	35,27	35,28
	11	0,02	7,5	39,64	39,66	39,59
	12	0,02	10	15,85	16,00	16,04
	13	0,05	5	75,43	75,45	75,50
	14	0,05	7,5	59,15	59,16	59,20
	15	0,05	10	80,28	80,35	80,33
	16	0,08	5	60,22	60,18	60,00
	17	0,08	7,5	66,22	65,56	65,26
	18	0,08	10	74,51	75,00	74,81

Table B3 DCF concentrations

Run	Feed (µg/l)	Effluent (µg/l)	%removal	Average	StDev
1,1	950	0,36977	99,96107685	99,96161	0,000747
1,2	975	0,3692	99,96213331		
2,1	950	0,363407	99,96174667	99,96271	0,00136
2,2	1000	0,363294	99,96367057		
3,1	975	0,347162	99,96439364	99,96287	0,002153
3,2	925	0,357519	99,9613493		
4,1	975	0,453708	99,95346587	99,95626	0,003946
4,2	1025	0,41977	99,95904684		
5,1	925	0,441132	99,95231001	99,95454	0,00316
5,2	925	0,399793	99,95677909		
6,1	1050	0,370624	99,9647025	99,9627	0,002828
6,2	975	0,383145	99,96070312		
7,1	1050	0,374836	99,96430133	99,9698	0,007775
7,2	1500	0,370554	99,97529643		
8,1	1100	0,361366	99,96714857	99,92608	0,058087
8,2	1125	1,293731	99,88500168		
9,1	1175	0,371225	99,96840642	99,95423	0,020051
9,2	950	0,569526	99,94004985		
10,1	950	0,417522	99,95605032	99,95731	0,001788
10,2	1075	0,445281	99,95857851		
11,1	1025	0,348519	99,96599811	99,96354	0,00348
11,2	900	0,350304	99,96107729		
12,1	975	0,349961	99,96410658	99,96202	0,002956
12,2	925	0,370677	99,95992684		
13,1	950	0,354541	99,96267985	99,96627	0,005077
13,2	1150	0,346612	99,96985981		
14,1	1175	0,355477	99,96974664	99,96707	0,003787
14,2	1000	0,356085	99,96439153		
15,1	1025	0,651502	99,93643885	99,95029	0,019594
15,2	975	0,349542	99,96414949		
16,1	1150	0,36236	99,96849043	99,96489	0,005088
16,2	900	0,348343	99,96129519		
17,1	1075	0,348373	99,96759322	99,96586	0,002452
17,2	975	0,349778	99,96412537		
18,1	1050	0,35057	99,9666124	99,96406	0,003608
18,2	950	0,365656	99,96150989		

Table B4: CBZ concentrations

Run	Feed (µg/l)	Effluent (µg/l)	%removal	Average	StDev
1,1	900	0,294074	99,96732508	99,96777	0,000629
1,2	925	0,294012	99,96821494		
2,1	900	0,295928	99,96711909	99,96807	0,001339
2,2	950	0,294383	99,96901235		
3,1	1025	0,302825	99,97045614	99,96878	0,002376
3,2	925	0,304362	99,96709601		
4,1	925	0,340806	99,9631561	99,96401	0,001201
4,2	1025	0,360246	99,96485405		
5,1	975	0,364456	99,96261991	99,9555	0,010075
5,2	925	0,477566	99,94837123		
6,1	1050	0,406089	99,96132488	99,95661	0,006667
6,2	925	0,444965	99,95189568		
7,1	1000	0,412877	99,95871233	99,9606	0,002664
7,2	975	0,365825	99,96247953		
8,1	925	0,295935	99,96800699	99,97089	0,004084
8,2	1225	0,321166	99,97378233		
9,1	1150	0,317692	99,9723746	99,97052	0,002627
9,2	925	0,289904	99,96865904		
10,1	950	0,308398	99,96753702	99,96807	0,000754
10,2	1075	0,337519	99,96860293		
11,1	1175	0,311155	99,97351872	99,97225	0,001799
11,2	1000	0,290261	99,9709739		
12,1	1200	0,413652	99,96552897	99,96824	0,003829
12,2	1000	0,290565	99,97094349		
13,1	1100	0,290867	99,97355752	99,97064	0,004127
13,2	900	0,290515	99,96772051		
14,1	1150	0,29472	99,97437221	99,97503	0,000927
14,2	1200	0,29181	99,9756825		
15,1	1025	0,290994	99,97161037	99,97213	0,000735
15,2	1050	0,287173	99,97265024		
16,1	1175	0,292519	99,97510473	99,97193	0,004485
16,2	925	0,288952	99,96876194		
17,1	1075	0,291819	99,97285406	99,97053	0,003285
17,2	900	0,28613	99,96820778		
18,1	975	0,283639	99,97090879	99,97077	0,000193
18,2	975	0,286306	99,97063528		

Table B5: IBU Data.

Run	Feed	Effluent	%removal	Average	StDev
1,1	1000	0,553437	99,94465631	99,95742	0,018055
1,2	1050	0,313011	99,97018944		
2,1	1075	1,119395	99,89587019	99,91442	0,026237
2,2	975	0,653495	99,93297492		
3,1	950	0,266711	99,97192513	99,97054	0,001965
3,2	925	0,285399	99,96914604		
4,1	1025	3,420038	99,66633773	99,62587	0,057231
4,2	1050	4,353284	99,58540154		
5,1	950	123,4527	87,0049762	93,35575	8,981347
5,2	925	2,714699	99,70651901		
6,1	950	1,921198	99,79776864	99,76197	0,050621
6,2	1050	2,875116	99,72617938		
7,1	950	2,824944	99,70263751	99,74113	0,054443
7,2	975	2,148593	99,77963151		
8,1	1025	0,577168	99,94369093	96,9613	4,21774
8,2	1150	69,24258	93,97890584		
9,1	1150	2,868401	99,75057387	98,01865	2,449306
9,2	1200	44,55922	96,28673164		
10,1	1150	6,841343	99,40510063	99,30748	0,138057
10,2	1000	7,901419	99,20985812		
11,1	1175	1,715727	99,85398065	99,85787	0,005497
11,2	900	1,244205	99,86175495		
12,1	1125	111,512	90,08781927	94,82508	6,699497
12,2	950	4,157778	99,56233911		
13,1	1075	9,181233	99,14593184	99,35973	0,302355
13,2	1000	4,264736	99,57352639		
14,1	900	4,612761	99,487471	99,42992	0,081385
14,2	1000	6,276241	99,37237588		
15,1	925	2,261609	99,7555017	99,81786	0,088186
15,2	975	1,167905	99,88021485		
16,1	1075	6,72884	99,37406144	99,45161	0,109674
16,2	1100	5,179196	99,52916399		
17,1	900	3,227572	99,6413809	99,53546	0,149793
17,2	1050	5,989811	99,42954182		
18,1	1125	13,22518	98,82442857	99,282	0,647099
18,2	1050	2,734563	99,73956541		

Table B6: Ammonia data

	NH3				
Run	**Feed**	**Effluent**	**% removal**	**Ave.**	**Std. Dev.**
	mg/l				
1,1	9,32	6	35,62	67,47025	45,03977752
1,2	8,8	0,06	99,32		
2,1	10,36	0	100,00	99,84359	0,221201287
2,2	9,59	0,03	99,69		
3,1	9,08	0,05	99,45	99,28268	0,235690787
3,2	9,05	0,08	99,12		
4,1	9,92	6,36	35,89	34,23898	2,330794343
4,2	8,53	5,75	32,59		
5,1	8,07	3,25	59,73	61,02223	1,831185799
5,2	8,2	3,09	62,32		
6,1	9,34	0,87	90,69	82,85734	11,07030709
6,2	8,49	2,12	75,03		
7,1	8,05	0,11	98,63	91,57521	9,981986211
7,2	8,59	1,33	84,52		
8,1	8,61	0,07	99,19	99,37492	0,265765843
8,2	9,15	0,04	99,56		
9,1	8,78	0,06	99,32	99,10069	0,305378444
9,2	8,07	0,09	98,88		
10,1	8,08	5,23	35,27	67,47292	45,5385825
10,2	9,19	0,03	99,67		
11,1	8,8	5,31	39,66	41,90371	3,174364201
11,2	8,63	4,82	44,15		
12,1	10	8,4	16,00	24,66667	12,25651754
12,2	10,8	7,2	33,33		
13,1	9,9	2,43	75,45	64,94887	14,85726867
13,2	8,89	4,05	54,44		
14,1	8,3	3,39	59,16	69,97686	15,30212658
14,2	13,8	2,65	80,80		
15,1	17,3	3,4	80,35	68,29841	17,0390254
15,2	9,6	4,2	56,25		
16,1	11,3	4,5	60,18	68,97738	12,44563558
16,2	9,9	2,2	77,78		
17,1	9	3,1	65,56	64,02778	2,160604054
17,2	12,8	4,8	62,50		
18,1	12,4	3,1	75,00	71,93396	4,336032149
18,2	10,6	3,3	68,87		

Table B7: NH^{4+} data.

	NH^{4+}				
Run	**Feed**	**Effluent**	**%removal**	**Ave.**	**Std. Dev.**
	mg/l				
1,1	9,88	6,36	35,63	67,43823	44,98712102
1,2	9,32	0,07	99,25		
2,1	10,98	0	100,00	99,85236	0,208791372
2,2	10,16	0,03	99,70		
3,1	9,62	0,05	99,48	99,32302	0,222350982
3,2	9,59	0,08	99,17		
4,1	10,51	6,73	35,97	34,29925	2,356789408
4,2	9,04	6,09	32,63		
5,1	8,54	3,44	59,72	60,96548	1,762825699
5,2	8,68	3,28	62,21		
6,1	9,89	0,92	90,70	82,83493	11,11959573
6,2	8,99	2,25	74,97		
7,1	8,52	0,12	98,59	91,54852	9,960344862
7,2	9,1	1,41	84,51		
8,1	9,12	0,08	99,12	99,35501	0,328377762
8,2	9,69	0,04	99,59		
9,1	9,3	0,06	99,35	99,1511	0,288125004
9,2	8,55	0,09	98,95		
10,1	8,56	5,54	35,28	67,43464	45,47299516
10,2	9,73	0,04	99,59		
11,1	9,32	5,63	39,59	41,84209	3,181718208
11,2	9,14	5,11	44,09		
12,1	10,6	8,9	16,04	24,68553	12,22983427
12,2	11,4	7,6	33,33		
13,1	10,49	2,57	75,50	64,95534	14,91307628
13,2	9,41	4,29	54,41		
14,1	8,8	3,59	59,20	70,07846	15,37804196
14,2	14,7	2,8	80,95		
15,1	18,3	3,6	80,33	68,35021	16,9389691
15,2	10,2	4,45	56,37		
16,1	12	4,8	60,00	64,56731	6,459148482
16,2	10,4	3,21	69,13		
17,1	9,5	3,3	65,26	63,88158	1,953847685
17,2	13,6	5,1	62,50		
18,1	13,1	3,3	74,81	71,77958	4,28447334
18,2	11,2	3,5	68,75		

Table B8: NH_3 - N Data.

	NH_3-N				
Run	**Feed**	**Effluent**	**%Removal**	**Ave.**	**Std. Dev.**
	mg/l				
1,1	7,67	4,94	35,59	67,45083	45,05346181
1,2	7,23	0,05	99,31		
2,1	8,52	0	100,00	99,8731	0,179468726
2,2	7,88	0,02	99,75		
3,1	7,47	0,04	99,46	99,32904	0,191609235
3,2	7,44	0,06	99,19		
4,1	8,16	5,23	35,91	34,26397	2,323397407
4,2	7,02	4,73	32,62		
5,1	6,63	2,67	59,73	61,02152	1,828601663
5,2	6,74	2,54	62,31		
6,1	7,68	0,72	90,63	82,77668	11,0991958
6,2	6,98	1,75	74,93		
7,1	6,62	0,09	98,64	91,54089	10,04033796
7,2	7,07	1,1	84,44		
8,1	7,08	0,06	99,15	99,3768	0,317152564
8,2	7,52	0,03	99,60		
9,1	7,22	0,05	99,31	99,13	0,255757759
9,2	6,64	0,07	98,95		
10,1	6,65	4,3	35,34	67,47076	45,44209619
10,2	7,56	0,03	99,60		
11,1	7,24	4,37	39,64	41,8627	3,142116002
11,2	7,1	3,97	44,08		
12,1	8,2	6,9	15,85	24,78076	12,62483058
12,2	8,9	5,9	33,71		
13,1	8,14	2	75,43	64,93797	14,83793647
13,2	7,31	3,33	54,45		
14,1	6,83	2,79	59,15	70,014	15,36287608
14,2	11,4	2,18	80,88		
15,1	14,2	2,8	80,28	68,24211	17,02653626
15,2	7,9	3,46	56,20		
16,1	9,3	3,7	60,22	67,08284	9,712510109
16,2	8,1	2,11	73,95		
17,1	7,4	2,5	66,22	64,24018	2,794532154
17,2	10,6	4	62,26		
18,1	10,2	2,6	74,51	71,73766	3,920402708
18,2	8,7	2,7	68,97		

Table B9: COD Data.

Run	CODi	CODf	%COD removal	COD Ave	Std. Dev
	mg/l				
1,1	120	103	14,17	12,35	2,57
1,2	570	510	10,53		
2,1	330	100	69,70	80,30	15,00
2,2	110	10	90,91		
3,1	1120	570	49,11	50,36	1,77
3,2	310	150	51,61		
4,1	840	240	71,43	72,08	0,92
4,2	220	60	72,73		
5,1	260	190	26,92	24,57	3,32
5,2	135	105	22,22		
6,1	205	145	29,27	29,63	0,52
6,2	150	105	30,00		
7,1	175	150	14,29	14,72	0,61
7,2	165	140	15,15		
8,1	630	470	25,40	51,73	37,24
8,2	670	147	78,06		
9,1	250	148	40,80	38,29	3,54
9,2	190	122	35,79		
10,1	380	182	52,11	41,41	15,13
10,2	560	388	30,71		
11,1	380	188	50,53	51,76	1,75
11,2	400	188	53,00		
12,1	350	155	55,71	48,80	9,77
12,2	370	215	41,89		
13,1	360	186	48,33	37,88	14,79
13,2	310	225	27,42		
14,1	220	200	9,09	19,36	14,52
14,2	540	380	29,63		
15,1	450	325	27,78	35,68	11,18
15,2	390	220	43,59		
16,1	450	149	66,89	48,55	25,94
16,2	480	335	30,21		
17,1	500	70	86,00	79,57	9,09
17,2	540	145	73,15		
18,1	520	150	71,15	64,15	9,91
18,2	280	120	57,14		

Table B10: Colour Data

Run	Feed	Effluent		Removal	Ave removal	Std. Dev.
				%	%	
1,1	87	27		68,97	52,60	23,15
1,2	69	44		36,23		
2,1	79	45		43,04	42,65	0,55
2,2	71	41		42,25		
3,1	262	99		62,21	52,94	13,12
3,2	71	40		43,66		
4,1	82	67		18,29	9,15	12,93
4,2	76	76		0,00		
5,1	74	52		29,73	23,30	9,09
5,2	83	69		16,87		
6,1	79	63		20,25	21,93	2,37
6,2	72	55		23,61		
7,1	67	50		25,37	32,02	9,40
7,2	75	46		38,67		
8,1	76	44		42,11	39,36	3,88
8,2	71	45		36,62		
9,1	75	13		82,67	70,28	17,52
9,2	38	16		57,89		
10,1	59	54		8,47	15,90	10,51
10,2	60	46		23,33		
11,1	58	63		-8,62	30,69	55,59
11,2	70	21		70,00		
12,1	73	36		50,68	40,59	14,28
12,2	82	57		30,49		
13,1	68	52		23,53	8,82	20,80
13,2	51	54		-5,88		
14,1	59	28		52,54	43,38	12,96
14,2	76	50		34,21		
15,1	85	41		51,76	40,38	16,11
15,2	69	49		28,99		
16,1	62	64		-3,23	-8,48	7,42
16,2	51	58		-13,73		
17,1	65	49		24,62	7,04	24,85
17,2	57	63		-10,53		
18,1	72	42		41,67	43,30	2,31
18,2	69	38		44,93		

Appendix C (GC –MS Analysis)

Table C1: GC - MS peak area

Name	RT	m/z	Area 0	Area 1	Area 2	Area 3	Area 4	Area 5	Area 6
IBU	8.758	160	1635	13180	79460	155297	441602	768353	1629957
CBZ	14.803	193	189	38835	266889	577853	1412991	192012	7266040
DCF	15.099	214	789	8185	74500	156413	412362	989887	1749398
Dihexyl phthalate – 3,4,5,6-d_4 (4µg)	15.555	153	6208767	6330109	7155450	6088942	6950008	6474305	5810212

Table C2: GC -MS Standard Curve Data

Pharmaceutical normalized	Point					
Ibu normalized with Dihexyl						
µg	0,1	0,5	1	2	4	8
Ibu peak area/Dihexyl peak area	0,0021	0,0111	0,0255	0,0635	0,1187	0,2805
Cbz normalized with Dihexyl						
µg	0,1	0,5	1	2	5	10
Cbz peak area/Dihexyl peak area	0,0061	0,0373	0,0949	0,2033	0,5245	1,2506
Diclo normalized with Dihexyl						
µg	0,1	0,75	1,5	3	6	12
Diclo peak area/Dihexyl peak area	0,0013	0,0104	0,0257	0,0593	0,1529	0,3011

Quantification Curves

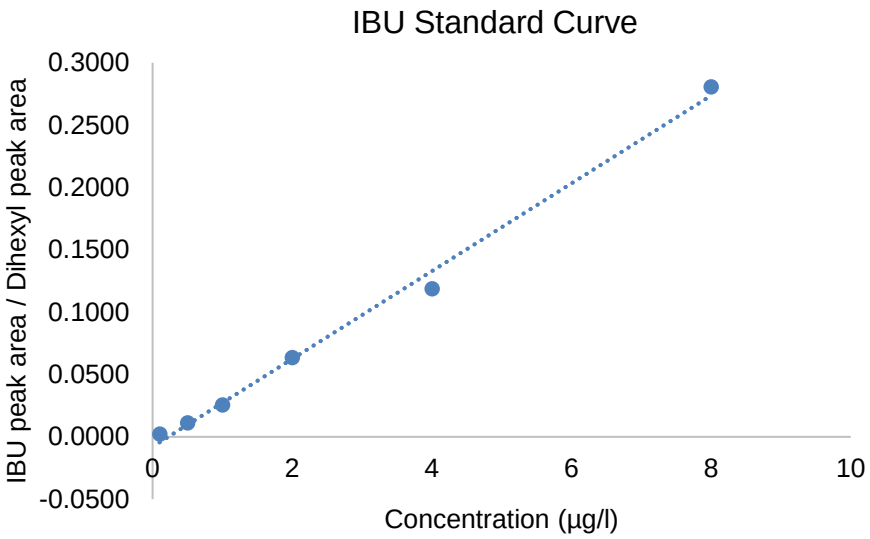

Figure C1: IBU standard Curve

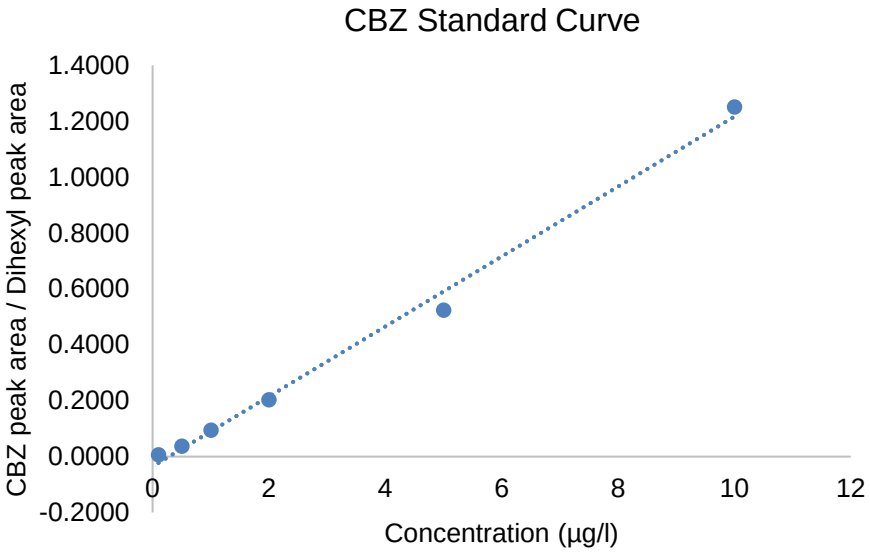

Figure C2: CBZ Standard Curve

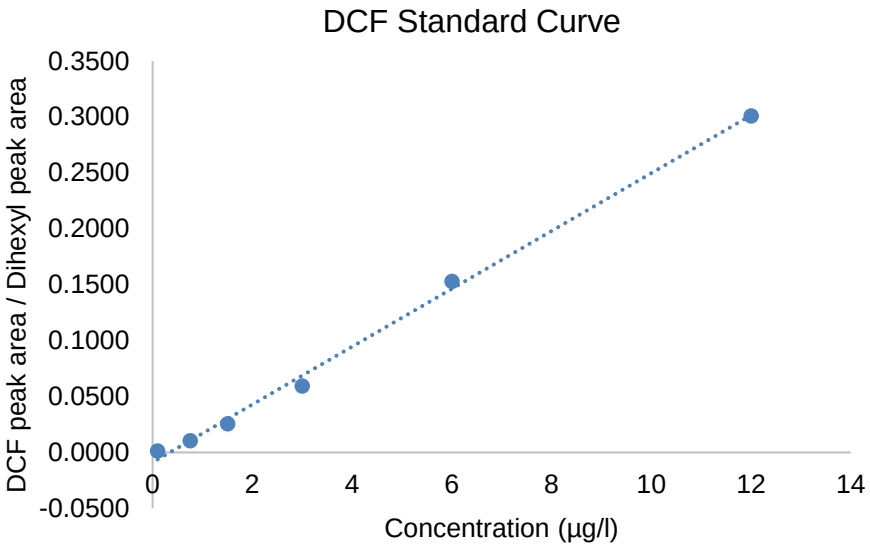

Figure C3: DCF Standard Curve.

Appendix D (Experimental Data)

Table D1: Run 1

Run 1								
Date	**Time**	Hours	DO mg/l	TDS ppm	V volts	EC µS/cm	Temp °C	pH
22/06/2022	20:43	0	9,79	2471	5,5	1235	19,2	4,04
	21:43	1	8,04	2563	5,5	1281	18,7	3,72
	22:43	2	8,47	2454	5,5	1229	18,8	3,62
	23:43	3	7,77	2433	5,4	1219	18,9	3,53
	00:43	4	7,97	2457	5,4	1228	19,7	3,46
	01:43	5	10,18	2578	5,4	1286	20,5	3,44

Table D2: Run Duplicate

Duplicate								
Date	**Time**	Hours	DO mg/l	TDS ppm	V volts	EC µS/cm	Temp °C	pH
2022/01/07	19:46	0	9,05	2559	7,3	1280	20,3	4
	20:46	1	7,22	2582	7	1286	20,4	3,56
	21:46	2	6,54	2586	7	1293	21,2	3,46
	22:46	3	7,55	2516	7	1250	21,6	3,65
	23:46	4	7,44	2575	7,1	1125	23,2	4,47
2022/02/07	00:46	5	7,36	2361	7,1	1181	22,6	6,24

Table D3: Run 1 conditions

Conditions		
Reaction Time	5	hrs
NaCl	0,08	M
pH	4	initial
I	1,5	A

Table D4: Run 2

Run 2								
Date	**Time**	Hours	DO mg/l	TDS ppm	V volts	EC µS/cm	Temp °C	pH
2022/05/08	16:53	0	9,65	1324	4	2649	18,3	4,02
	17:53	1	8,56	1254	4,5	2510	18,1	3,55
	18:53	2	9,76	1291	4,5	2580	17,2	3,4
	19:53	3	9,22	1203	4,5	2412	16,7	3,47
	20:53	4	9,03	1186	4,5	2379	17,5	3,8
	21:53	5	9,94	1096	4,5	2198	16,3	5,46

Table D5: Run Duplicate

Duplicate								
Date	**Time**	Hours	DO mg/l	TDS ppm	V volts	EC µS/cm	Temp °C	pH
2022/05/08	22:51	0	9,81	1319	5,5	2638	17	4,02
	23:51	1	9,36	1315	5,5	2629	17,1	4,04
2022/06/08	00:51	2	9,9	1306	5,5	2613	17,1	3,55
	01:51	3	9,9	1253	5,5	2573	17,8	3,68
	02:51	4	9,75	1230	5,5	2473	17,4	4,03
	03:51	5	9,75	1144	5,5	2286	18,7	6,03

Table D6: Run 2 Conditions

Conditions		
Reaction Time	5	hrs
NaCl	0,08	M
pH	4	initial
I	1	A

Table D7: Run 3

Run 3								
Date	**Time**	Hours	DO mg/l	TDS ppm	V volts	EC µS/cm	Temp °C	pH
2022/03/07	21:00:00	0	9,41	2583	11	1291	17,8	4,02
	22:00	1	9,4	2588	10,5	1295	17,8	3,39
	23:00	2	10,09	2607	10	1203	18	3,29
2022/04/07	00:00	3	9,26	2548	10	1277	19,5	3,61
	01:00	4	10,32	2560	10	1281	21,1	3,45
	02:00	5	9,05	2322	10	1262	21,4	6,26

Table D8: Run Duplicate

Duplicate								
Date	**Time**	Hours	DO mg/l	TDS ppm	V volts	EC µS/cm	Temp °C	pH
2022/06/07	04:57	0	9,91	2549	9	1274	17,6	4,01
	05:57	1	9,62	2565	8,5	1281	19,2	3,52
	06:57	2	8,49	2501	8,5	1252	20	3,46
	07:57	3	9,14	2597	8,5	1205	20	3,88
	08:57	4	9,87	2323	8,5	1162	20,7	6,06
	09:57	5	9,01	2243	8,6	1122	21,1	6,83

Table D9: Run 3 Conditions

Conditions		
Reaction Time	5	hrs
NaCl	0,08	M
pH	4	initial
I	2	A

Table D10: Run 4

Run 4								
Date	**Time**	Hours	DO mg/l	TDS ppm	V volts	EC µS/cm	Temp °C	pH
2022/04/07	02:36	0	9,41	468	9	935	16,5	4,05
	03:36	1	8,51	418	8,5	838	18,4	3,38
	04:36	2	9,71	437	8,5	875	17,7	3,64
	05:36	3	9,75	473	8,5	945	18,4	3,46
	06:36	4	8,75	508	8,4	1017	18,7	3,49
	07:36	5	8,35	462	8,1	925	19,5	3,41

Table D11: Run Duplicate

Duplicate								
Date	**Time**	Hours	DO mg/l	TDS ppm	V volts	EC µS/cm	Temp °C	pH
2022/04/07	08:15	0	9,67	460	12	921	17	4,04
	09:15	1	8,73	448	11,5	896	16,7	3,76
	10:15	2	9,89	441	11,3	882	17,6	3,64
	11:15	3	8,68	477	10,9	944	16,8	3,59
	12:15	4	9,34	476	10,5	952	17,9	3,62
	13:15	5	9,66	472	10,5	941	18,1	3,46

Table D12: Run 4 Conditions

Conditions		
Reaction Time	5	hrs
NaCl	0,02	M
pH	4	initial
I	1	A

Table D13: Run 5

Run 5								
Date	**Time**	Hours	DO mg/l	TDS ppm	V volts	EC µS/cm	Temp °C	pH
2022/05/07	17:02	0	9,59	473	13,6	945	17,7	4,02
	18:02	1	8,82	508	13	1016	18,6	3,28
	19:02	2	9,6	530	12,5	1060	20	3,3
	20:02	3	8,72	495	12	911	21	3,39
	21:02	4	9,25	485	11,9	970	21,8	3,36
	22:02	5	7,97	527	11,5	1052	21,2	3,34

Table D14: Run Duplicate

Duplicate								
Date	**Time**	Hours	DO mg/l	TDS ppm	V volts	EC µS/cm	Temp °C	pH
2022/07/07	04:30	0	9,97	475	14	950	18	4,01
	05:30	1	9,52	461	12,9	923	19,7	3,79
	06:30	2	10,05	467	12	935	20,9	3,57
	07:30	3	9,86	501	12	1002	21	3,49
	08:30	4	9,76	507	11,5	1010	21,4	3,43
	09:30	5	9,83	538	11,5	1036	21,9	3,36

Table D15:Run 5 Conditions.

Conditions		
Reaction Time	5	hrs
NaCl	0,02	M
pH	4	initial
I	1,5	A

Table D16: Run 6

Run 6								
Date	**Time**	Hours	DO mg/l	TDS ppm	V volts	EC µS/cm	Temp °C	pH
27/07/2022	08:17	0	9,32	603	15	1207	17,4	4
	09:17	1	9,84	590	13,5	1191	19,7	3,64
	10:17	2	10,16	613	12,5	1225	21,7	3,47
	11:17	3	8,07	650	12	1306	23,1	3,33
	12:17	4	10,07	662	12	1328	23,7	3,3
	13:17	5	7,51	643	12	1283	24	3,28

Table D17: Run Duplicate

Duplicate								
Date	**Time**	Hours	DO mg/l	TDS ppm	V volts	EC µS/cm	Temp °C	pH
27/7/2022	14:00	0	9,56	459	18,5	919	17,9	4,01
	15:00	1	9,28	468	15,5	936	23,2	3,67
	16:00	2	8,09	499	14,5	999	25	6,3
	17:00	3	9	521	14	1042	25,3	6,36
	18:00	4	9,04	531	13,5	1061	26,5	6,33
	19:00	5	9,07	527	13,5	1055	26,5	6,25

Table D18: Run 6 Conditions

Conditions		
Reaction Time	5	hrs
NaCl	0,02	M
pH	4	initial
I	2	A

Table D19: Run 7

Run 7								
Date	**Time**	Hours	DO mg/l	TDS ppm	V volts	EC µS/cm	Temp °C	pH
2022/09/07	09:07	0	9,75	862	7	1724	18,2	4,05
	10:07	1	9,12	802	6,5	1603	19,2	3,76
	11:07	2	9,6	871	6,5	1752	19,6	3,54
	12:07	3	9,57	840	6,5	1681	19,9	3,45
	13:07	4	9,34	807	6,5	1612	20	3,41
	14:07	5	9,08	868	6,5	1735	19,6	3,4

Table D20: Run Duplicate

Duplicate								
Date	**Time**	Hours	DO mg/l	TDS ppm	V volts	EC µS/cm	Temp °C	pH
2022/09/07	19:50	0	9,61	861	7,9	1722	18,7	4,01
	20:50	1	8,74	820	7,5	1640	19,8	3,74
	21:50	2	8,91	869	7,5	1735	19,6	3,55
	22:50	3	7,88	881	7,5	1759	19,1	3,41
	23:50	4	9,02	875	7,1	1661	19,8	3,39
2022/10/07	00:50	5	9,49	876	7,1	1757	19,9	3,32

Table D21:Run 7 Conditions

Conditions		
Reaction Time	5	hrs
NaCl	0,05	M
pH	4	initial
I	1	A

Table D22: Run 8

Run 8								
Date	**Time**	Hours	DO mg/l	TDS ppm	V volts	EC µS/cm	Temp °C	pH
2022/08/08	23:28	0	9,62	913	9,5	1826	18,5	4,08
2022/09/08	00:28	1	8,84	852	9	1705	19	3,53
	01:28	2	8,69	919	9	1836	19,4	3,37
	02:28	3	8,71	928	9	1891	19,6	3,31
	03:28	4	9,61	801	9,5	1715	19,6	4,51
	04:28	5	9,65	818	9,5	1636	19,7	5,54

Table D23: Run Duplicate

Duplicate								
Date	**Time**	Hours	DO mg/l	TDS ppm	V volts	EC µS/cm	Temp °C	pH
2022/10/08	18:51	0	10,17	904	8	1808	16	4,024
	19:51	1	8,32	912	7,5	1828	18,4	3,5
	20:51	2	8,61	909	7,5	1818	19,7	3,37
	21:51	3	9,01	861	7,5	1722	19,7	3,7
	22:51	4	8,48	831	8	1662	19,5	6,32
	23:51	5	8,67	790	8	1580	19,7	6,44

Table D24: Run 8 Conditions

Conditions		
Reaction Time	5	hrs
NaCl	0,05	M
pH	4	initial
I	1,5	A

Table D25: Run 9

Run 9								
Date	**Time**	Hours	DO mg/l	TDS ppm	V volts	EC µS/cm	Temp °C	pH
2022/11/08	00:36	0	9,82	947	10,5	1894	17,5	4,03
	01:36	1	7,48	866	9,5	1734	17,3	3,47
	02:36	2	8,86	898	9	1796	19,2	3,36
	03:36	3	8,12	931	9	1761	19,2	3,5
	04:36	4	7,51	812	9	1703	20,5	3,52
	05:36	5	6,66	879	9	1764	24,4	3,54

Table D26: Run Duplicate

Duplicate								
Date	**Time**	Hours	DO mg/l	TDS ppm	V volts	EC µS/cm	Temp °C	pH
2022/12/08	16:28	0	10,08	909	10	1818	16,6	4,074
	17:28	1	10,54	867	10	1806	17,1	3,73
	18:28	2	8,01	891	10	1789	18,1	3,42
	19:28	3	9,11	810	10	1751	19,8	3,33
	20:28	4	10,51	801	10	1601	20,8	5,32
	21:28	5	11,66	823	10	1646	21,4	7,19

Table D27: Run 9 Conditions

Conditions		
Reaction Time	5	hrs
NaCl	0,05	M
pH	4	initial
I	2	A

Table D28: Run 10

Run 10								
Date	**Time**	Hours	DO mg/l	TDS ppm	V volts	EC µS/cm	Temp °C	pH
15/08/2022	17:22	0	10,02	456	9,5	910	15,3	4,03
	18:22	1	9,08	430	9	862	21,3	3,98
	19:22	2	10,47	456	9	908	17,5	3,54
	20:22	3	10,46	435	9	868	17,7	3,47
	21:22	4	11,01	453	9	907	18,5	3,33
	22:22	5	11,13	535	8,5	1070	18,4	3,31

Table D29: Run Duplicate

Duplicate								
Date	**Time**	Hours	DO mg/l	TDS ppm	V volts	EC µS/cm	Temp °C	pH
15/08/2022	22:57	0	9,96	489	11	977	16,7	4,05
	23:57	1	9,25	449	10	898	17	4,01
16/08/2022	00:57	2	9,85	473	9	981	17,1	3,83
	01:57	3	10,01	501	9	893	17,6	3,64
	02:57	4	10,21	499	9	999	18,01	3,21
	03:57	5	10,78	519	9	1039	18,5	3,14

Table D30:Run 10 Conditions

Conditions		
Reaction Time	5	hrs
NaCl	0,02	M
pH	4	initial
I	1	A

Table D31: Run 11

Run 11								
Date	**Time**	Hours	DO mg/l	TDS ppm	V volts	EC µS/cm	Temp °C	pH
17/08/2022	17:28	0	9,95	468	11,5	938	17,1	4,05
	18:28	1	8,68	468	10,5	940	19,3	3,86
	19:28	2	9,06	462	10	925	19,6	3,51
	20:28	3	8,02	478	9,5	957	20,8	3,27
	21:28	4	9,48	472	9,5	945	20,8	3,19
	22:28	5	8,97	483	9,5	962	20,9	3,16

Table D32: Run Duplicate

Duplicate								
Date	**Time**	Hours	DO mg/l	TDS ppm	V volts	EC µS/cm	Temp °C	pH
17/08/2022	22:55	0	10,23	467	15,5	937	17,2	4,07
	23:55	1	10,9	450	14	906	18,7	3,78
18/08/2022	00:55	2	10,75	463	13	923	20,3	3,48
	01:55	3	10,43	456	13	905	21,3	3,32
	02:55	4	10,58	476	12,5	946	20,9	3,31
	03:55	5	10,58	500	12,5	999	20,9	3,25

Table D33: Run 11 Conditions

Conditions		
Reaction Time	5	hrs
NaCl	0,02	M
pH	4	initial
I	1,5	A

Table D34: Run 12

Run 12								
Date	**Time**	Hours	DO mg/l	TDS ppm	V volts	EC µS/cm	Temp °C	pH
25/08/2022	19:54	0	9,6	457	16,5	915	20	4,01
	20:54	1	9,98	432	14,5	861	21,8	3,73
	21:54	2	9,85	461	14,5	376	24	3,36
	22:54	3	10,42	472	13	944	25	3,35
	23:54	4	9,71	491	13	982	22,2	2,35
26/08/2022	00:54	5	9,33	530	12,5	1063	22,6	2,96

Table D35: Run Duplicate

Duplicate								
Date	**Time**	Hours	DO mg/l	TDS ppm	V volts	EC µS/cm	Temp °C	pH
29/08/2022	14:32	0	10,27	4,83	20	966	17,3	4,05
	15:32	1	9,5	4,6	18	923	19,6	3,95
	16:32	2	9,63	509	16	1021	23,1	3,75
	17:32	3	9,2	486	15	971	22,6	3,49
	18:32	4	10,22	498	15	995	24,1	3,35
	19:32	5	8,84	513	15	1027	23,6	3,27

Table D36: Run 12 Conditions

Conditions		
Reaction Time	5	hrs
NaCl	0,02	M
pH	4	initial
I	2	A

Table D37: Run 13

Run 13								
Date	**Time**	Hours	DO mg/l	TDS ppm	V volts	EC µS/cm	Temp °C	pH
19/08/2022	20:46	0	10,57	832	6	1662	17,9	4,04
	21:46	1	9,9	826	6	1649	18,4	3,74
	22:46	2	10,11	774	6	1550	18,1	3,43
	23:46	3	10,79	775	6	1548	18	3,28
	00:46	4	10,61	836	6	1679	18,2	3,13
	01:46	5	10,56	829	5,9	1656	18,3	3,13

Table D38: Run Duplicate

Duplicate								
Date	**Time**	Hours	DO mg/l	TDS ppm	V volts	EC µS/cm	Temp °C	pH
20/08/2022	02:16	0	10,28	887	6,5	1774	18	4,02
	03:16	1	10,21	881	6,5	1762	18	3,01
	04:16	2	10,54	879	6,5	1759	18	3,41
	05:16	3	10,7	876	6,5	1741	18	3,22
	06:16	4	8,87	942	6,5	1882	17,2	3,22
	07:16	5	11,06	942	6,5	1884	18,2	3,24

Table D39: Run 13 Conditions

Conditions		
Reaction Time		hrs
NaCl		M
pH	4	initial
I		A

Table D40: Run 14

Run 14								
Date	**Time**	Hours	DO mg/l	TDS ppm	V volts	EC µS/cm	Temp °C	pH
20/08/2022	07:34	0	10,19	877	8,5	1762	17,8	4,05
	08:34	1	10,78	878	8	1745	17,5	3,68
	09:34	2	10,83	858	8	1717	18,6	3,58
	10:34	3	10,91	860	8	1721	18,5	3,48
	11:34	4	9,04	866	7,5	1736	18,2	3,26
	12:34	5	9,44	848	7,5	1703	18,5	3,16

Table D41: Run Duplicate

Duplicate								
Date	**Time**	Hours	DO mg/l	TDS ppm	V volts	EC µS/cm	Temp °C	pH
26/08/2022	01:30	0	10,43	877	9	1753	20	4,06
	02:30	1	9,28	818	9	1634	19,6	3,73
	03:30	2	9,54	871	8,5	1741	19,3	3,57
	04:30	3	10,74	862	8	1731	20,3	3,24
	05:30	4	9,51	871	8	1721	20,3	3,24
	06:30	5	9,4	852	8	1706	19,1	3,23

Table D42: Run 14 Conditions

Conditions		
Reaction Time	5	hrs
NaCl	0,05	M
pH	4	initial
I	1,5	A

Table D43: Run 15

Run 15								
Date	**Time**	Hours	DO mg/l	TDS ppm	V volts	EC µS/cm	Temp °C	pH
26/08/2022	16:10	0	10,13	890	10	1776	16,8	4,06
	17:10	1	10,67	847	9	1697	19,6	3,67
	18:10	2	9,27	856	9	1711	20,6	3,52
	19:10	3	10,63	834	8,5	1670	20,9	3,24
	20:10	4	10,6	900	8,5	1793	22,4	3,2
	21:10	5	10,57	911	8,5	1827	21,8	3,02

Table D44: Run Duplicate

Duplicate								
Date	**Time**	Hours	DO mg/l	TDS ppm	V volts	EC µS/cm	Temp °C	pH
29/08/2020	19:55	0	10,71	890	10	1780	18	4,05
	20:55	1	10,43	830	9	1656	18,1	3,75
	21:55	2	10,19	846	9	1689	19,2	3,55
	22:55	3	10,22	855	9	1711	19,3	3,37
	23:55	4	11,96	826	8,5	1656	19,9	3,3
30/08/2022	00:55	5	10,99	866	8,5	1735	19,4	3,24

Table D45: Run 15 Conditions

Conditions		
Reaction Time	5	hrs
NaCl	0,05	M
pH	4	initial
I	2	A

Table D46: Run 16

Run 16								
Date	**Time**	Hours	DO mg/l	TDS ppm	V volts	EC µS/cm	Temp °C	pH
26/08/2022	21:34	0	10,12	1259	5,5	2518	19,1	4,05
	22:34	1	11,33	1184	6	2358	19	3,89
	23:34	2	10,54	1183	5,5	2368	19,3	3,52
27/08/2022	00:34	3	11,8	1181	5,5	2362	19,2	3,36
	01:34	4	11,53	1247	5,5	2497	19,1	3,21
	02:34	5	11,97	1243	5,5	2490	19,1	3,2

Table D47: Run 16.2

Duplicate								
Date	**Time**	Hours	DO mg/l	TDS ppm	V volts	EC µS/cm	Temp °C	pH
17/08/2022	03:04	0	10,37	1274	6	2553	18,8	3,07
	04:04	1	8,96	1202	6	2411	18,5	4,6
	05:04	2	8,93	1153	6	2304	18,4	3,73
	06:04	3	10,17	1232	6	2466	18,8	3,36
	07:04	4	9,02	1224	6	2446	18,8	3,35
	08:04	5	9,19	1272	6	2551	19,1	3,3

Table D48: Run 16 Conditions

Conditions		
Reaction Time	5	hrs
NaCl	0,08	M
pH	4	initial
I	1	A

Table D49: Run 17

Run 17								
Date	**Time**	Hours	DO mg/l	TDS ppm	V volts	EC µS/cm	Temp °C	pH
27/08/2022	08:18	0	10,26	1216	7,5	2437	19,1	4,06
	09:18	1	9,51	1170	7,5	2344	19	3,67
	10:18	2	11,41	1194	7,5	2377	21,7	3,39
	11:18	3	10,28	1204	7	2407	20,2	3,33
	12:18	4	11,02	1233	7	2425	20,8	3,34
	13:18	5	11,12	1231	7	2466	20,8	3,23

Table D50: Run Duplicate

Duplicate								
Date	**Time**	Hours	DO mg/l	TDS ppm	V volts	EC µS/cm	Temp °C	pH
27/08/2022	13:45	0	10,08	1271	7	2541	19	4,06
	14:45	1	9,53	1181	7	2531	19,8	3,64
	15:45	2	10,21	1192	6	2521	20,1	3,31
	16:45	3	9,88	1205	6	2499	20,5	3,37
	17:45	4	9,73	1222	6	2481	20,9	3,34
	18:45	5	9,8	1243	6,5	2489	21,2	3,29

Table D51: Run 17 Conditions

Conditions		
Reaction Time	5	hrs
NaCl	0,08	M
pH	4	initial
I	1,5	A

Table D52: Run 18

Run 18								
Date	**Time**	Hours	DO mg/l	TDS ppm	V volts	EC µS/cm	Temp °C	pH
27/08/2022	18:04	0	9,8	1286	9	2572	19,9	4,07
	19:04	1	9,73	1194	8,5	2380	21,2	3,54
	20:04	2	9,46	1201	8	2408	21,6	3,4
	21:04	3	8,18	1258	8	2516	21,9	3,22
	22:04	4	10,01	1227	8	2452	21,8	3,16
	23:04	5	10,59	1338	8	2668	26,6	3,23

Table D53: Run Duplicate

Duplicate								
Date	**Time**	Hours	DO mg/l	TDS ppm	V volts	EC µS/cm	Temp °C	pH
29/08/2022	09:07	0	10,2	1288	7,5	2570	15,8	4,04
	10:07	1	10,11	1242	7,5	2476	17,5	3,58
	11:07	2	10,25	1201	7	2402	18,4	3,46
	12:07	3	10,88	1197	7	2390	19,2	3,22
	13:07	4	10,91	1294	7	2583	19,2	3,23
	14:07	5	10,81	1287	7	2573	19,4	3,23

Table D54: Run 18 Conditions

Conditions		
Reaction Time	5	hrs
NaCl	0,08	M
pH	4	initial
I	2	A